Advanced Bottom-Up Engineering of Living Architectures

COMPASS

ENGINEERING LIFE GUIDED BY NATURE

This paper must be cited as: Gaspar, V. M., Lavrador, P., Borges, J., Oliveira, M. B., & Mano, J. F. Advanced Bottom-Up Engineering of Living Architectures. *32*(6), 1903975. *Advanced Materials* (2020). https://onlinelibrary.wiley.com/doi/full/10.1002/adma.201903975

Title: Advanced Bottom-up Engineering of Living Architectures

Vítor M. Gaspar, Pedro Lavrador, João Borges, Mariana B. Oliveira, João F. Mano**

Dr. V.M. Gaspar, P. Lavrador, Dr. João Borges, Dr. Mariana B. Oliveira, Prof. João F. Mano*
Department of Chemistry, CICECO – Aveiro Institute of Materials
University of Aveiro
Campus Universitário de Santiago, 3810-193, Aveiro, Portugal
E-mail: vm.gaspar@ua.pt, jmano@ua.pt

Keywords: Tissue Engineering, Living Building Blocks, Bottom-up Assembly, 3D Bioarchitectures

Abstract
Bottom-up tissue engineering is a promising approach for designing modular biomimetic structures that aim to recapitulate the intricate hierarchy and biofunctionality of native human tissues. In recent years, this field has seen exciting progress driven by an increasing knowledge of biological systems and their rational deconstruction into key core components. Relevant advances in the bottom-up assembly of unitary living blocks toward the creation of higher order bioarchitectures based on multicellular-rich structures or multicomponent cell–biomaterial synergies are described. An up-to-date critical overview of long-term existing and rapidly emerging technologies for integrative bottom-up tissue engineering is provided, including discussion of their practical challenges and required advances. It is envisioned that a combination of cell–biomaterial constructs with bioadaptable features and biospecific 3D designs will contribute to the development of more robust and functional humanized tissues for therapies and disease models, as well as tools for fundamental biological studies.

1. Introduction

Tissue engineering and regenerative medicine (TERM) strategies have been for long regarded as the next-generation medical treatments owing to their potential to repair, improve, or replace tissues/organs that exhibit defective functions resulting from trauma, chronic diseases or ageing.[1, 2] Over the past decades, this field has witnessed a tremendous evolution motivated by an accumulating body of knowledge on human tissues development, homeostasis regulation, and inflammation/regeneration processes.[3-5] Adding to this, such fundaments have also been key for rapidly advancing the fabrication of complex microphysiological systems using well-designed bioinstructive materials that aim to recapitulate human disease hallmarks in vitro.[6]

This deepened understanding of tissue-specific microenvironments and recognition of their fundamental modular nature has revealed that different cell populations and their supportive extracellular matrix (ECM) represent the core effectors in human biological systems and are essential for life.[7, 8] During the processes of organogenesis and morphogenesis, such elements self-orchestrate tissue development from a nano- to macrostructural organization in a dynamic mode involving both cell–cell crosstalk (e.g., via soluble mediators, vesicles, etc.) and dynamic cell–matrix biochemical and biophysical interactions. This highly bioregulated interplay remains active throughout our lifetime with constant ECM synthesis, biochemical modification, and remodeling in response to biological and environmental

factors, as well as to tissue injury.9 Loss-of-function at both cellular and ECM level dysregulates tissue homeostasis and prompts the onset of numerous life-threatening pathologies.9

Recreating these building blocks and their intricately controlled crosstalk is essential when designing tissue engineered platforms that aim to repair/substitute the complex 3D architecture of tissue-specific microenvironments and their biological functions.10 Despite significant advances, the inclusion of key biocomponents in ex vivo engineered constructs and their arrangement into structurally ordered and physiologically functional microtissues remains a demanding challenge.11

Aiming to recapitulate such components, conventional tissue engineering strategies have explored "top-down" approaches, involving cell seeding in supporting porous 3D scaffolds aiming to mimic the native ECM physiochemical and biomechanical cues.12, 13 In top-down tissue engineering, cells are expected to attach/proliferate, and ultimately completely populate a prefabricated 3D biodegradable scaffold, while simultaneously depositing de novo formed ECM along time. Up-to-date, numerous scaffold types have been engineered to better recapitulate tissues microarchitecture, physiology, and ECM soft/stiff spatiotemporal biomechanical rearrangements.14 The latter often encompasses the inclusion of mechanical stimulation and/or biomolecules (e.g., growth factors, cytokines, etc.) for tailoring biomaterials to better recapitulate in vivo tissue microenvironments biomolecular signaling and mechanobiology.15, 16 However, cells immobilization in preformed ECM-mimetic supporting scaffolds is highly challenging, often resulting in low cell seeding density and heterogeneous spatial distribution.17 Despite recent progress in biocompatible scaffolds fabrication techniques (e.g., 3D printing, two-photon polymerization, lithography, etc.) or on the use of bioderived decellularized matrix (dECM) tissue-specific templates, top-down scaffold-based approaches generally fail to mimic the unit-repetitive modular design found in native human tissues (i.e., nephrons, lobules, islets, etc.).18

These limitations and the accumulating knowledge of human developmental biology has supported bioinspired bottom-up approaches in the form of self-assembling multicellular modules and/or cell–ECM mimetic biomaterial constructs.

Scaffold-free cell-rich structures and scaffold-based cell–biomaterial bottom-up tissue engineering strategies are more suitable for replicating the natural intricacies and modularity of human tissues/organs.19 These building blocks can then be combined into multiscale microtissues in a hierarchic and programmed assembly mode with a biospecific design. This is critical since organ-like microarchitectures are needed not only to replicate living structures functionality, but also to identify key parameters and their roles in determining engineered tissues function. Advancing biomimetic designs in this direction is essential for accelerating regenerative medicine approaches, but also in the context of developing preclinical drug screening models. Also, it is now recognized that hierarchical tissue organization naturally limits the accumulation of somatic mutations.20, 21 Thus, bottom-up assembly of hierarchical constructs might also contribute to guide the differentiation of naive stem cells upon implantation and reduce the possible risks of cell-based therapies. From a bioengineering perspective, it is more valuable and intuitive to construct a repertoire of selected biofunctional cell-rich modules rather than immediately attempting to mimic the

full complexity of natural tissues. When contemplating clinical translation, optimizing biofunctionality while minimizing complexity is essential.22

Bottom-up tissue engineering provides a unique design flexibility, allowing to freely combine each building block to carry out distinct tasks in multiple layouts with tissue-biomimetic features, and only then assessing the final biofunctionality of multiscale-assembled microtissues. The cellular rich building blocks can be engineered via different approaches including self- or guided/programmed cell assembly (Figure 1) that enable user-controlled spatial distribution of different cell populations.19

Ultimately, by establishing a library of biofunctional modular units that is representative of: i) a key biological function from a specific tissue or organ, ii) the underlying matrix that supports the cell modules and provides essential cues for their bioactivity, researchers will be able to advance tissue engineered constructs toward more realistic clinical applications. In this progress report, we provide an up-to-date outlook on current strategies for assembling bottom-up tissue engineered constructs and include a critical perspective on the key role that modular cell–biomaterial assemblies will play in the upcoming years for building biofunctional microtissues with a truly pro-regenerative potential.

2. Cell-rich Assemblies

2.1. "2.5D" Multicellular sheet-like assemblies

The current understanding that cells naturally self-organize into highly ordered multicellular structures which precede tissue and organ formation has laid the foundation for the development of advanced methodologies that aim to recapitulate the high cellular density of human tissues. Cell sheet technologies take advantage of close cell–cell interactions to autonomously engineer microtissues without the use of biodegradable cell-supportive scaffolds. As mentioned earlier, their presence can hinder proper cell–cell communication, spatial arrangement and its degradation byproducts can influence cell physiology.23, 24 Their degradation can also originate areas rich in ECM deposition that can hinder communication between neighboring cell clusters.25 Native tissues and organs are densely populated by numerous cell types that are enclosed in a vast framework of tissue-specific matrix that allows efficient cellular intercommunication, directing fate and function at the microscale. This cell-rich 3D environment with well-orchestrated ECM presentation leads to higher order physiological function seen in living tissues.26 Pursuing this design philosophy is essential for building up different types of tissues such as cardiac, renal, and hepatic that generally operate at high cell densities.27-29

In this context, cell sheets arise as scaffold-free high cell density microstructures that aim to recapitulate the contiguous assembly of cells seen in living tissues, thus attempting to retain its structural and functional cues.30 Here, cells are cultured and proliferate in adhesive substrates until confluent layers are generated. These cell-rich sheets are then harvested with methodologies that should maintain cell sheet integrity and allow it to be easily transferred. Thus, cell sheet harvesting with proteolytic enzymes (e.g., trypsin, dispase, etc.) has been discontinued because these can affect cell integrity, as well as disrupt essential intercellular junctions and cell surface proteins.31, 32

The emergence of smart surface engineering refined the control on cell detachment and enabled cell sheet harvesting in mild conditions. In this sense, Okano's group has popularized cell sheet applications by designing a temperature-dependent harvesting substrate, which is commercially

available under the brand name UpCell.27, 33 The poly(N-isopropylacrylamide) coating undergoes a sharp change in wettability from 37 to 32 °C, which spontaneously peels the cell sheet from the surface at room temperatures.23, 25 Still, this one-time use system is expensive, detachment time may vary significantly, and it can be difficult to handle due to the low range of temperature that triggers the peeling process.34, 35 Thermally expandable hydrogel sheets or multilayered coatings are being explored as an alternative to this technology that facilitate transfer and stamping of cell sheets with spatially controlled cell adhesion.36-38 Other sophisticated harvesting systems have been developed over the years exploring different cell-friendly stimuli, including electroactive substrates, pH-responsive coatings, and photoactivatable surfaces, that change their wettability on-demand.39, 40 In this context, hematoporphyrin-containing films for light-induced cell sheet harvesting of human-bone-marrow-derived mesenchymal/stromal stem cells (MSCs) were successfully developed.41 Light-responsive titanium dioxide (TiO2) nanodots films also offer spatial control over cell detachment and can be used for aligning cell sheets in predetermined directions.42 Alternatively, magnetic forces can hold cells in place until harvesting is intended.6 Magnetite cationic liposomes modified with RGD (arginine-glycine-aspartic acid) cell-adhesive peptide were used as smart coatings for developing fibroblast cell sheets, which were stabilized under a magnetic field and could be moved as a contiguous microtissue on-demand.43 Also, cells internalizing magnetic nanoparticles can be forced to assemble over different surfaces to create cell sheet-like structures.44 More recently, Park and co-workers embedded magnetic nanoparticles in thin hydrogel sheets for efficient harvesting of endothelial progenitor cell sheets.45 Using a bioinspired approach, researchers have also developed a cellulose-dopamine coating which enabled cellulase-assisted enzymatic harvesting with minimal cell damage as recently reported.35

Monolayer cell sheets are built with millions of cells, but their sheet-like fragile structure is hard to manipulate and does not offer enough microtissue depth in comparison to thick native tissues.46 However, researchers can assemble thicker constructs just by stacking cell sheets, taking advantage of the cell-dense vast ECM network that naturally intertwines the different cell sheets into a contiguous and integral multilayered microtissue.47 Their versatility extends beyond stacking single cell-type sheets, but also enables rich combinations of multiple cell types, thus more accurately mimicking heterogenous native tissues. The crosstalk signaling present in tissues plays a key role in influencing cell fate and potentiating biofunctionality.48 Cells from closely related osseous tissues (i.e., periodontal ligament and jaw bone) assembled into a co-cultured cell sheet exhibited enhanced osteogenic potency and were more structurally similar to the native periodontal tissue in vivo.49 Still, although some improvements can be achieved with randomized distribution of cell populations, reconstituting tissue-specific biological function relies on recapitulating its hierarchic cellular organization patterns. For instance, the liver's ability to perform more than 500 different functions is associated with its repetitive functional units (liver lobules) that are organized in a hierarchic multiscale manner.50 Precisely engineered culturing and harvesting substrates can direct the spatial arrangement of different cell populations in cell sheets design, contributing toward more complex and in vivo-like assemblies. In this context, straightforward approaches such as microcontact printing of ECM proteins using rationally designed stamps have been explored to enable spatial control over cellular adhesion layouts during cell sheet manufacturing.51, 52 By controlling nonadhesive and cell adhesive areas, researchers engineered hepatocyte modules surrounded by endothelial cells, achieving a co-patterned liver-like microtissue that maintained the ability to synthesize albumin and urea (Figure 2A,B).53, 54 In addition, other advanced methodologies (e.g., microfluidics chips and dielectrophoretic55/magnetic patterning56) that permit cell spatial organization were also explored for designing liver-like cell-rich lobules with biomimetic distribution[57] or for fabricating microvessel-like cell sheets that recapitulate key

features of perfusable vascularized networks.58 Apart from controlling cell distribution and harvesting in in vitro cultured substrates, cell sheets have also been recently processed as scaffolds-free 3D bioinks. Using an elegant approach, researchers used extrusion bioprinting to fabricate sheet-based constructs that showed an increased structural integrity in comparison to standard cell-aggregates owing to their in vitro produced ECM.59

Still, engineering a functional microtissue requires more than just controlling the spatial location of different cells and cell types, but also cellular alignment. In fact, many tissues in the human body (e.g., skin, skeletal muscle, myocardium, brain, and cartilage) show regional and directional 3D anisotropy that is essential for their mechanical and biological functions.64 For instance, the myocardium is assembled from multiple layers of cardiomyocytes aligned along several directions throughout the whole tissue in a 3D anisotropic organization that is required for efficient electrical propagation and synchronized contractility.65 Researchers have demonstrated that layered cardiomyocyte sheets rapidly establish electrical communications via functional gap junctions, achieving 3D-like myocardial tissues with elongated cardiomyocytes and synchronized macroscopic pulsations.66, 67 These bioengineered microtissues possessed elongated cardiomyocytes resembling the native cardiac muscle, which maintained spontaneous pulsations for more than 1 year postimplantation.31, 68 Moreover, the cardiac microtissues show intrinsic angiogenic potential, which is essential for fostering favorable host tissue integration and preventing ischemia.69, 70 Alternatively, researchers have engineered a 3D anisotropic skeletal muscle tissue by stacking myoblast sheets with a defined alignment as seen in Figure 2C,D.60 Interestingly, anisotropy from top layers was transferable to layers underneath due to the self-organization capacity of myoblasts. Also, cell sheets with different orientations were designed by stacking perpendicularly aligned differentiated myotube layers that do not self-organize, thus generating multioriented constructs.

Nevertheless, not all morphological aspects can be recapitulated by stacking cell sheets in a stratified manner. In fact, some architectural features of native tissues include tubular structures (e.g., trachea, blood/lymph vessels, or intestines) with specific 3D conformations and different cells at specific locations (i.e., wall versus lumen).62 Inspired by organisms development, stacked cell sheet constructs can be maneuvered toward such configurations by twisting, rolling, or wrapping into desired tubular forms.71 Multilayered cardiomyocyte sheets wrapped around a resected rat aorta formed a functional myocardial tube that integrated with the host tissue and exhibited well-defined sarcomeres with contractile behavior.72 Their flexible nature can also be exploited for replacing the damaged epithelial lining in tracheas.73 Vascular media and adventitia tubules have been assembled by rolling fibroblast and smooth muscle cell (SMCs) sheets, achieving 0.3 mm wall-thick constructs able to sustain supraphysiological mechanical stresses.74 Other researchers have designed 3D anisotropic hMSCs tubules by rolling cell sheets cultured on aligned ECM substrates.61 The tubular vascular grafts were then matured in static or dynamic (i.e., bioreactor) conditions. Ultrastructure analysis revealed distinct parallel grooves for bioreactor-matured tubules that fused in thicker walls (0.25 vs 0.17 mm in static samples) and exhibited mechanical and vasodilation features resembling the native arterial wall (Figure 2E,F). However, these studies do not include endothelial cells in the composition of the tubules, a critical aspect since these structures play a key role in their native counterparts.74 To address this, researchers have developed 3D macroscopic tubular tissues by a stress-induced rolling of cell sheets containing arrangements of endothelial cells, SMCs and fibroblasts in a layered fashion (Figure 2G,H).62 Moreover, by controlling cell orientation in the 2D surface template, they could fabricate tubules with circumferentially and longitudinally oriented SMCs, thus mimicking the anisotropy seen in native tunica media and adventitia. Aiming to achieve more complex architectures, self-folding co-cultured cell sheets were obtained by culturing cells in origami-inspired micromolded alginate substrates that release cell assemblies upon

enzymatic degradation with alginate lyase.75 The resulting dodecahedron microstructures give rise to 3D co-culture cell-rich assemblies via a self-folding process mediated by cell–cell traction force (Figure 2I,J).

It is important to note that thick microtissues (i.e., >50–100 μm) often become necrotic before sufficient neovascularization develops, which can be overcome by incorporating endothelial cells, either in co-culture or as individual layers, capable of forming microvascular networks.76 Moreover, laser-assisted bioprinting can be used for guiding human endothelial cells to form tubule-like structures on top of cell sheets.77 Micropatterning of electrochemical-responsive substrates has also allowed the harvesting of human umbilical vein endothelial cells (HUVECs) in the form of capillary-like luminal structures.78 Previous studies also demonstrated that functional vascularization improves integration with host tissues.79 The characteristic intercapillary network of specific tissues is a key parameter to take into account in the bottom-up design process.80 For instance, the heart has a narrower intercapillary distance (<25 μm) than other tissues. Hence, when assembling cardiac tissues, it is important to optimize the ratio of noncardiomyocyte cells as they can affect the contractility of the engineered 3D construct and possibly cause arrhythmia.76, 81

Overall, multilayered cell sheet constructs can be stacked on top of one another to engineer specific stratifications seen in hierarchic organs. Cell sheets can also be deformed into tubular shapes that are prominent in certain tissues, as well as the vast vascular network. When in contact with vascular beds or host organs, cell-rich sheet constructs naturally integrate onto tissue interfaces and develop functional intervascularization. Over the last decade, cell sheets have been bioengineered into different tissues, ranging from small vessels, cardiac microtissues, hepatic-like lobules, skeletal muscle, cornea, and others.24 Functional prevascularized and perfusable cardiac microtissues have been successfully developed, but the stacking process is still manual and operator dependent.82, 83 Recently, an advanced automated cell sheet stacking technology was developed by Okano's group, and is envisioned to shift current cell sheet designs toward large scale manufacturing and translation into clinical applications.47 Adding to engineered cell sheets, other scaffold-free assemblies such as 3D multicellular aggregates (e.g., spheroids,84 fibers,85 dense membranes, etc.)86 have been receiving an increasing focus for bottom-up tissue engineering and for establishing organotypic preclinical disease models.

2.2 3D Multicellular Assemblies

2.2.1 Spherically Shaped Multicellular Aggregates

Cell-rich 3D aggregates are valuable building blocks for fabricating organotypic microtissues owing to their closer correlation to living organs gene expression patterns,87 multidimensional cell–cell interplay, and pH/nutrient/oxygen diffusion gradients.88 Engineered multicellular 3D constructs better recapitulate these intrinsic functions since cells are immediately driven toward 3D-like microaggregates in in vitro culture platforms, in contrast to the initial 2.5D monolayer setting of cell sheets.89-91 The resulting structures display a more realistic physiological response at early timepoints and intrinsically include microenvironment specific (bio)chemical/physical cues that support their biological performance.91

Cell-rich 3D clusters fabrication takes advantage of intercellular adhesion mechanisms (e.g., cadherin and integrin-mediated)92, 93 to create self-assembled structures comprising single, or multiple cell types, unlocking the potential to fabricate heterotypic cell constructs more similar to the cellular heterogeneity of human tissues.94, 95 Upon in vitro maturation, these seamless 3D microaggregates secrete de novo ECM frameworks in which cells reside and exchange interactions, adding to their biofunctionality and biomedical applicability. To date, numerous technologies have been developed for the rapid manufacture of scaffold-free 3D cellular

aggregates via culture and proliferation in nonadhesive setups, including forced floating and hanging drop platforms, multiarrayed micromolds, and microfluidic chips.96, 97 These well-established methods have been employed by researchers for high-throughput generation of multicellular microaggregates exhibiting rod-, toroidal-, or honeycomb-like architectures, as well as spherical morphologies (i.e., 3D spheroids, Figure 1).97-99

In particular, self-assembled 3D spheroids have rapidly arisen as attractive cell-rich unitary building blocks for recapitulating in vivo organs functional units since 3D multicellular aggregates with spherical shapes are also observed during tissue morphogenesis.100 3D spheroids exhibit tissue-specific features, shape reproducibility, size versatility, ease of handling, bioprocessing, and potential for upscaled production.97, 101 The latter poses a critical aspect when researchers envision the clinical application of cell-dense multiscale constructs that require millions of 3D spheroidal functional units.88, 102, 103

To date, advanced monotypic (single culture) and heterotypic (co-culture) scaffold-free 3D multicellular spheroids have been developed as in vitro microphysiological systems for modeling pathophysiology of human diseases or as unitary building blocks for tissue engineering of cardiac, hepatic, vascular, or neuronal tissues, among others.89, 90, 104 In the context of tissue engineering and regeneration, 3D spheroids have been employed as angiogenic stimulating units (i.e., via secretion of trophic factors—VEGF, PDGF)93 or as functional blocks for the assembly of prevascularized microtissues.90 Progresses in this field indicate that 3D spheroids comprising heterogeneous cell populations better recapitulate the complexity of human tissues and exhibit a more pro-regenerative capacity. In a recent study, 3D co-culture spherical constructs comprising HUVECS and human bone marrow MSCSs (hBM-MSCs) were fabricated for improving bone regeneration (Figure 3A). Upon implantation into chick femur bone defects endothelial-skeletal 3D clusters improved collagen II and angiogenic proteins expression in the osteogenic niche. More importantly, an increased mineralization and bone volume deposition was obtained for 3D HUVEC-HBMSCs co-culture spheroids when compared to the sham defect group (Figure 3A).105 The establishment of functional tubular-vessel-like networks with positive blood perfusion have also been reported in co-cultured 3D spheroids comprising human osteoblasts (hOB) and human dermal microvascular endothelial cells (HDMECs) upon implantation into mouse dorsal skin models.106 This evidences the tissue integrative properties of prevascularized 3D spheroid building blocks and the importance of taking this into consideration when engineering implantable cell-rich 3D assemblies. By using a similar strategy, 3D MSCs–OECs (outgrowth endothelial cells) co-culture spheroids were established in nonadherent agarose micromolds to function as elementary units for prevascularized microtissues formation. The established 3D spheroids demonstrated a significant pro-angiogenic potential in in vivo chick chorioallantoic membrane (CAM). assays, accompanied by close tissue integration, and their culture under xeno-free conditions potentiates their applicability in bottom-up tissue engineering (Figure 3B).107 It is worth to reference that in vitro culture of cell-rich assemblies under xeno-free conditions is an important parameter for cell-based therapies application in a more realistic clinical setting.

Despite their recognized validity for regenerative medicine applications, these examples mainly employ nonlinked, individual spheroids. Also, the spherical morphology restricts the geometrical complexity of fabricated 3D multiscale microtissue assemblies.89 For bioengineering larger and more intricately patterned tissues, 3D cell-rich spherical aggregates must be processed through advanced methodologies.93 In this sense, researchers are advancing 3D spheroids postproduction bioprocessing by using microplatforms that promote spheroid-spheroid fusion and by taking advantage of automated biofabrication technologies (e.g., 3D bioprinting) that build-up spheroid-based living architectures with user-defined geometries.102

Spheroids fusion occurs when spatially adjacent spheroids establish physical contact and coalesce into a more cohesive single tissue, a spontaneous process that occurs during biological development and that is fundamental in myocardial and skeletal tissues formation.102, 108 This process is then followed by cell self-organization into distinct layers within the resulting microtissues, similarly to what occurs during human organs development.108 Also, taking advantage of nonadhesive poly(dimethylsiloxane) (PDMS) microchamber arrays, the fabrication of robust neurospheroid networks was established through fused neuronal processes protruding from spatially adjacent 3D neurospheroids of rat cortical cells (Figure 3C). During optimization, the authors discovered that PDMS microchambers with 100 μm diameter and depth were optimal for promoting oxygen diffusion to 3D neurospheroids and for assuring constructs viability.109 The interconnected/fused 3D spheroid neuronal network was then implanted in cortical tissue and exhibited excellent integration into cortical tissues as observed by the establishment of functional synaptic connections with host neurons. Random 3D microscale spheroids fusion has also been employed for creating 3D millimeter-scaled tissues with complex geometries (e.g., star, square, triangle, etc.) in nonadherent micromolded platforms (Figure 3D).110, 111 The microfabricated tissues comprising co-cultured HUVECs and MSCs 3D spheroids as unitary building blocks showed autonomous deformation, contractility and formed self-assembled vascular structures in high deformation regions.111 This resulted in spatially modulated secretion of pro-angiogenic growth factors and specific vascular patterns.111

To achieve more precise spatial positioning and user defined-patterns, 3D spheroids can be processed though 3D bioprinting/robotic assembly or magnetic-based manipulation.2 In this sense, Mironov's group bioprinted multicellular 3D spheroids into customized millimeter-sized vascular tubular constructs with well-defined topology and cellular composition as a result of spheroid-spheroid fusion (Figure 3E).112 This groundbreaking approach, alongside with Kenzan's method113 for bioprinting 3D spheroids (up to 500 μm) into needle arrays which are removed after spheroids fusion, are envisioned to contribute for the fabrication of evermore complex cell-rich biospecific constructs with controlled architectural features. Yet, to date, such strategies still require specialized equipment, extensive troubleshooting, and the maturation of bioprinted microtissues along time. Alternatively, 3D spheroids magnetic manipulation using preprimed cells with magnetoferritin nanoparticles has also been explored to generate structurally defined microtissue rings for tissue engineering, but the biofunctionality and long-term safety of such constructs remains to be elucidated.114, 115 Adding to the opportunities that arise from the establishment of dense 3D spheroid assemblies the development of 3D multicellular organoids in vitro is also becoming increasingly relevant in numerous fields of research including tissue engineering and regenerative medicine, disease modeling, and drug discovery.116, 117

Human 3D organoids are highly relevant as building blocks for bottom-up tissue engineering since their assembly is reminiscent of tissues organogenesis and morphogenesis. Generally, 3D organoids are composed of stem cells (i.e., human adult/embryonic stem cells, or human pluripotent stem cells (hPSCs)) that undergo in vitro proliferation, directed differentiation, cell-sorting, lineage commitment, and self-assembly into higher order 3D architectures.118 Interestingly, upon in vitro maturation, 3D organoids generate highly organized cell-rich structures that somewhat recapitulate the complex structural features and physiological responses of the tissues their cells were derived from.119, 120 Despite their organotypic features it is important to emphasize that current organoidgenesis in vitro is only possible under a highly controlled microenvironment often including a complex cell culture medium that contains multiple factors (i.e., small molecules and growth factors) for precisely guiding cellular differentiation and also an ECM-mimetic hydrogel to further provide bioinstructive

cues (i.e., Matrigel).118 To date, these multicellular systems have been increasingly employed in advanced bottom-up engineering of numerous tissue types such as kidney, liver, or pancreas. In fact, researchers have been recently able to develop pancreatic islet organoids from human embryonic stem cell derived pancreatic progenitor cells.121 The cells spontaneously aggregated in vitro under controlled culture conditions and formed robust multicellular spheroid-shaped organoids with controlled size and cellular heterogeneity. Upon maturation the resulting 3D organoids exhibited functional insulin secretion after a glucose challenge. It is important to emphasize that such organoids were assembled using a unique hydrogel platform (i.e., Amikagel) and that the development of biofunctional organoids in fully scaffold-free conditions remains to be demonstrated to the best of our knowledge.121 There is no doubt that these are highly promising microphysiological constructs, however most in vitro generated organoids still generally lack key cellular constituents of the tissues they aim to recapitulate. In this context, researchers are actively developing new strategies for including stromal, immunological, and vascular components in these 3D multicellular assemblies.120, 122 It is envisioned that advances in these important aspects will have a significant impact in the development of more physiomimetic building blocks for bottom-up tissue engineering.

2.2.2 Fiber-Shaped Multicellular Aggregates

Fiber-shaped constructs are highly valuable for bottom-up tissue engineering applications due to their ease of processability into higher order living architectures and similarity to multidirectional native anatomic structures, including blood vessels, neurons, lymph vessels, ligaments, and tendons.123 In fact, the exacerbation of the length of one single dimension in fiber-shaped materials enables the spatially unconfined deposition of continuous structures. This unique potential has been leveraged by the rapidly emerging field of 3D printing/bioprinting which explores the potential of long fiber-shaped materials to create personalized implants and tissue engineered cell-laden constructs with highly specific architectures and functionality.124-126 Moreover, know-how from the textile industry, namely, knitting, weaving, and reeling has been transposed for the bottom-up tissue engineering of fibrous structures due to its potential for generating biofunctional micro/macroscale constructs with improved bioactivity and mechanical properties.127 Interesting advances in this field include, but are not limited to, the fabrication of cell-laden hydrogel yarns for tendon bioengineering through mechanical stimulation128 or the fabrication of vessel-like networks with cell-laden collagen fibers.129

Despite the versatility of fiber-shaped constructs, few reports describe the fabrication and exploitation of fully scaffold-free cell-rich fibers. In this context, Takeuchi's group pioneered the production of meter-long cellular microfibers.130 By using a double-coaxial microfluidics device, researchers were able to fabricate core–shell fibers comprising alginate crosslinked with calcium ions (diameters ranging from 100 to 200 μm) (Figure 4A). Such hollow structures were laden with mixtures of cell suspensions and ECM proteins, the latter capable of forming gelled structures at in vitro cell culture temperature conditions or in the presence of thrombin and maintained high cell viability. Cells from different sources including fibroblasts, cardiomyocytes, endothelial, and pancreatic cells could be processed in the shape of long fibers in the presence of specifically selected and optimized ECM proteins. In this approach, the alginate shell was easily removed from fiber constructs formed by fibroblasts or MIN6m9 cells (a mouse pancreatic beta cell line) using alginate lyase. Importantly, the generated cellular microfibers maintained shape and structural integrity after this process. Although this study represented a breakthrough in the use of elongated cellular fiber-shaped materials, the use of relatively stiff gel-forming ECM proteins as a determinant factor for the success of fibers' formation did not warrant a fully scaffold-free character to the achieved microfibers. Moreover, the assembly of microfibers as higher order constructs was restricted to alginate-coated units,

while the handling of cell/ECM-only structures may pose additional challenges to the precise assembling of macrometric constructs.

In an effort to surpass the possible toxicity of enzyme-mediated methods to degrade alginate reported in primordial studies,130 a method based on mechanical action to retrieve fibers composed of bone marrow MSCs and collagen was suggested.134 While this study avoided the use of possibly toxic enzymes, the rapid formation of the cellular fibers (24 h) was still dependent on the addition of ECM proteins. Also based on the co-axial microfluidic-based extrusion of cell suspensions inside hollow alginate tubes, other researchers reported the formation of scaffold-free centimeter-long microfibers built solely from primary human chondrocytes (Figure 4B).131 After four days of incubation and cellular aggregation, alginate tubes were removed by a postprocessing technique that involved their dissolution in sodium citrate. Cellular strands matured in vitro for 3 weeks in chondrogenic medium could be bioprinted into macrometric constructs with clinically relevant sizes. Interfiber fusion was observed as early as 12 h of contact, and complete merging was obtained after 7 days of in vitro maturation.

Alternative approaches to microfluidic-based fabrication of cellular fibers were suggested based on the patterning of growth channels prepared by laser micromachining135 and more recently, by micromolding.85 These strategies have been exclusively directed for the preparation of tendon single fibers, and are highly dependent on specific equipment and selective patterning of adhesive proteins into nonadhesive agarose molds.

The scaffold-free generation of fiber structures via 3D bioprinting as also been recently materialized through the extrusion of hMSCs cell-rich bioink into a medium containing alginate microgel particles (Figure 4C).132 To generate the supporting baths, microgels with different average sizes (7 and 409 μm) were assembled via dual crosslinking of methacrylated and oxidized alginate (OMA), and subsequently crosslinked with calcium. This disruptive approach allowed high-resolution bioprinting of hMSC-rich 3D filaments even with curved, corner, and X-shaped configurations due to the shear-thinning and self-healing properties of the engineered supporting bath, and regardless of microgels size (Figure 4C). The 3D bioprinted cell-rich filaments presented high cellular viability postprinting and the smaller microgels bath allowed to obtain maximum printing resolution of hMSCs filaments as exhibited by the 3D printed anatomic shaped constructs (Figure 4C). To confer mechanical cues and stability during microtissues maturation postprinting the OMA bath was photocrosslinked. This allowed long-term culture and fusion of stem-cell-rich aggregates into denser 3D microtissues, as well as maintained their differentiation potential toward osteogenic and chondrogenic lineages.132

Nevertheless, most approaches targeting the preparation of microfibers are still focused on the achievement of multicellular bulk structures. A high degree of cellular compaction, however, may lead to poor oxygen and nutrients diffusion during maturation periods, culminating in loss of cellular viability and function in fibers' core regions. To tackle this challenge, microporous tissue strands were prepared by adding a porogen agent—alginate microbeads—to cellular suspensions before extrusion inside a hollow alginate tube (Figure 4D).133 Fibers comprising adipose-derived MSCs (ASCs) generated by this methodology showcased approximately 25% porosity and high pore interconnectivity. When compared to bulk nonporous strands, porous counterparts showed improved long-term in vitro cellular viability, as well as higher efficacy on the induction of both the osteogenic and chondrogenic differentiation on the aggregated cells (Figure 4D).

An overall analysis of current technologies available for the fabrication of scaffold-free cellular fibers enabled identifying opportunities in this rapidly growing, yet still poorly explored field. In this context, fiber-based textile engineering processes are particularly interesting for tailoring the mechanical properties (e.g., tensile stress/strength, Young's modulus, and elongation at break) of multifiber assemblies to better recapitulate the biomechanical features of native tissues.136 Relevant examples of textile techniques for such applications include knitting (e.g., allows control over interfiber porosity, higher through-plane strength, and stretchability), braiding (e.g., tailoring of load-bearing properties, tensile strength, and abrasion resistance), or the less mechanically demanding weaving process (e.g., tunable mechanical anisotropy and allows improved control over cell distribution), and winding of fibers onto 3D tubular constructs.137, 138 Furthermore, architectural manipulation of multiple fibers, each containing HUVECs, fibroblasts, or hepatocytes, allowed different cells to be interfaced in predefined patterns across braided assemblies.138 The braiding process resulted in vastly different mechanical properties, with differences on the range of three orders of magnitude.138 Future approaches based on the knitting and/or printing of co-cultured fibers or fibers comprising different cell types (or in distinct stages of differentiation/maturation) may pave the way for the fabrication of architecturally precise and hierarchic constructs that better recapitulate the features of human tissues with fibrillar structures.

From the former examples it becomes clear that the assembly of 3D cellular aggregates into higher order structures provides an exciting approach to generate cell-dense tissues from the bottom-up. However, from a critical perspective, cells self-assembly in both 2.5D sheets and 3D multicellular aggregates (e.g., spheroids, fibers, etc.) still occurs in a stochastic mode that does not fully recapitulate the highly controlled process of tissues morphogenesis at a unicellular level. Aiming to address this uncertainty, cutting-edge technologies for bottom-up tissue engineering have focused on the synthetic engineering of cell membrane surface to imprint biospecific cues and preprogram cell-rich scaffold-free assemblies with precise cell–cell selectivity and spatiotemporal organization. In the following section, we highlight these emerging paradigms and present the most recent advances of these approaches.

2.3. Unitary cell surface bioengineering

In the context of bottom-up tissue engineering, the manipulation of cell surface to promote a programmed self-assembly into higher order 3D bioarchitectures, represents a powerful approach for assembling unitary cellular building blocks into highly controlled microtissues (Figure 1). Although cells can be coated with hard shells139 we will mainly focus on soft surface modifications140 and on precisely programmed surface engineering141 allowing cells to be molded and organized into more complex structures.

Currently, cell surface modification is facilitated by the knowledge of various bioconjugation chemistries together with synthetic biology approaches (e.g., genetic engineering) and other methodologies that include the inclusion of multifunctional micro- and nanosized agents capable of connecting multiple cells. Adding to this, the vast array of available biorthogonal coupling chemistries, as well as their specific binding nature, allow for the construction of surface modified cellular modules leading to precise hierarchic architectures.142 Because different cell types can be functionalized differently, researchers can control the cellular spatial arrangement in bottom-up assembled constructs.

In particular, cell surface glycoengineering arisen as an elegant metabolic cell engineering concept that exploits intrinsic sialic acid biosynthesis pathways in order to install reactive functional groups at cells surface. Cell functionalization takes place upon unnatural

monosaccharides uptake and incorporation within the sialoglycan metabolism, which is responsible for continuous remodeling of natural sialic acid end-capping residues in live cells.143 Bertozzi's group pioneered this biotechnological cellular hijacking tool by exposing at the cell surface biorthogonal ketone and azide groups available for oxime and click-chemistry conjugations, respectively.144, 145 Since then, advances in biorthogonal chemistry have presented this field with additional sialoglycan-compatible groups such as biotin, alkyne, alkene, and thiols. More recently, other innovative strategies incorporating arylazide photocrosslinkers, bifunctional sialoglycan analogues (e.g., azide-alkyne) and caging groups capable of neutralizing surface negative charge and inducing cell aggregation, have been reported.143, 146, 147

Among these strategies, azide-glycoengineering is by far the most explored alternative, owing to its high in vivo chemical stability, unique presence in the body, as well as the growing popularity of strain-promoted copper-free azide-alkyne cycloaddition (SPAAC) reactions with fast kinetics at physiological conditions under the absence of catalysts.148 Still, a lack of cell selectivity in co-culture conditions is one of glycoengineering main limitations, but this can be overcome via delivery with cell-penetrating and targeted nanoassemblies (e.g., liposomes). In line with this, researchers were able to improve cell-selectivity and surface engineering efficacy by administering ligand-targeted liposomes loaded with azidosugars.149 This allows for precise cell attachment of imaging/therapeutic agents, biomaterials, nanocarriers, or even other surface-modified cells.

Unsurprisingly, glycoengineering represents an enabling technology for various biomedical applications, namely, both live cell,150, 151 and extracellular vesicle labeling/tracking,152 drug-based cancer theranostics,153 as well as cell-based chemo- and immunotherapies.154, 155 Despite an impressive body of literature on these recent advances, tissue engineering concepts exploiting this biomachinery phenomenon are still at their youth. Glycoengineering of typically nonadherent human Jurkat cell surfaces imparted them with extra free thiol groups, thus stimulating spontaneous self-aggregation into clusters.156 Importantly, this can allow allocation of typically nonadherent cell lines (e.g., immune cells) in bottom-up assemblies of heterogenous cell-rich building blocks as it will be further discussed. Alternatively, coupling of immunostimulants to live cells has recently been reported via a glycoengineering strategy.154 The concept of incorporating immune cells in engineered assemblies, i.e., immunoengineering, is on the forefront of developing clinically relevant immunomodulatory tissues.157 Translation of this technology to other cell types in the future, could be exploited for fast-generating spheroid building blocks or allowing more sophisticated and hierarchic assemblies via thiol-reactive incorporation (e.g., alkyne, norbornene, maleimides, or photocrosslinkable alkenes). Cells with norbornene-bearing surfaces have now been successfully generated, which could allow for light-enabled precise spatial control of cell–cell interactions.158 However, although norbornene-sugar incorporation efficiency is still limited in present attempts, other photocrosslinkable groups have shown promising results (i.e., acrylamide).159 Cells exhibiting triple-orthogonal surface engineering have also been reported, which could allow for more complex heterogenous configurations of cell–cell interactions.159 Alternatively, cell surface-grafting strategies are starting to emerge, either as controlled radical polymerization or anchoring telechelic synthetic polymers, in order to re-engineer cell surface functionality and interactions.160, 161

However, surface modification can elicit possible phenotypic and biofunctional alterations that are yet to be fully understood.156 The usage of smart biodegradable cell linkages with on-demand dynamic anchoring of cells may help overcoming some of those concerns. With this rationale, a biocompatible and chemically detachable cell glue system based on biorthogonal

linkers connecting glycoengineered cells was successfully developed.162 Azide-containing cells were functionalized with bioreducible tetrazine and trans-cyclooctene linkers containing internal disulfide bonds, achieving fast cell–cell gluing upon mixing the two different cell groups. Then, the established cell glue network could be disassembled after natural glutathione ($5 \times 10{-}3$ m) administration, showcasing the reversible glue behavior (Figure 5A). Another elegant way of obtaining on-demand control over cell–cell interactions was recently achieved by using bioengineered azide mammalian cells surface to contain β-cyclodextrin, which forms an inclusion complex with trans-azobenzene via host–guest interactions.163 The azobenzene trans-to-cis conversion can then be triggered by photoactivation, dissociating the inclusion complex in a reversible manner. Using this rationale, photoactive azobenzene functionalized with cell recognition moieties (azo-aptamer) were used to enable cell–cell interactions between cyclodextrin-modified cells and azobenzene-bound cells, a process that could be easily reversed by light exposure. The photocontrolled manipulation of cell–cell interactions could also be useful in developing user-defined hierarchic cellular-rich assemblies.

This advanced technology has been explored in recent studies to direct drugs and nanoassemblies toward tumors, while also monitoring its progression.166 Moreover, by exploiting the tumor-homing properties of MSCs, researchers have used glycoengineered MSCs as nanoparticle beacons, irreversibly trapping nanoconstructs in tumor sites.150 Due to the high reactivity, bioorthogonal character and biocompatibility of this azide-DBCO chemistry, such rationale could be translated to glycoengineered tissue constructs (GTCs), where exposed azides allow postimplantation follow-up and signal for subsequent GTC-targeted nanoassemblies containing bioinstructive cues. Recent research efforts have achieved encouraging results supporting this novel strategy. For instance, glycoengineered azide-chondrocytes could be readily tracked via near-infrared (NIR) imaging 4 weeks after subcutaneous implantation in mice.167 Moreover, DBCO-650-labeling not only provided improved contrast imaging, but also preserved chondrogenic potency and showed minimal adverse effects on cartilage formation over traditional cell tracking fluorescent probes (i.e., DiD). In a similar approach, the migration of glycoengineered human ASCs (hASCs) in ischemic hindlimb mouse model was also tracked.151 Again, NIRF-labeling via DBCO-Cy5 probe showed notable biocompatibility, in particular over DiD-based labeling, and allowed efficient in vivo monitoring of intramuscularly administered hASCs for 2 weeks, in particular their co-localization in ischemic sites. In a follow-up study, this technology was used to allocate glycol chitosan nanoparticles containing different imaging probes in hASCs.168 However, rapid uptake of these clickable nanoassemblies was observed within 1 h of incubation. When envisioning the generation of nanoenabled cell clusters for tissue engineering, avoiding intracellular uptake is a critical parameter. To this end, photoswitchable nanoparticles were covalently bound to living cell membranes via a similar glycoengineering strategy.169 Site-specific membrane localization of upconversion nanoparticles in human embryonic kidney 293 (HEK293) cells was evident in fluorescence microscopy studies, which inspires future studies where spatial bioactive presentation can be tuned by external triggers and achieve localized differentiation in hierarchic constructs.

Tracking the fate of transplanted cells is essential for pursuing optimal tissue engineering applications, and this is facilitated in GTCs designs.170 As demonstrated by Bertozzi's group, nonpenetrating azide-binding probes can enable 3D spatiotemporal in vivo imaging of developing zebrafish.171 Because these probes are not transferable across cells, the addition of different reporters at various time intervals allow for differential labeling of tissue layers and display time-sensitive imaging of GTCs development. Another unique feature of glycoengineering is the sensitivity to different intracellular metabolisms that can distinguish cell subtypes and thus monitor stages of human breast cancer.172 Similarly, incorporation of

azido-sugars was significantly increased during cardiac hypertrophy.173 Dysregulation of sialoglycan biosynthesis is also found in neurological disorders and central nervous system injuries.174 These recent findings inspire novel applications in cell-based therapies and tissue engineering with innate pathophysiological-responsive monitoring.

Holistically, it is important to discuss the limitations of the aforementioned technologies in bottom-up tissue engineering and potential improvements. The dynamic nature of the cell membrane and its refined biomachinery does allow researchers to introduce superficial reactive moieties and use cells as building blocks in chemically driven interactions among other cells, biopolymers, and nanoassemblies. However, dynamic surface glycan recycling and inevitable cell division processes ultimately restrict the timeframe for appreciable surface reactivity. This issue raises concerns about whether long-term feeding of cells with unnatural sugars can lead to unexpected effects on cell and microtissue development.175 Moreover, the importance of spacers on the stability of such cell-networks requires further studies. Indeed, the risk of using complementary cells for strain-promoted alkyne-azide cycloaddition with insufficient spacer length could result in membrane fusion among adjacent cells.176 Hence, alternative cell surface engineering approaches using nanocarriers as crosslinking points have also been extensively investigated.

Nanosized fusogenic liposomes can efficiently fuse with cell membranes upon uptake, thus incorporating their phospholipidic content in living cell membranes.177 This phenomenon has inspired Yousaf's group to reprogram cell surfaces to display specific functional groups in order to accelerate 3D tissue assemblies.178 This approach takes advantage of a pioneering biorthogonal chemistry based on ketone and oxyamine catalyst-free conjugation with fast kinetics at physiological conditions and in the presence of serum.179

Using this approach, researchers have reprogrammed nonadherent Jurkat cells with photolabile-oxyamine and ketone groups, achieving rapid multicellular 3D spheroid assemblies via intercellular oxime linkages.164 Upon UV illumination, the microtissue disassembled into individual cells. In the same study, fibroblasts transformed with photolabile oxyamines readily adhered to aldehyde-containing interfaces. The reprogramed cells could then be selectively detached from the material upon UV illumination. In addition, large multilayered microtissues containing MSCs and fibroblasts sheets were easily assembled with this technology (Figure 5B). Photo-disassembly of tissue multilayers can then be locally triggered resorting to photomasks during UV exposure, which enables the fine remodeling of microtissue hierarchy.

Liposomal fusion instructs chemoselective cell clustering, locking cells in place until sufficient matrix is produced and elicits microtissue formation and cell spreading. This oxime cell-coupling tool allows easy access to the generation of robust 3D modules with various geometries (e.g., circular, bar, and square) and accelerated assembly times.179 Also, its fast kinetics have recently enabled in-flow spheroid and tissue assembly via microfluidics.180 Cell cluster morphology and assembly times can be tuned by controlling flow rate, channel distance and cell density, and the cell modules are stable, thus not requiring seeding in Matrigel or other supporting ECM-mimetic scaffolds. Recently, scaffold-free tissue-like models (e.g., hepatic and cardiac) have been developed using this innovative tool.181, 182 Heterogenous cell populations can be rapidly programmed to self-assembly into dense multilayered tissue modules for biomedical applications. This flexible biotechnological tool is also compatible with current 3D bioprinting technologies where cells could act both as ink and glue, while biosacrificial layers could be achieved by including photoresponsiveness within the oxime linkage, as demonstrated in the study by Luo et al.164 It is important to note that the fusogenic capacity varies significantly among cell types.183 Although this could represent a limitation to

liposome-driven cell assembly strategies, this phenomenon could be exploited for differential cell modification in co-culture conditions. However, to date further studies are still required to ascertain the potential of this approach.

Alternatively, oligonucleotide-based technologies (e.g., DNA aptamers) have also been employed for establishing programmed cell–cell connectivity into higher order cell-rich 3D microtissue constructs. This approach is inspired by the orthogonal hydrogen bonding of nucleic base pairs naturally observed in DNA, an interaction that demands a specific template for complete binding of two complementary nucleotide sequences.184 Such unique cross-reactivity has led to significant advances in other fields (e.g., DNA origami and patterning, synthetic nanopores, and molecular motors).185 For bottom-up tissue engineering, this selectivity has been materialized by anchoring single-stranded DNA (ssDNA) into living cells membrane to modulate cell–cell interactions between complementing aptamer sequences. This chemical reprogramming can be performed under typical cell culture conditions and does not require cells genetic manipulation. Such strategy has been explored in a seminal work, where ssDNA aptamer sequences were used as binding agents for building selective connectivity among cells. The complementary oligonucleotide sequences were introduced in different cells surface via selective chemistry between modified ssDNA aptamers (i.e., phosphine or difluorinated cyclooctyne) and glycoengineered nonadherent Jurkat cells decorated with azide moieties (via glycocalyx engineering with N-azidoacetylmannosamine sugars).165 By using specifically matched ssDNA the authors were able to establish large 3D cell aggregates of typically nonadherent cells with DNA clustering being evident at cell–cell interfaces (Figure 5C). Interestingly, a precise control over cellular ratios (1:50) resulted in the formation of rosette-like microtissue assemblies with controlled cell neighboring (Figure 5C), confirming the DNA-mediated cell programming. Overall, these authors further demonstrated that the kinetic parameters of 3D microtissues assembly via defined cellular connectivity depend on DNA sequence complexity, density, and cell concentration.

An important advantage of duplex DNA technology is the possibility to reverse DNA-mediated cellular assemblies into their unicellular building blocks via controlled melting or degradation.165 This linkage reversibility can allow for cells selective isolation/purification,186 or for templated cells inclusion in higher order ECM-mimetic structures as clusters which then disassemble and migrate to specific areas alike in some pathologies. This technology could therefore be of interest also for investigating fundamental cell migration studies. Using DNA-programmed assembly of cells, it is also possible to incorporate components of the mesenchyme, such as fibroblasts, allowing the precise engineering of stem cell niches that capture stromal contributions. It is clear that this technology allows a precise control over individual cell–cell interactions and may enable direct examination and manipulation of juxtacrine cell–cell and cell–ECM interactions during tissue maturation.

These methods have unprecedentedly expanded our ability to precisely manipulate cells behavior or adhesion properties. Nevertheless, from a developmental biology perspective, multicellular self-assembly into complex tissue structures is driven mainly by genetically programmed routines activated at specific time frames to induce biologically relevant and dynamically orchestrated physiological responses.187-189 Recent, approaches have therefore started to use synthetic biology tools to explore self-regulated cell–cell adhesion mechanisms in an attempt to better emulate in vivo biosystems features in in vitro bioengineered 3D microtissue assemblies. In fact, various genetically encoded circuits have already been developed for establishing complex biologically driven patterns at the cell population level. These include the encoding of: i) adhesion-driven assemblies (i.e., phase separation), of ii)

lateral inhibition where neighboring cells have different fates, a characteristic process in vertebrates neuronal development, of iii) mechanically driven assemblies that can originate tree-like or fractal patterns, or the use of iv) "reaction-diffusion programing" of biological spatial pattern formation, also termed the "Turing/Gierer–Meinhardt model."190 The latter is based on activator–repressor species that govern spatial patterns formation via different diffusion rates. Such interactions are considered to be key in embryonic development and respond to changes in tissue size.190 This mechanism is also particularly valuable since simple synthetically programmed genetic networks can originate complex and recurrent patterns which have the ability to self-regenerate when disturbed.190 These strategies therefore add an attractive layer of complexity and dynamism to the formerly discussed cell surface engineering approaches and better recapitulate tissues morphogenesis.

Taking inspiration on these processes, a recent study reported an elegant generation of genetically programmed multilayered 3D microtissue assemblies evocative of dynamic 3D structures observed during embryonic development.141 Specifically, the authors designed genetic circuits that combined adhesion-driven (i.e., cadherins) and lateral inhibition via synNotch receptors at the cell–cell interface to create complex self-organized 3D microtissues with cell-signaling induced morphologic spatial rearrangements (Figure 5D). In turn, these dynamics generated new cell–cell interactions and reorganizations as a result of cell type diversification and asymmetry.

It is clear that cutting-edge cell surface modifying technologies enable researchers to sculpt cellular behavior and allow the fabrication of precisely programmed cell-rich microtissues in in vitro culture. Yet, other biomaterial-based approaches are also moving bottom-up tissue engineering forward by imparting biointegrative/bioinstructive cues on cellular building blocks and by unlocking the build-up of highly organized cell–biomaterial assemblies. The following chapters will focus on different cell–biomaterial assemblies and their importance toward the creation of more in vivo-like microtissues.

3. Cell-Biomaterial Assemblies

3.1. Macromolecular cell surface functionalization via Layer-by-Layer

In recent decades, the LbL assembly technology has emerged as a simple, robust, and highly versatile engineering methodology to modify diverse inorganic and organic surfaces, including eukaryotic cells.191 LbL technology has rapidly evolved to become a well-established tool for functionalizing surfaces,192 and fabricating elegant and stable electrostatic, and nonelectrostatic-driven multilayered cellular-rich architectures with multiple functionalities and advantages.193 Its simplicity and cost-effectiveness (no specific or expensive equipment is required), as well as mild processing conditions turned it into a powerful technology for cell surface functionalization in the context of bottom-up tissue engineering strategies. In fact, the LbL assembly process can be performed under physiological conditions entirely in aqueous solutions. This means that there is no need for the use of organic and/or harmful solvents or extreme pH, ionic strength, and temperature conditions, thus turning it into a very appealing tool when dealing with biomolecules which have not only limited solubility in nonaqueous solutions, but are also highly prone to lose their biological activity. In addition, it is a highly versatile technology both in terms of the substrates, building blocks, and intermolecular interactions that can be used to fabricate simple, organized, as well as more intricate architectures.194-198 Moreover, an unprecedented source of building blocks including biological materials such as nucleic acids, enzymes and other proteins, peptides, polymers, viruses, or even cells can be used to functionalize the substrate surface, provided that the

individual constituents show complementary interactions. Such versatility enables the fabrication of a plethora of continuous, molecularly uniform, and scalable thin films, as well as multilayered surfaces and devices with precisely tailored physicochemical, mechanical and biological properties, including multilayered thin films, free-standing multilayered membranes, core–shell particles, hollow multilayered capsules, or even 3D tissue-like structures across multiple length scales.192 This is a key advantage over monolayer-based systems, thus turning LbL surface engineering technique into a highly suitable and powerful technology for a wider range of biomedical applications, including tissue and cell surface engineering, enabling a high degree of control over cell–surface, cell–biomaterial, and cell–cell interactions.199-201

However, notwithstanding the tremendous progress, only in the last few years the LbL assembly technology has extended well-beyond its importance for the functionalization of hard and soft inanimate charged surfaces, proving to be a suitable bottom-up strategy for functionalizing animate and dynamic surfaces, including living cells.191, 202, 203
Such multilayered assemblies are intended to engineer hierarchically ordered 3D cellular architectures to emulate the complex organized structure and function of natural tissues and organs. Akashi's group has pioneered the research in this field by proposing the build-up of biocompatible tissue constructs comprising L929 fibroblast-based cellular multilayers and native ECM components, including cell adhesive proteins.199 The authors have reported the use of fibronectin (FN) and gelatin (G) to prepare nanometer-size-based multilayered films on the cell surface by simply repeating the alternate immersion of a cell monolayer-modified glass substrate into FN and G aqueous solutions, under physiological conditions, using the dip-assisted LbL methodology (Figure 6A). In-between each protein deposition step, washing steps were required to remove weakly adsorbed molecules and avoid the cross-contamination of protein aqueous solutions. The successful growth of unlabeled and fluorescently labeled FN/G multilayered coatings comprising different number of layers (i.e., film thickness) was confirmed on a solid surface by employing quartz crystal microbalance (QCM) and fluorescence intensity, respectively. A linear increase in the frequency shift and fluorescence intensity was seen upon increasing the number of layers, thus indicating an increase in the thickness of the film covering the cell surface. The influence of the (FN/G)n multilayered coating on the possible build-up of 3D L929 fibroblast multilayers was assessed by confocal laser scanning microscopy (CLSM) and compared with solely FN-coated and uncoated cells.199 It was found that, the (FN/G)n multilayered coating was homogeneous and that there was the need for at least 7 bilayers (≈6 nm film thickness, Figure 6A) and having the FN as the outermost layer (i.e., (FN/G)n/FN) to enable the adhesion of more cell layers, leading to higher order 3D fibroblast-based cellular assemblies. Furthermore, the nanofilms showed high intercellular adhesion, being easily peeled off from the glass substrate. However, the same behavior did not happen either on the single FN-coated (≈2.3 nm thick layer) or on the uncoated cells. This indicates that, after seeding the first cell monolayer, no additional cell layers could be included, irrespective of having the first cell monolayer uncoated or coated with a single FN layer. The reason behind this result is explained in light of the motifs displayed by the FN chemical structure. Although FN displays RGD moieties in its structure, such motifs are intrinsically required for regulating the adhesion of FN to the first layer of cells. Therefore, the FN per se is unable to bind to a second layer of cells, thus inhibiting the build-up of cellular multilayers.

Besides the development of 3D hierarchically stacked constructs encompassing multilayers of L929 fibroblast cells,199, 207 several studies in the literature recalling to the use of the FN/G biomolecular recognition for LbL assembly of different cell types have been reported.208, 209 Those artificial 3D tissue-like constructs include the fabrication of vascularized blood vessels.210 However, the fabrication of artificial 3D tissue constructs by solely resorting to the

dipping LbL methodology is quite challenging. First of all, it is a time-consuming process owing to the numerous depositions and rinsing steps. As such, it raises film stability concerns since the deposited layers might be endocytosed before the adsorption of subsequent layers. Furthermore, it requires large amounts of materials for each adsorption step, as well as solid surfaces. Moreover, the multilayered coating is very thin, showing a film thickness in the nanometer-size range. Hence, researchers have been looking for alternative deposition methodologies to process such multilayered coatings in a fast pace and, simultaneously, develop thick and more robust 3D tissue models emulating the structure and function of natural tissues. One simple methodology that has been used to significantly speedup the LbL assembly process and which does not require the use of solid substrates, is the centrifugation-assisted LbL approach in which individual cells, collected by centrifugation after trypsinization, are alternatively incubated in the native ECM proteins FN and G using centrifugation.208 After each deposition step, the cells are rinsed with buffer solution, to remove unbound molecules, followed by centrifugation. This deposition methodology has been used to successfully develop a variety of 3D human tissue models, including liver,211 skin,212 and blood/lymph-vascularized human stromal models.213 However, the centrifugation-assisted LbL methodology requires multiple centrifugation steps to separate the cells from the adsorption protein solutions, which may damage cell membranes and reduce viability, during the build-up process. Akashi and co-workers have investigated the effect of the centrifugation cycles on cell viability and have demonstrated that after submitting the uncoated hepatocyte carcinoma (HepG2) cell line to several centrifugation steps more than 90% of the cells were nonviable. However, in the case of the (FN/G)9-coated cells, the same number of centrifugation cycles ended-up with a cell viability over than 85% and extensively reduced the leakage of cytosolic enzyme lactate dehydrogenase, showing that the LbL coating extensively protects cells from centrifugation-derived physical stress (Figure 6B).204 Despite these findings, one should not transpose the results gathered with the HepG2 cells and FN/G multilayered coating to other cell types and LbL constituents as the cell viability might by influenced by the cell type, LbL film composition and thickness. Nevertheless, physical stress can be avoided by resorting to filtration-assisted LbL technology which assures high viability and efficiency to the FN/G coated cells. The filtration-assisted LbL methodology has been employed to engineer 3D human tissue constructs, including vascularized cardiac microtissues,214 liver,211 and blood vessels.215 Using a different approach, researchers also demonstrated that the LbL assembly technology can be combined with automatic inkjet printing of single cells and ECM proteins to precisely develop 3D human microtissue chips in a rapid and automatic mode.216 Such technology hold great potential for in vitro high-throughput preclinical drug screening, as well as to study cell–biomaterial interactions.

In spite of immense reports on the fabrication of thin film-coated cell surfaces, 3D cellular multilayers, and the establishment of human micro/macrotissue constructs by resorting to biological specific interaction between FN and G multilayers, one can also combine fibronectin with other natural ECM proteins, such as collagen,217 or cytocompatible and negatively charged naturally occurring glycosaminoglycans, including heparin, or hyaluronic acid to modulate cell functions.218, 219 Adding to this, one could move beyond ECM proteins for cell coating, since they entail limited stability, high costs and batch-to-batch variability. Recent approaches focused on developing LbL-based multilayered micro/macrotissue constructs by resorting to a library of modular ECM-mimetic synthetic peptides, including peptide amphiphiles and multidomain peptides, comprising a repertoire of short different cell-binding motifs derived from ECM proteins. Those peptides are advantageous owing to their easy and cost-effective synthesis, biocompatibility, biodegradability, self-assembling capability into fibrillar nanostructures in aqueous media, and customized bioactivity, which turns them into suitable molecular building blocks for engineering artificial ECM-mimetic constructs to direct

cell fate.220-222 Such peptide library would encompass the widely studied FN-derived RGD and laminin-derived IKVAV (isoleucine-lysine-valine-alanine-valine) biofunctional peptide sequences, known to modulate cellular functions at the tissue and organ levels, among many others, opening new avenues in the molecular design of innovative ECM-like biomaterials for addressing a number of different tissue engineering applications.223, 224 When envisioning the assembly of dense LbL-built microtissues important aspects regarding nutrients/oxygen availability and neo-vascularization must be considered to assure cellular viability and biofunctionality in denser microtissue constructs.

Cell surface functionalization and LbL-based microtissues assembly, via surface engineering can also be alternatively performed by resorting to protein/polymer combinations. These mainly involve the use of collagen ECM mimetic component to functionalize cells surface. In a recent approach, researchers developed collagen type I/alginate (COL/AA)5 multilayer thin films for generating 2.5D cell sheet constructs after in vitro maturation for 4 days.225 The underlying hypothesis for successful films assembly was based on natural collagen interaction with the cell membrane and also its electrostatic interaction with negatively charged alginate biopolymers. The intrinsic collagen cell-selective interactions and reactivity toward negatively charged biopolymers was also leveraged for individual MSCs surface functionalization with multilayered thin films. In this work the collagen type I/hyaluronan (COL/HA) multilayered film did not fully covered cells surface, this important aspect resulted in an improved cytoprotection in unfavorable suspension culture conditions, supported MSCs colony-forming ability and also their osteogenic differentiation.226 This study is particularly relevant for bottom-up tissue engineering approaches since the assembled mesh-like film was composed of two major ECM components. Such could lay the foundation for using ECM mimetic surface functionalized MSCs as biofunctional building blocks in multiscale multicomponent cell–biomaterial assemblies in the future.

From another approach, various polymer/polymer combinations including cationic polymers have also been used for cell surface functionalization due to their electrostatically driven interaction with negatively charged cell membrane surfaces.227 However, their use generally elicits cytotoxic effects and cell lysis, including the formation of nanosized cell membrane pores, which may result in cell death.228-231 In addition, most polycations are known to quickly transpose the cell membrane and accumulate intracellularly, thus turning them generally useless for functionalizing the cell surface. Nevertheless, one cannot extrapolate and take this as the global picture. It is crucial to bear in mind that the propensity of the polycations to damage the cell membrane and induce cytotoxic effects on cells is strongly dependent on several properties, including polymer functional groups, concentration, molecular weight, conformation, charge density, hydrophobicity, deposition temperature and exposure time, as well as on the type of cells used.205 This means that, depending on the assembly conditions and cell type, the same polycation can be cytotoxic or noncytotoxic to the cells, thus proving that the cell functions are extremely sensitive to the surface chemistry nature. In an attempt to mitigate polycations' cytotoxicity and decrease the propensity to disrupt the cell membrane, other cell surface engineering approaches have emerged as promising tools for re-engineering the molecular landscapes of cell surfaces. One possibility concerns the decrease of the polycation charge density through the synthesis of block copolymers, grafting neutral polymers to polycations,232 and further functionalization of the cell surface via electrostatic interactions. Moreover, a multilayered coating can be attempted directly on the cell surface by employing an automated filtration process, as well as exploiting the electrostatic interactions between the cationic graft copolymer and oppositely charged materials.232, 233 For instance, it has been demonstrated that poly(l-lysine)-graft-poly(ethylene glycol) (PLL-g-PEG) could be adsorbed on the cell membrane surface with minimal accumulation in the intracellular compartments, whereas PLL

showed high cytotoxicity, destroyed the cell membrane, accumulated intracellularly, and decreased the cell viability.205 The influence of the percentage of backbone lysine groups grafted to PEG chains (grafting degree) on pancreatic islet viability has been assessed after cell exposure to the copolymers. It was found that the PLL toxicity decreased while decreasing the charge density (Figure 6C). However, keeping fixed the concentration of the graft copolymer and the grafting degree, and increasing the PEG chain length led to a decrease of the PLL cytotoxicity. The authors also studied the influence of the PLL molecular weight on its cytotoxicity to cells. As expected, polycations with higher molecular weight showed higher toxicity in comparison with their lower molecular weight counterparts. Another strategy to modify the cells surface in a LbL fashion while assuring cell viability, comprises the use of PLL-g-PEG-biotin (PPB) cationic copolymer and streptavidin multilayers by exploiting the highly specific, stable, and strong biological interaction between streptavidin and biotin motifs (Figure 6D).192 After the electrostatic deposition of the PPB cationic copolymer onto the negatively charged cell surface, the streptavidin entity adsorbs onto it through biotin–streptavidin biospecific interactions. Moreover, since streptavidin encloses four binding sites for biotin, a biotin fraction still remains available, thus enabling the adsorption of further PPB/streptavidin layers until reaching the desired film thickness (Figure 6D). It has been demonstrated that such strategy is a very efficient and stable methodology to build-up biocompatible, PEGylated multilayer thin films on cell surfaces,192 being an attractive methodology to control the extracellular microenvironments and regulate cell behavior. In a similar application, islet surface modification through the alternating adsorption of biospecific biotin-bovine serum albumin/streptavidin multilayers onto a hydrophobic-driven biotin-PEG-lipid functionalized lipid bilayer of the cell membrane has also been explored.234

Besides protein/protein, polymer/polymer, and protein/polymer hybrid nanofilms generated by biomolecular recognition and electrostatic driving forces, other intermolecular interactions can also be used to drive film growth and functionalized cell surfaces. Covalent bond-based chemical approaches have also been used to coat cell surfaces using polymers functionalized with orthogonally reactive moieties. For instance, recent studies focused on the fabrication of a covalently crosslinked multilayered thin film of poly(vinyl alcohol) (PVA) by assembling thiol-modified PVA (PVA-SH) and pyridyl disulfide-functionalized PVA (PVA-PD) multilayers on pancreatic islets surface.235 However, before the generation of the multilayered coating, the cell membrane surface was first functionalized with maleimide reaction groups using a maleimide-PEG-functionalized phospholipid (Mal-PEG-lipid). Then, thiol-modified PVA was covalently bound to the Mal-PEG-lipid modified cell surface through thiol-ene reaction. Stable PVA-based multilayers were then generated on cells surface by sequential deposition of PVA-SH and PVA-PD multilayers via thiol-disulfide exchange reaction. This methodology has great potential for improving the transplantation of pancreatic islets (Langerhans), possibly eliminating the need for self-monitoring and insulin injection in patients with insulin-dependent diabetes mellitus (type I).

Moreover, similar assemblies can be developed through the sequential adsorption of other polymers via covalent bonds.236, 237 More recently, the efficient assembly of biorthogonal, covalently stabilized polymer multilayers on pancreatic islet surfaces through the sequential deposition of PEG-azide-functionalized hyperbranched alginate (ALG) biopolymer (PEG-azido-ALG) and methyl-2-diphenylphosphinoterephthalate-functionalized poly(amido amine) (MDT-PAMAM) dendrimers via Staudinger ligation reaction was reported (Figure 6E).206 These researchers also compared the assembly process by purely resorting to covalent bonds with that co-mediated by covalent bonds and electrostatic interactions by manipulating the degree of positive charge of MDT-PAMAM via shielding with different amounts of glutaric anhydride (GA). The assemblies completely generated by covalent bonds showed a higher

degree of surface inhomogeneity in comparison with those obtained by combining electrostatic and covalent interactions. Such behavior was assigned to the inhomogeneity of the basement coating created after the adsorption of the PEG-azide layer via NHS coupling onto pancreatic islets when compared with the coating obtained via electrostatic adsorption of PAMAM dendrimers.

Another very interesting approach to overcome the cytotoxicity induced by most polycations and trigger cell surface engineering concerns the development of hydrogen bonded LbL films. Inspired by this approach yeast living cell surfaces were functionalized with nonionic and biocompatible hydrogen-bonded tannic acid (TA) and poly(N-vinylpyrrolidone) (PVPON) multilayers.238 However, before the deposition of the TA/PVPON multilayers, yeast cells were modified with a poly(ethyleneimine) (PEI) precursor layer to allow adhesion. It was found that, notwithstanding the cytotoxicity induced by the basement PEI monolayer, the assembly of at least (TA/PVPON)3 bilayers sustained a high cell viability for at least 6 days of culture. Such behavior was expected and is the result of the low exposure of cells to toxic polycations, as well as to the highly permeable LbL shell generated by hydrogen-bonded layers. Moreover, the fact that the TA, a natural polyphenol, entails antioxidant properties and is capable of scavenging free radicals, extensively contributes to protect cells against damage. In a similar report, researchers have developed a rapid, conformal, and stable coating of various types of living pancreatic islets with hydrogen-bonded TA/PVPON [239] and TA/poly(N-vinylcaprolactam) (PVCL) multilayers, [240] under physiological conditions, aiming at treating Type 1 diabetes. It was demonstrated that the hydrogen-bonded multilayers were more effective than electrostatic-driven LbL assemblies, keeping cell viability and functionality up to 7 days in culture. Moreover, hydrogen-bonded shells showed immunomodulatory cryoprotective properties, as demonstrated by the reduced pro-inflammatory cytokine production when incubated with macrophages and diabetogenic cells.

Adding to macromolecular cell surface modification, other strategies exploiting cell–materials interplay, namely, nano- and microparticle–cell interactions have been investigated for bottom-up tissue engineering as it will be showcased in the following sections.

3.2. Nanoparticle enabled bottom-up assemblies

3.2.1 Nanoparticle-coordinated Cell Clustering / Microtissue Aggregation

Nanoparticles are defined as colloidal materials with subcellular/sub-micrometer sizes ranging from 1 to 1000 nm.241, 242 In recent decades, these systems have attracted significant interest due to their numerous biomedical applications ranging from controlled delivery of hydrophilic/hydrophobic therapeutics, to multimodal bioimaging, biosensing and diagnostics.243, 244 Up-to-date, functional nanosystems have been formulated from a plethora of inorganic and organic materials including synthetic block-copolymers,245 natural origin biopolymers, and peptides/proteins that endow them with unique bioactivity, biocompatibility, biodegradability, and chemical versatility.246 This chemical flexibility and their high surface-to-volume ratio has been widely acknowledged and explored via precise chemical functionalization to imprint multifunctional features including cell/tissue targeting, adhesivity, and response to different stimuli.247, 248 So far, numerous types of nanoparticles have been fabricated to precisely adapt or respond to magnetic fields, temperature, ultrasound, pH/redox/hypoxic microenvironments, enzymes, light, among others.249, 250 This responsiveness may trigger changes in nanoparticles color, shape, size or originate complete disruption and prompt cargo release.251 Adding to this, nanoparticles physicochemical

properties have received significant focus due to their influence in the overall biological performance of these systems. Among these, particle size is particularly important at the nano–bio interface since multiscale interactions can be established with cells surface or intracellular organelles. Particles surface chemistry (i.e., charge, functionality, etc.) and shape (i.e., spherical, square, rod, elliptical, circular disks, etc.)252 are too recognized to play a critical role in cellular internalization kinetics and cytotoxicity.

Owing to their physicochemical properties, nanoparticles have also been recently explored in the context of bottom-up tissue engineering for promoting the assembly of cellular building blocks into higher order 3D clusters. The most recent studies have explored nanoparticles as membrane-adhesive mediators of cell aggregation or as structural supports for preformed 3D agglomerates. Different researchers have pursued this strategy in the form of either hyperbranched polyglycerols or dendrimeric intercellular linkers for rapidly forming multicellular structures.253, 254 Recently, IKVAV-functionalized polyamidoamine dendrimers coated with hyaluronic acid were used as adhesive particulates for rapidly compacting ASCs into 3D spheroid structures (Figure 7A).255 These membrane-binding particles effectively maintained spheroids compactness in presence of competitive adhesion from tissue culture plates, while enhancing their proliferation and paracrine secretion of angiogenic factors. The potential of this nanobridging phenomenon has also been illustrated in recent applications where researchers have successfully glued together biological tissues and accelerated wound closures.256, 257 Catechol-functionalized liposomes have also been recently used to promote tissue–tissue adhesion and could be an interesting technology for bridging cell-rich 3D modules.248 Conversely, polymeric nanoparticles adsorbed on cell membranes of spheroids can be used for slowing down spheroid spreading processes on adhesive substrates (Figure 7B).258 Controlling spheroid fusion and compartmentalization could be an interesting feature for bottom-up bioprinting-based approaches using 3D spheroids as unitary building blocks.

Attempting to explore nanoparticles for cell surface modification, Irvine's group has developed maleimide-functionalized liposomes that readily attach to thiol groups expressed at T-cell membrane proteins.260, 261 With this approach, researchers managed to immobilize nanoparticles loaded with immunomodulatory drugs at the surface of T-cells, allowing for specialized cargo delivery to the linked T-cells and thus modulating its behavior locally.261 More recently, smart protein nanogels that adhere to the plasma membrane were produced. These systems serve as reduction-responsive cell backpacks that release their cargo in the presence of the characteristic increase in redox activity at T-cells surfaces.262 In terms of augmenting cell aggregation, protein–protein interactions can also drive colloidal assembly, which could be a pathway for establishing nanoenabled cell-dense modules with nanoparticulated reservoirs of bioinstructive signals.263 On the other hand, a recent pioneering study focused on the use 20 nm carboxylated polystyrene nanoparticles as “nanostickers” capable of effectively maintaining single cells as large cohesive aggregates.264 In this study, a cadherin-depleted S180 murine cell line characterized for its extremely poor cell–cell adhesion was used to illustrate the potential of nanostickers to glue cells together into cell-rich structures.

Looking forward, advanced nanoconstructs anchored to cell membranes can extend their activity while function as bioreservoirs of small molecules/morphogens for driving stem cells differentiation or committing terminally differentiated cells to specific phenotypes. Previously, this elegant perspective of combining bioactive cell patterning and modular self-assembly was limited by a lack of affordable and efficient precision chemistry strategies. However, throughout the last decade, the maturing fields of nanotechnology, bioconjugate chemistry, and drug delivery have provided researchers with a remarkable toolbox of biodegradable/smart

biomaterials, sophisticated surface modification strategies and frameworks for bioactive controlled release. With the advent of biorthogonality, emerging cellular backpacks and cutting-edge membrane-engineering strategies (e.g., glycoengineering, liposomal fusion, boronic acid, or maleimide-based chemistries), could translate to the form of scaffold-free, clickable modular assemblies containing different ratios of bioactive nanoparticles for bottom-up tissue engineering.

Adding to cell-membrane bound strategies, biomaterial-in-cell strategies using nanoparticles that are readily internalized by cells have also been explored for on-demand cell self-aggregation into engineered 3D microtissues. Specifically, PLL magnetic nanoparticles (MNPs) that immediately respond to static magnetic fields have been employed to generate magnetically levitated multicellular 3T3-L1 preadipocyte microtissues within 24 h of culture.265 Interestingly, prolonged culture under adipogenic conditions resulted in the formation of 3D adipospheres exhibiting specific lipidic contents, thus evidencing biofunctionality. Also, levitated 3D spheroids derived from white adipose tissue (WAT) cells were able to recapitulate key aspects of WAT organogenesis. Positive and negative magnetophoresis could also be leveraged for assembling 3D cell-dense architectures (e.g., ring-shaped, three-pointed star, rectangular, etc.) under different magnet configurations as it will be further discussed.266 The use of magnetically active cells to generate 3D assemblies must however be subjected to further fundamental studies such as those already reported,267 since our understanding of the long-term effects in cells biofunctionality and the degradation of these nanoparticles in living dynamic microtissues is still in its infancy.

Even considering possible long-term effects, this technology remains highly attractive for more complex bottom-up tissue engineering. Recently, magnetic assembly was explored for precise fabrication of endothelial 3D spheroids and for their inclusion into prefabricated magnetic vascular tree-like templates. This magnetic confinement and prolonged culture induced 3D endothelial multicellular spheroids maturation and fusion into a higher order construct that exhibited morphologic and phenotypic stability.268 The manipulation of spheroids into user-defined shapes/patterns was explored by using a disruptive approach that brought forward a paradigm shift in magnetic-based spheroid manipulation.259 This involved the generation of Janus spheroids where cells and particles are segregated into distinct domains in a ECM-like microenvironment, aiming to reduce MNPs internalization and thereby avoid possible adverse effects on cell viability (Figure 7D). The resulting Janus constructs present lower MNPs internalization in comparison to standard spheroids and demonstrated the ability to fuse together into more complex 3D vascular tissue tube constructs via magnetic guidance.259 It was also discovered that the strength of the magnet largely affected 3D spheroids fusion into the desired tubular shape, with constructs established with a weak magnet (i.e., 10% of maximum magnetic field) exhibiting faster inner ring contraction than their counterparts (Figure 7Di,ii).

3.2.2 Bioinstructive and 3D bioprocessed nanoparticle-based assemblies

Beyond engineering cells surface and operating as cellular aggregators, nanoparticles are also attractive for imparting different bioinstructive cues (e.g., growth factors, cytokines, mechanical, and electric/magnetic stimuli), further enabling engineered microtissues 3D maturation and improving biofunctionality.269, 270 Particularly, the incorporation of nanoparticles with stimuli-responsive features in bottom-up bioarchitectures development is highly valuable owing to their potential for loading different biochemical cargos and for spatiotemporally controlling biophysical signals presentation to cellular building blocks.271

In this context, Laponite nanosilicates (Laponite is a trademark of the company BYK Additives Ltd.) have been recently employed to generate bioinstructive gradients of different growth factors (e.g., VEGF, FGF, and PDGF) for promoting endothelial sprouting, or for establishing osteochondral interfaces in cell–biomaterial assemblies (via rhBMP-2 and TGF-β3).272, 273 In another elegant approach, researchers have exploited the potential of magneto-responsive nanoparticles for patterning biochemical gradients (i.e., BMP-2) in human MSCs–agarose scaffolds and established robust osteochondral constructs in vitro.274 Strikingly, this strategy resulted in spatially controlled osteogenic gene expression and tissue mineralization, as well as the formation of a bone–cartilage interface after 28 days of maturation in vitro. Apart from magnetism, temperature and light (e.g., visible, near-infrared, etc.) also represent promising alternatives for on-demand generation of gradients of bioinstructive molecules that ultimately guide cell differentiation and modulate 3D microtissues physiology in vitro.275-277 Recently, mechanoresponsive nanoparticles have too been formulated to provide bioactive molecules presentation upon deformation by biomechanical forces, thus unlocking the possibility to engineer constructs with biomechano-interactive signals similar to those naturally present in living tissues.278 These studies represent a stepping stone in highlighting the versatility of stimuli-responsive nanoparticles for providing biochemical gradients in tissue-scale constructs, evidencing possible future trends in this field.

Adding to their transported bioactive cargo, nanomaterials' physicochemical features can also be exploited as modulation mechanisms to develop and mature on-demand 3D microtissues with complex biofunctionality. This has been the case of load-bearing and complex electroactive tissues (e.g., cardiac, nerve, and skeletal muscle).279 In this regard, several electrically conductive nanomaterials, such as graphene, carbon nanotubes, and silicon/gold nanowires, provided promising outcomes in cardiac tissue engineering.280, 281 By impregnating gold nanowires in alginate scaffolds researchers were able to enhance the electrical interconnectivity of engineered cardiac 3D microtissues and improve cardiomyocytes phenotype, expression of contractile function markers and ability to generate synchronous contractions.282 More recently, incorporation of silicon nanowires in human induced pluripotent stem-cell-derived cardiomyocytes enabled the assembly of electrically conductive cardiac 3D spheroids with enhanced cell–cell junctions, contractile machinery maturation, and decreased spontaneous beat rate, which could be beneficial for reducing arrhythmia post-transplantation.283 Also, nanoparticles comprising conducting polymers (e.g., polypyrrole) were employed to trigger biomolecules delivery upon stimulation with weak external electrical fields, that are known to impact cell processes in angiogenesis, cardiomyogenesis, neurogenesis, and osteogenesis and could thus enable on-demand microtissue maturation along time.284, 285

Notwithstanding their potential for bottom-up tissue engineering, most of these studies describe the use of overly simplistic nanoparticle containing scaffolds, being unable to fully recapitulate native ECM composition, nor tissues complex architecture or anatomical scale. To overcome such drawbacks, researchers are actively developing nanoparticle functionalized bioinks and exploiting advanced additive manufacturing techniques to build-up 3D microtissue constructs with tailored microenvironments allied to biospecific designs.286

Nanoparticles incorporation in bioinks is highly valuable as it can improve the mechanical performance of natural-based biomaterials (e.g., gelatin and fibrin)286 and allows bioactive cues' tailored presentation, as well as to introduce electrical properties in the final assemblies.286, 287 Interestingly, it is being increasingly recognized that nanoparticles inclusion in bioinks also improves shear-thinning, a fundamental aspect for enhancing printability and resolution (Figure 8A).288, 289 From the plethora of nanomaterials currently being pursued in 3D nano-bioprinting strategies, Laponite nanoparticles are widely explored

due to their innate bioactivity (i.e., osteogenic/angiogenic), mechanical resistance, and sustained delivery of bioinstructive signals (e.g., growth factors).290, 291 Recent evidences corroborate that Laponite nanosilicates incorporation in PEG-based photocrosslinkable bioinks enabled sustained VEGF delivery which directed rapid HUVECs migration toward 3D bioprinted constructs.292 Such nanoengineered Laponite/PEG-diacrylate bioinks displayed improved shear-thinning properties, high mechanical stability, increased printing fidelity, and suitable cytocompatibility post-crosslinking.293 An improvement to this design was achieved by incorporating nanosized Laponite in GelMA/κ-carrageenan and exploiting nanoengineered ionic covalent entanglement (NICE) in a bioink with innate bioactivity (i.e., GelMA cell adhesive domains).294 With this synergistic approach, it was possible to bioprint large vertical structures and different human-scale 3D anatomical structures with improved mechanical strength, toughness and elasticity (Figure 8B). Cells laden in such bioprinted constructs also maintained high cell viability over 120 days, indicating the potential of this approach for long-term bottom-up tissue engineering applications.

Other silica-based nanoparticles with cationic surface charge have been exploited to improve the printability and shape fidelity of anionic polysaccharide bioinks (i.e., alginate/gellan gum) via the establishment of electrostatic interactions. This approach resulted in enhanced mechanical robustness of large-scale ear-shaped 3D constructs and high cell viability. Importantly, the observed mechanical improvement was highly dependent on polymers molecular weight, nanoparticles surface chemistry, concentration and size, being mainly observed for particles (<100 nm).298 Such indicates that various parameters must be carefully investigated to achieve optimal mechanical properties of printed constructs always taking as reference those of the native tissues one aims to recapitulate.299

Recently, the use of inorganic nanoparticles to endow cell-laden bioinks with electric conductivity has been explored for materialized 3D bioprinted constructs for application in cardiac tissue engineering. In this context, researchers explored the development of an electroactive bioink comprising inorganic gold nanorods (34 × 25 nm) and GelMA hydrogel. Gold nanoparticles inclusion improved bioink shear-thinning properties and printability, while also enhanced cardiac cell adhesion/organization versus its pristine GelMA counterpart (Figure 8C).295 In addition, such gold nanocomposite bioink could install electroconductive bridges connecting adjacent cardiac bundles and promoted electrical communication in 3D printed constructs. This resulted in increased cell–cell interactions, cardiac phenotypic expression as well as synchronized contractile frequency of bioprinted cardiac constructs (Figure 8C). Similarly, an alginate-based nanostructured bioink with embedded silver nanoparticles was used for bioprinting chondrocytes into 3D bionic ears, which could successfully receive electromagnetic signals (Figure 8D).296 These are highly elegant approaches to generate electroactive microtissue constructs, nevertheless their in vivo applicability and long-term biocompatibility in cardiac microenvironment is an important aspect to be further evaluated.

Adding to this, magnetic iron nanoparticles were exploited to recapitulate the anisotropy of human cartilage in bottom-up engineered 3D constructs.300 Such nanomaterials have been used to direct collagen alignment during bioprinting, thus enabling the fabrication of multilayered chondrocyte-laden constructs with intercalating layers of aligned/random collagen fibers. Interestingly, bioprinting of such constructs led to enhanced collagen I and II expression, highlighting the importance of architectural control when envisioning to recapitulate intrinsically anisotropic human tissues in bottom-up engineered cell–biomaterial assemblies.300 This attention on faithfully recapitulating tissues complex architecture using nanoparticles in the bioprinting process was further demonstrated by the inclusion of melanin nanoparticles (≈500 nm) in a silk fibroin/PEG-acrylate nanoengineered bioink. In this elegant

strategy melanin nanoparticles innate light absorption was hypothesized to improve light-induced 3D bioprinting resolution in the z-axis while assuring embedded NIH/3T3 fibroblasts viability.297 By reducing light penetration depth, nanoparticles enabled 3D projection stereolithography bioprinting of otherwise impracticable empty/tilted structures such as tubes or stairs, and enabled the fabrication of fully perfusable vascular networks with high printing precision (Figure 8E).

In practice, the described bottom-up engineering technologies that are based on, or include nanomaterials, are envisioned to assist researchers in modulating mechanical properties and the local biochemical microenvironment/mechanical cues, allowing one to better guide living microtissues morphogenesis and maturation during in vitro culture before in vivo application. Advances in cell-membrane-functionalized nanoparticles,301 may further contribute for selective particle–cell docking and for a higher control over cell–cell spatial patterning in co-cultured 3D aggregates in a foreseeable future. Adding to these opportunities, it has been recently demonstrated that nanoparticles could potentially function as nanosensors for monitoring the early immune response to implanted tissue engineered constructs,302 or for mapping oxygen distribution/dynamics within 3D bioprinted constructs.303 Generating microtissues with built-in biocompatible nanosensors could be essential for further understanding and noninvasively monitor the physiological changes upon their implantation in real-time.

3.3. Microparticle enabled bottom-up assemblies

3.3.1. Microparticle-coordinated Cell Clustering / Microtissue Aggregation

Microparticles, i.e., structures ranging from 1 to 1000 μm, have for long been the platform of choice for various biomedical applications,304, 305 with numerous reports exploring microcarrier formulations for focal delivery and controlled release of therapeutics, as injectable tissue-defect fillers, as biosensing tools, or as cell-expansion systems in static/dynamic in vitro cultures.306, 307

Along the last decades, the exponential evolution of precision particle fabrication techniques (i.e., electrodynamic jetting, molding/microarrays,308 or microfluidics)309, 310 has contributed for improving the manufacture of microparticles with tailored surface chemistry, degradation and porosity.311 Particulates with variable surface topography, stiffness, tunable size, and complex shapes have also been successfully engineered.312, 313 This technological progress, combined with particles physicochemical versatility, have provided the foundation for also exploring microparticles as injectable cell-encapsulating platforms and for in vitro disease modeling.84, 314 More recent endeavors have focused on exploring microparticles as building blocks for modular bottom-up tissue engineering by taking advantage of their role as orchestrators of cellular aggregation and of their bioinstructive cues for 3D microtissues maturation.306, 311, 315 We will focus on cell–particle surface interactions at the material–bio interface rather than cell encapsulation which will be further discussed in hydrogel-based platforms.

In this sense, the establishment of cell–microparticle unitary blocks and their progression into modular 3D aggregates has been materialized by using cell-scaled solid microparticles as supporting/adhesive platforms (i.e., >2 μm to several hundred micrometers), as opposite to smaller particles which may be extensively internalized by cells when no cell-membrane anchoring technology is installed.315 The control over microparticle–cell aggregates size and morphology is key when envisioning 3D microtissues build-up and is highly dependent on

microparticle formulations monodispersity,316 cell density,84 and culture conditions (i.e., static/dynamic).317 3D cell–microparticle assemblies biointegration and overall biofunctionality is also vital in the context of bottom-up tissue engineering and recognized to be largely influenced by: i) cells and microparticles spatial distribution/density, ii) the existence of cell–particle anchoring ligands (i.e., antibodies, ECM mimetic proteins/biopolymers, etc.),305 and iii) the presence of bioinstructive morphogens (e.g., growth factors, cytokines, etc.).318 These fundamental design considerations and processing know-how have enabled researchers to fabricate 3D constructs where particle–cells adhesion is random or directed.319 Both approaches can warrant the application of bioengineered microtissues in bottom-up tissue engineering and regenerative medicine.

Random cellular adhesion to microfabricated spherical particles is by far the most explored alternative owing to its simplicity, low cost, and possibility to produce dense 3D microtissues which guide cell fate.320 Using this concept, researchers have explored gelatin and heparin microparticles for loading BMP-4/noggin bioactive molecules and to support the establishment of pluripotent stem cell agglomerates in vitro. During culture, the controlled release of soluble mediators actively bioinstructed 3D cellular aggregates toward specific phenotypes, thus demonstrating the advantages of using microparticles as cell-adhesive and delivery platforms.321 In a similar approach, the controlled release of TGF-β1 from gelatin microparticles impregnated in human-periosteum-derived cells (hPDCs) micromasses induced significant cellular differentiation toward chondrogenic lineage and the expression of chondrogenic biomarkers.322 Microparticle-guided 3D microtissues random assembly was also recently explored through the fabrication of surface-decorated microparticles with human E-cadherin fusion protein cell–cell adhesion biomimetic ligands that improved cells proliferation and formation of dense MSCs-rich 3D aggregates (Figure 9A).323 However, when envisioning in vitro generated 3D microtissues implantation, the establishment of highly dense constructs is generally deleterious due to decreased oxygen/nutrients diffusion. Recent efforts have been made toward surpassing these issues through the development of VEGF165-functionalized microcarriers, or of oxygen releasing microparticles that increased the viability of 3D cellular masses cultured in microparticulated platforms.324, 325 The latter is a particularly elegant approach that has proven valuable for providing a timely supply of oxygen to microparticle adhered human-periosteal-derived cells which preserved their osteogenic differentiation even under hypoxia.325
Adding to these technologies, open porous microparticle platforms have also received a significant focus for 3D microtissues assembly owing to their improved gases/nutrients and waste metabolites exchange with the surrounding microenvironment. Recently microporous particles technology was advanced with the fabrication of highly open porous polyhydroxyalkanoate (PHA) microspheres (OPMs; 300–360 μm in diameter, Figure 9B), which are able to harbor stem cells in their interconnected network while also assuring a higher cell viability and continuous proliferation in comparison to their less porous counterparts.326

Aiming to further control microtissues shape, researchers used microarray platforms to promote the fusion of cell–particle microaggregates as an attempt to generate geometrically defined higher order assemblies.320 This pooling and spatial confinement resulted in the bottom-up establishment of macrosized and shape defined tissue constructs (Figure 9C). Programmed particle–cell microagglomerates confinement and directed assembly into larger assemblies can also be established via magnetism, sound, mechanical forces, and light.319, 327

Despite these exciting advances, assuring a precise control over cells adhesion in specific microparticle regions remains remarkably challenging. While the dynamic nature of microparticles–cells interactions and aggregations allows researchers to explore ex vivo 3D

microtissues assembly, due to its underlying concepts such interactions are inevitably random and with limited control over cell-specific adhesion. Recent studies have reported exciting results on the development of microparticles displaying anisotropic/heterogenic regions for programmed/guided cell adhesion. In particular, spatially designed cellular microenvironments in spherical particles volume have been generated by using segmented microcapillaries to eject microdroplets containing multiple types of collagen and sodium alginates.328, 329 This resulted in the fabrication of anisotropic microspheres with hemispheres containing two ECM microenvironments with different mechanical properties. On another approach, biomimetic anisotropic PCL particles (≈70 μm) exhibiting fuzzy and smooth surfaces in either side were used to selectively adhere fibroblasts and endothelial cells (Figure 9D). In vitro cell culture of endothelial cells added stepwise to Janus particles smooth side, induced different prostacyclin secretion by endothelial cells. These particles demonstrated higher affinity toward fibroblasts as opposite to hepatocytes, opening new avenues for cell isolation based solely on particles morphological features.330 Selective cells isolation in antibody-functionalized microparticles has also been successfully demonstrated, further contributing toward the toolbox of available approaches for biospecific control over cell–particle adhesion.314 In the long-run such strategies can be valuable for assembly of heterogeneous microtissues in which the build-up process is self-regulated by cells spatial distribution on particles surface. One could hypothesize that combining this approach with genetic cell surface engineering could yield living constructs with bioregulated architectures.

3.3.2 Bioinstructive and 3D bioprocessed microparticle-based assemblies

As aforementioned, it is well established that the orchestrated presentation of different bioinstructive cues (e.g., growth factors, cytokines, mechanical, magnetic/electric, etc.), either via their spatiotemporally controlled presentation or in the form of biochemical gradients, is also essential for providing a close-to native microenvironment and further potentiating engineered microtissue maturation in vitro.331 In this sense, besides functioning as building blocks for cellular aggregation and microtissues maturation, microparticles have also been employed as delivery systems for controlled release of bioactive molecules in bottom-up cell–biomaterial assemblies. This strategy has been successful in guiding the fate of microparticle-adhered cell unitary blocks, or through incorporation in cell-laden bioinks. The latter is particularly valuable, since the direct incorporation of growth factors in bioinks results in rapid diffusion, often reducing bioactive molecules overall concentration comparing to that achieved with sustained presentation via microparticle-mediated controlled delivery.332 Researchers have explored these microparticles features for instance by incorporating gelatin microparticles loaded with either VEGF or BMP-2 into bioinks for achieving accelerated osteodifferentiation and regional angiogenesis on bioprinted 3D living constructs with well-defined architecture.333, 334 Adding to this, microparticles loaded with growth factor/cytokine rich cell-derived secretomes have also been employed as bioinstructive building blocks and are currently being envisioned for potentiating advanced 3D bioprinting strategies in the future.335

In addition, to biochemical signals, the inclusion of mechanical cues in bottom-up engineered constructs via microparticles inclusion was also fruitfully demonstrated in recent works. An elegant approach, involved MSC-laden PLA microparticles embedding within GelMA-gellan gum bioinks, functioning as unitary building blocks for providing both cellular components and mechanical reinforcement. This approach increased up to twofold the compression modulus of bioprinted 3D constructs.336 On a different setup, β-tricalcium phosphate microparticle incorporation were used for tuning 3D constructs stiffness,337 as well as to induce osteodifferentiation and mimicking the mineral fraction present in calcified cartilage.338, 339

The inclusion of cell-laden microparticles in bioinks developed for advanced 3D biofabrication adds a layer of processability to these building blocks and allows the engineering of microparticle-based living constructs with biospecific tissue designs that would be otherwise difficult to obtain through other bottom-up processing technologies. However, it is important to emphasize that including dense polymeric microparticles in living tissue constructs is an unnatural approach and may generate nutrient/oxygen diffusion limitations, during long-term maturation of microtissues in vitro, an important parameter that must be considered at early design stages when modulating cell–microparticles density/concentration.

Apart from particles for bottom-up tissue engineering approaches, also cell-laden hydrogels processed as nano/microgel particles or fibers provide a seamless supporting matrix to build-up and mature 3D microtissues as it will be discussed in the following sections.

3.4. Hydrogel-based platforms for biomimetic bottom-up assembly

3.4.1. Cell-laden ECM mimetic hydrogels

Utilizing biomaterial-based ECM mimicking matrices for pursuing tissue-specific features and biomolecular gradients unravels the potential to achieve high-quality biological modules with flexible and augmented biofunctionality that can support cell adhesion, proliferation and ultimately de novo tissue morphogenesis. In essence, hydrogels are highly hydrated and self-supporting 3D networks with porous or fibrillar-like internal architectures similar to native ECM. These building blocks can be based on: i) natural sources, i.e., self-assembling peptides, engineered proteins, polysaccharides, and decellularized ECM; ii) synthetic polymeric materials and iii) hybrid hydrogels arising from the combination of different monomers/nanocomposites in the hydrogel network. The organization, composition, and structural features of the ECM vary significantly across tissues, hence, a universal building block may be unrealistic.340 In a bottom-up perspective, hydrogels are advantageous due to their flexible design nature, derived from their polymeric framework and its amenability to be chemically tailored to better reproduce key ECM features (e.g., adhesion site density, biomolecule immobilization, matrix stiffness, stretchability, degradability, etc.). Moreover, their ease for obtaining cell-laden structures, sustaining proliferation, as well as providing 4D bioarchitectures that can be altered and matured through embedded cells activity or by specific stimuli are highly desirable in such bioengineering strategies.

The specificity of ECM-like microenvironments materialized through the encapsulation of living healthy and fully functional cells poses several challenges to the development of spatially controlled cell-laden hydrogels: i) the effective three-dimensionality of the intended patterns that ii) simultaneously enable the compatibility of the 3D-assembled hydrogels with cell encapsulation via cell adhesion, but that can also direct the fate and function of the engineered bioarchitecture. By now, the importance of scaling-up cell–matrix interactions to the third dimension is unquestionable because it affects the biological activity of the final construct.341 Despite the unambiguous importance of exposing cells to 3D-controlled cues, the patterning of hydrogel matrices has been mostly achieved solely on a 2D perspective and frequently of a multistep nature or resorting to top-down reactions based on photolithographic methods. For example, photosensitive S-2-nitrobenzyl-cysteine moieties immobilized on a nonadhesive agarose matrix allow for UV-induced uncaging of sulfhydryl groups at specific regions, where maleimide-terminated peptides containing the fibronectin binding domain can be precisely tethered to the matrix framework via thiol-ene up to a 1.5 mm depth.342 In this way, cell adhesion can be spatially controlled, unlike in tissue-derived materials (e.g., collagen and fibrin), which contain randomly dispersed cell adhesion domains. Currently, with emerging

multiphoton-based lithography, researchers have now successfully reported true 3D patterning of multiple growth factors with subcellular precision and interconnectivity (Figure 10A).342, 343 Beyond that, orthogonal photodegradation has been exploited to engineer cell-laden hydrogels with intricate and perfusable cavities and microchannels with user-controlled shapes and location (Figure 10B–E).344-346 Alternatively, in a truly biomimetic approach, Culver and co-workers have exploited two-photon lithography for manufacturing cell-laden PEG-based hydrogels with precise 3D cell immobilization based on native tissue sections as biological blueprints.347 These hydrogels were rendered cell-degradable by imparting the PEG-diacrylate backbone with matrix metalloproteinase-sensitive peptide (GGPQGIWGQGK). Here, the researchers imaged cross-sections of different tissues (e.g., retina, cerebral cortex, heart, etc.) and were able to precisely match the hydrogel patterning to the original tissue vascular bed. This image-guided 3D photopatterning successfully recapitulated the neural stem cell niche seen in the subependymal zone of mice (Figure 10F). The versatility of this technology allowed them to pattern distinct bioactive peptides on regions of interest and accurately recreating vascular and neural progenitor staining of the biological tissue section. Moreover, the advent of photoinitiator-free strategies based on the [2 + 2] cycloaddition of maleimide groups at physiological conditions will foster the development of truly multiphoton click chemistry reactions for engineering cell microenvironment niches in hydrogel structures.348, 349
Wiley-VCH.
Despite the relevance of top-down patterning techniques that enable the precise control of hydrogels chemistry on a 3D space and over time, the self-assembly of precisely designed hydrogels through spontaneous intermolecular interactions benefiting from easy injectability and tailoring of biophysical properties of ECM-mimetic structures could further potentiate these applications.221, 350 However, contrarily to the abovementioned examples of top-down patterning of 3D hydrogels, reports of exclusively bottom-up hydrogel assembly strategies targeting the precise positioning of biochemical patterns and gradients in 3D are still limited. Recent works have begun to utilize molecular self-assembly to generate hydrogel 3D bioarchitectures capable of continuously expanding their network similar to the growth of living tissues in nature.351 Here, instead of growth factors, researchers manipulated oxygen concentration to engineer complex 3D shapes and also intricate out-of-plane buckling by inhibiting growth at specific regions. This is the first study for generating self-assembled hydrogel architectures inspired by the bottom-up morphogenesis process of living tissues, but cell-friendly conditions will still need to be attained for achieving relevant cell-laden hydrogel structures.

The ability of synthetic or recombinant short peptide sequences to function as hydrogelators has been used as the driving principle of one of the most commonly reported strategies to prepare bottom-up self-assembled hydrogels.350, 352-355 The use of amino acid sequences is an interesting approach due to their possible similarity with native ECM features capable of driving cell adhesion and other cell response phenomena, which include cell migration, apoptosis, mechanotransduction, vascularization, among others. Moreover, most of reported amino acid sequences used for the preparation of hydrogels are widely considered biocompatible, potentially biodegradable and nonimmunogenic.356 The mechanism of hydrogelation of peptide blocks is generally regulated by noncovalent interactions which drive their assembly into fibrous structures that entangle in the form of 3D highly hydrated solid structures in the presence of stimuli such as ions, enzymes, temperature, pH changes or exposure to light.356-359 Although the mechanisms driving the formation of supramolecular hydrogels are mostly based on noncovalent bonds, researchers' recently reported the assembly of amphiphilic peptides through nonweak interactions convertible to covalent bonding.360 Self-assembled networks based on nanofiber peptides include vast applications on neural, myocardial and wound regeneration.361-363 The cell-friendly conditions under which the

spontaneous assembly occurs, along with the ability to tailor the biochemical composition to mimic ECM cues, enabled the exploitation of bottom-up self-assembled peptide hydrogels as promising cell encapsulating matrices. The dispersion of hepatocyte-like spheroids in a RAD16-I peptide hydrogel showed that the generated 3D hydrogel significantly tailored cellular proliferation and presented matured differentiation profiles.364 Indeed, it has been recently disclosed that the bioactivity of amphiphile mimetic peptides (e.g., brain-derived neurotrophic factor, BDNF) can be augmented in 3D hydrogels due to conformationally improved peptide–cell interactions in these systems, which not only encourages cell infiltration but increases functional maturation of the construct.365 A co-assembly system of peptide amphiphiles designed to form nanofibers targeting cartilage repair was also proven promising for tissue regeneration based on a cell encapsulation approach.366 Indeed, the decoration of peptide segments with the TGF-β1 binding epitope (i.e., HSNGLPL sequence), which is exposed in high density to encapsulated cells and damaged tissues due to the collapsing of the hydrophobic alkyl chains in the amphiphilic molecule, promoted the chondrogenic differentiation of mesenchymal stem cells encapsulated within the hydrogel and boosted the formation of hyaline cartilage in osteochondral defects in in vivo rabbit models. Hydrogels based on other peptide amphiphiles with bioactive domains as IKVAV, or with a tenascin-C-mimetic configuration, showed potential as cell encapsulation and regeneration matrices for inner ear and neural repair.367-370

Native tissues can display different degrees of anisotropy and spatially varying stiffness, that are key players in guiding cell migration, organization, and function.340 Beyond their flexibility for designing self-assembled hydrogels with tunable biochemical and mechanical features, peptide amphiphiles can be also explored for developing biomimetic constructs. In an innovative study, researchers have exploited a C16G3RGDS peptide amphiphile for programing cell-driven contraction of compressed collagen hydrogels in defined regions.371 Here, cells served as bioactuators capable of mechanically transforming hydrogels into curved structures, thus remodeling the dense collagen stroma toward a more native-like organization found in human cornea. In fact, these 4D self-curved tissues presented superior ECM organization and orthogonally aligned cells over planar substrates. Alternatively, an interesting study designed by DeForest group exploited fusion proteins as hydrogel crosslinkers to fabricate bioarchictectures that respond to user-defined stimuli such as calcium (e.g., calmodulin-based proteins) and light (e.g., photosensitive light, oxygen, and voltage sensing domain 2, LOV2).372 In this study, the unique semisynthetic protein-PEG hydrogel matrices yielded tunable stiffness-patternable features which could be cycled on demand to investigate 3D cellular response to cyclic loading, a key aspect that native ECM is subjected to but was yet to be replicated in cell-laden hydrogel constructs (Figure 10G). In another sophisticated work, researchers have manufactured core–shell hyaluronic-based hydrogels with distinct biochemical and biophysical features.373 Cell adhesion site density, enzymatic degradability, and mechanical stiffness could be hierarchically presented in a core–shell bioarchitecture by varying the macromer/crosslinker ratios and timing of introduction of the interfacial crosslinking agents that covalently functionalized hydrogels at the liquid-gel interface. The biorthogonal tetrazine-trans-cyclooctene ligation here used occurs in aqueous conditions with extremely fast kinetics and without using any specialized equipment, catalyst, or triggering stimuli. The responses of human mesenchymal stem cells encapsulated in these hydrogels were assessed according to the different properties of the core–shell bioarchitectures. For homogenous (i.e., core = shell) stiff hydrogels, cells remained spherical ≈7 days in those nondegradable and nonadhesive platforms, whereas MMP-degradable gels with few adhesion sites were sufficient to foster cells spreading. The researchers could then assemble heterogenous hydrogels with spatially resolved properties, such as stiff-to-soft transitions from shell to core, as well as increasing MMP degradability or adhesion site density toward the core. Recently, the

same group has now devised multilayered hydrogel channels with three different cell populations spatially patterned across its interfaces, thus yielding functional bioarchitectures more closely resembling native arteries.374 Another relevant strategy to obtain cellularly graded hydrogels exploits the self-healing phenomena that is characteristic of dynamic covalent hydrogel networks. Using this approach cell-laden hydrogels based on 2-acrylamidophenylboronic acid and poly(vinyl alcohol), which readily self-assembled in aqueous conditions were successfully fabricated.373 Due to the dynamic nature of boronic-diol bonds, these hydrogels exhibited significant self-healing capacity, which was exploited for establishing a gradient of two different cell types (e.g., lung fibroblasts and breast cancer cells) initially cultured separately on different hydrogels. After cutting each cell-laden hydrogel block, two halves were merged together due to their natural self-healing features and simultaneous cell migration could be observed across the healed interface of the newly formed binary hydrogel. This current design could be further improved by including ECM-mimetic domains eliciting adhesion or matrix remodeling. In the future, the preparation of cell-laden hydrogels with distinct customizable microenvironments will undoubtedly be essential for manufacturing advanced bottom-up bioarchitectures.

Noncovalent interactions (e.g., host–guest inclusion complexes, avidin–biotin, and nucleotide base pairs) are attractive not only for self-assembling bottom-up hydrogels, but also because they can be engineered to endow the hydrogel networks with unique features owing to its reversible and adaptive nature. In host–guest interactions, the binding readiness between opposing pairs is convenient because it partially recapitulates the constant adaptiveness of native ECM and embedded cells, thus being promising for modulating the biochemical 3D environment.375 For instance, the well-known host–guest β-cyclodextrin/adamantane pair can be used for tackling the dynamic mechano-regulation of cell–substrate interactions.376 Adjusting ratios of host/guest monomers allowed the precise tailoring of the initial mechanical properties of the hydrogel, while the subsequent addition of free competing host molecules enabled softening of the material on-demand. In comparison to previously reported systems based on UV irradiation or temperature as sources of mechanomodulation, the authors hypothesize that this host–guest system could allow handling cells with high viability as compared to potentially damaging stimuli. Synthetic adamantane and cyclodextrin derivatives are commercially available and can be easily installed into a plethora of polymers, including polysaccharides such as hyaluronic acid that are frequently used for designing cell-bearing bottom-up hydrogels with shear-thinning properties.377, 378 The ability of such hydrogels to withstand high deformations has seldom been studied. To this end, researchers have explored acrylated-β-cyclodextrin and adamantane-hyaluronic acid as macro-crosslinkers of ductile polymers prepared through the polymerization of N,N-dimethylacrylamide monomers.379 This novel strategy yielded highly swollen cell-laden hydrogels with outstanding resistance to fatigue, i.e., up to 80% compressive deformation for over 1000 cycles. The high viability observed for encapsulated cells after deformation cycles makes these hydrogels promising materials for mechanostimulation and interesting candidates for reproducing tissues subjected to cyclic deformation such as cartilage.

Alternatively, natural host–guest pairs like streptavidin–biotin have also enabled the processing of cell-laden structures.377, 380 For example, living cells modified with avidin were used as hydrogel crosslinkers through direct interaction with biotinylated 1,4-benyl-dicarbonxamide supramolecular gelators capable of being easily modified and with the ability to self-assemble.380 The stability achieved in this system, in opposition to the comparatively poor binding verified on polymeric molecules, drove selective and faster proliferation of different cell types. However, drawbacks associated with the avidin–biotin pair and cyclodextrin-based inclusion complexes include the difficult scale-up production of molecules modified with the

streptavidin–biotin pair and the poor in vivo application of cyclodextrin-based pairs due to low binding affinity.381 To overcome such limitations, Kim's group suggested novel supramolecular hydrogel assemblies based on hyaluronic acid modified with pumpkin-shaped cucurbit[6]uril (CB[6]) or diaminohexane groups.381 The highly selective and strong CB[6]–diaminohexane interaction allowed cell encapsulation on self-assembled hydrogels,382 which could then be later modularly modified by treating the hydrogel with multifunctional tags-CB[6], which included RGD domains to promote cell adhesion, FITC probes for in vivo detection,381 or TGF-β3 and dexamethasone to regulate mesenchymal stem cells' chondrogenic differentiation.383 Other interesting systems can comprise dock-and-lock (DnL) mechanisms based on engineered proteins and anchoring proteins attached to multiarm crosslinker polymers, which can instantly lock onto recombinant “docking” domains under physiological conditions.384 Hydrogels prepared using this chemistry displayed a remarkable ability to recover from deformation cycles with self-healing properties independently from mechanical disruption, while enabling cytocompatible encapsulation and injection of mesenchymal stem cells.

Owing to their several attractive features, including controllable sequences, precise recognition, and low toxicity, DNA building blocks have evolved considerably in the last decades for designing advanced hydrogel systems.385 However, hydrogels based on spontaneous nucleotide pairing are still scarce, and the majority of reported technologies are dependent on enzymes,386 pH changes and temperature variations to promote DNA fragmentation.387 In fact, the decoration of macromolecules (e.g., polymeric chains and peptide sequences) with complementary nucleotide sequences has rendered the most effective and stimulus-free cell-compatible self-assembling of hydrogel micro- and macroscopic units.388, 389 In this context, progress in 3D bioprinting enabled by DNA fragments hybridization has progressed significantly over the last years. Researchers have developed a novel class of bioinks based on a polypeptide–DNA conjugate (bioink A) and complementary DNA linkers (bioink B).389 Upon co-injection under physiological conditions both inks immediately formed a stable hydrogel that enabled high cell viability and the precise printing of multilayered structures with any intended shape. In addition, due to its polypeptide and nucleic backbone, the millimeter-sized bioarchitectures were naturally degradable through the action of nucleases or proteases. Recently, carboxymethylcellulose-based hydrogels crosslinked by self-complementary DNA interactions (duplex nucleic acids) and donor–acceptor (dopamine-bipyridinium) redox-mediated switchable bonds yielded stimuli-responsive networks with dynamic stiffness and simultaneous self-healing and shape memory properties.390 Double network hydrogels that self-assemble entirely from noncovalent interactions, i.e., DNA hybridization and host–guest inclusion complexes between cucurbit[8]uril (CB) and phenylalanine functionalized carboxymethylcellulose have also been reported.391 The resulting fully interpenetrating supramolecular network exhibited remarkable stretchability, ductility, shear-thinning and thixotropic properties. Moreover, the use of DNA motifs for programming constructs self-assembly is a unique strategy because such DNA motifs can potentially be recognized and processed by embedded cells or enzymes.392 Hence, they can signal for the enzymatic machinery of cell lysates and instruct them to synthesize functional proteins, thus assembling biorelevant protein-producing hydrogels.393

Considering the versatility and interchangeable features of cell–biomaterial hydrogel assemblies, their combination into higher order 3D bioarchitectures with well-defined and complex geometries that recapitulate the anatomic features of different human tissues is envisioned to open new avenues toward their application in numerous clinical scenarios. This potential is starting to be materialized with the advent of biofabrication technologies that allow

cells and biomaterials precise processing and positioning under conditions that assure maximum viability and biofunctionality.

3.4.2 Advanced 3D bioprocessed cell-laden hydrogels

The latest advances obtained in cell-laden hydrogel bioprinting technologies have enabled the development of extremely sophisticated cell-hydrogel living architectures in native ECM-mimetic microenvironments laden with multiple cell components and exhibiting evermore biospecific designs, as well as human anatomic-scale. Aiming to fabricate such constructs, researchers have produced pie-shaped alginate hydrogels with three cell types (i.e., amniotic-fluid-derived stem cells, smooth muscle cells, and aortic endothelial cells), containing spatially defined heterogeneous multiple cell distribution across the bioprinted construct by using an in-house modified thermal jet printer.394 Inkjet bioprinting takes advantage from picoliter drop generation on-demand and high printing speeds for manufacturing 3D cell-laden hydrogel building blocks with high controlled spatial deposition of cells and biomaterials.395 Beyond allowing one to spatially control cell distribution, this technology has also enabled the fabrication of fibroblast-laden vascular-like tubes with appropriate horizontal/vertical bifurcations via an alginate-based bioink and piezoelectric jet printers.396 In addition, inkjet-based bioprinting has been employed for producing layered structures with two different alginate-based bioinks, namely, 3D checkerboards, concentric/halved circular patterns, and other complex layouts with high precision (≈100 μm).397 These bioinks were also combined with MMP-sensitive PEG for producing 3D perfusable channels via a sacrificial layer-based method. Recently, inkjet-spray bioprinting that avoids the use of crosslinking baths has been developed for scalable manufacturing of layered hydrogel structures via an alginate/saponified GelMA-based bioink (Figure 11A).395 By incorporating ECM-mimicking GelMA within the inkjet bioprinting process, this work improved the design over other attempts solely comprising alginate-based bioinks and could produce large-scale hydrogel structures with improved cell proliferation/spreading and collagen expression. This technology allowed faster bioprinting (≈3–23-fold) than the previously highlighted studies and is compatible with printing of heterogeneous hydrogel constructs. Moreover, GelMA blending improved hydrogels mechanical properties (i.e., compressive modulus, ≈10–25 kPa), an important aspect when foreseeing the biomedical applicability of such constructs. Despite this, the range of biomaterials compatible with inkjet processes is limited, and the fabrication of mechanically reinforced/thick 3D bioprinted constructs with tissue-like cell densities is highly challenging to materialize through this modality.398

To bridge this gap, extrusion-based bioprinting is a valuable alternative as it allows bioink deposition at high cell densities and the manufacturing of large scale 3D constructs, being one of the most widely established bioprinting technologies due to its relative simplicity and versatility.398 Using this approach cryopreservable cell-laden microgels have been employed as off-the-shelf bioinks for on-demand extrusion-based bioprinting of modular 3D constructs.402 Alternatively, microfluidic-produced norbornene-functionalized hyaluronic acid/PEG-diacrylate microgels were employed as densely packed granular inks for 3D printing purposes, envisioning the design of particulated bioinks composed entirely of bundled microgels (Figure 11B). For obtaining the extrudable granular ink, cell-laden microgels containing NIH/3T3 fibroblasts were produced upon visible light photocrosslinking and subsequently compacted upon vacuum-driven filtration before printing, while maintaining high cell viability (≈70%) during both processes. Such shear-thinning jammed microgel inks could be printed into diverse 3D constructs which could be stabilized with posterior interparticle photocrosslinking for producing mechanically robust architectures.

However, from a critical perspective the packing density of these microgels must be carefully addressed to allow a compromise between 3D microtissues cellular density and the availability of nutrients/oxygen, as well as removal of metabolites during in vitro maturation. Aiming to address this important aspect, recent endeavors have focused on the potential of aqueous two-phase emulsion bioinks (i.e., immiscible GelMA/polyethylene oxide) for bioprinting hydrogel constructs with predesigned internal porous architectures.403 The obtained pore-forming bioprinted 3D constructs displayed enhanced cell viability, spreading and proliferation over standard nonporous GelMA hydrogels across three different cell types (i.e., human hepatocellular carcinoma cells, human umbilical vein endothelial cells, and mouse embryonic fibroblasts). Although an elegant strategy for bioprinting pore-forming constructs with superior biological properties, these approaches still do not allow precise architectural control over vascular networks, a critical aspect in bottom-up tissue engineering. In this context, advanced multilayered coaxial extrusion systems have been employed for bioprinting core–shell hydrogels with prevascularized networks in a one-step process that allows researchers to obtain a more precise control over vascular frameworks, being superior to conventional sacrificial templating approaches.404 In this approach, alginate comprising the innermost channel provided structural support during extrusion, while the final framework was permanently fixed by covalent photocrosslinking between GelMA/4-arm PEG-tetracrylate in the blend bioink. These researchers were able to assemble perfusable cell-laden hydrogel tubular 3D constructs that displayed highly organized cell spatial distribution, as well as tubular topology with gradually increasing, periodically varying or constant outer/inner diameters, thus achieving biologically relevant vascular networks with heterogeneous architectures.

Adding to this discussion, it is important to emphasize that 3D bioprinting of native-like cannular tissues (e.g., gastrointestinal tract, trachea, urinary bladder, urethra, blood vessels, etc.) should attempt to replicate not only the multilayered layout of such biological architectures, but also its varying multicellular composition.405 To address this requirement, a digitally coded microfluidic-based multichannel coaxial extrusion system was developed to allow continuous bioprinting of perfusable tubular structures with on-demand control over the number of concentric layers (i.e., up to 3 multilayers) spanning across user-defined lengths, while using tissue relevant cell types in separate bioinks.405 Using this elaborate system, vascular tissues were produced with human smooth muscle cells SMCs/HUVECs, while bioprinting tubular urothelial structures containing human urothelial cells (inner layer) and human bladder SMCs (outer layer). Bioprinting of geometrically defined multicellular tubular hydrogels represents an important step toward creating biomimetic cannular microtissue constructs. Still, replicating the typical multimaterial composition of native tissues represents one of the most challenging aspects in modular bottom-up tissue engineering. Aiming to tackle this, microfluidic-based extrusion platforms were engineered for extruding more than a single bioink simultaneously.406 Multimaterial extrusion platforms can now successfully bioprint up to seven different cell-laden hydrogel bioinks with fabrication speeds (up to 15 times faster) unmatched by conventional devices.399 With this technology, bioprinting of several complex structures, such as multilayered cuboids, blood vessel-like rings, and miniaturized organ-like constructs with multiple bioinks was successfully achieved (Figure 11C). In this work, researchers have demonstrated the outstanding capacity for rapid continuous bioprinting of constructs with various cell types and material compositions that can be spatially controlled over defined locations or gradients. However, printing speed in such system is still a limiting factor when considering large-scale constructs engineering.286 Recently, the integration of a microfluidic device capable of rapidly switching between multiple bioinks in a stereolithography-based platform equipped with dynamic mirror microdevice (DMD)

technology has been employed for enhancing multi-biomaterial bioprinting.400 Such device enabled the rapid 3D bioprinting of constructs with various bioinks containing different cell types, namely, musculoskeletal interfaces (e.g., C2C12, fibroblasts, and HUVECs) and tendon–bone interfaces (e.g., human MSCs, fibroblasts, and osteoblasts) (Figure 11D). This work uniquely combines the multi-biomaterial processing in multichannel microfluidic systems with the fast fabrication times and high spatial resolution of stereolithography-based bioprinting. Alternatively, the DMD capacity for dynamically projecting complex layouts has been employed for rapid 3D bioprinting of prevascularized constructs with functional endothelial networks that can anastomose with host circulation.407 With this technology, researchers bioprinted hepatic 3D constructs with well-defined hexagonal lobule units of hepatic cells derived from human-induced pluripotent stem cells.408

Notably, another important addition to the toolbox of advanced light-enabled bioprinting has been recently disclosed. Volumetric bioprinting represents a groundbreaking technology that can materialize cell-laden hydrogels at unprecedented speed and allows their manufacturing with innumerous complex geometrical features at high-resolution.401 Inspired by the principles of computed tomography, the researchers irradiated a rotating cylinder containing photocrosslinkable bioink (i.e., GelMA), photoiniator and cells with a sequence of 2D light patterns that intersect and elicit spatially resolved 3D bioprinting at sites of multiple exposures. Due to this, construct dimensions do not dictate printing time, unlike conventional bioprinting approaches. In fact, human auricle models (4.14 cm3; Figure 11E) fabricated by the volumetric approach were printed at unparalleled rates versus extrusion-based printing (i.e., up to 250 times faster) and digital light processing photomanufacturing (i.e., up to 75 times faster), while also exhibited smoother surfaces unlike the other techniques which presented filament/voxel-paved surface artifacts. Interestingly, one of the unique features of volumetric bioprinting is to produce free-floating structures without using any sacrificial hydrogel templates. To demonstrate the potential of this feature, a functional ball-and-cage cardiac valve that enabled unidirectional flow was fabricated. Such valve design cannot be reproduced by extrusion-based or DMD-based bioprinting technologies without resorting to sacrificial templates. Also, researchers were able to bioprint several complex constructs (e.g., trabecular bone and meniscus) with relevant cell types (e.g., MSCs and articular chondroprogenitor cells, respectively) and high cell viability. However, current limitations of this approach, such as limited spatial control over multicellular and multi-biomaterial distribution that are achieved in recent microfluidic-based bioprinting, should be carefully considered.

The governing principles of hydrogels that can readily self-assemble via noncovalent/covalent interactions can be translated into the design of catalyst-free bioinks with improved bioprinting viability and ease of printability. Microfluidic-based templating strategies have been devised for bioprinting self-assembled ECM-derived components (e.g., collagen type I) via transient supporting bioinks (i.e., alginate).409 Alternatively, in an innovative approach, researchers have demonstrated the potential of self-assembling peptides for bioprinting a variety of ECM proteins and biomolecules (i.e., fibronectin, collagen, keratin, elastin-like proteins, hyaluronic acid, etc.) with high cell viability, thus serving as a versatile tool box that can provide tunable bioink composition and structural control.410 Because collagen self-assembles at neutral pH, collagen bioinks can be readily bioprinted via simple pH modulation. Interestingly, researchers have recently combined this principle with the second generation of freeform reversible embedding of suspended hydrogels (FRESH v2.0) and successfully demonstrated 3D bioprinting of organ-scale human heart with patient-specific anatomical architecture and synchronized contractions of cardiac ventricles containing human embryonic stem-cell-derived

cardiomyocytes (Figure 11F).125 Alternatively, bioprinting tissue beads and organ-specific dECM hydrogels could represent other rapidly expanding parallel strategies attempting to harness the complex material composition of native tissues that could play a role in orchestrating their biospecific functions.398, 411 Due to their viscoelastic characteristics, such bioinks could also benefit from improved shear thinning properties, which are known to play a role in maintaining cell integrity during the bioprinting process.412 Hydrogels with self-healing behavior (e.g., host–guest interactions) can also function as supporting baths for accommodating extruded bioinks.413 Although hydrogel viscoelasticity has proven to be beneficial in influencing cell behavior (e.g., proliferation, spreading, differentiation, and bioactivity) due to mechanical similarities with ECM, they can be associated with lower mechanical stiffness which may difficult the bioprinting of large scale structures.414 In this context, bioinks can be mechanically reinforced by intercalating deposition of melted robust biomaterials (i.e., PCL) facilitating bioprinting of voluminous tissues with enhanced structural integrity and without compromising cell viability.415, 416 Other approaches comprise biocompatible benzimidazole-based biomolecule that can accelerate exchange dynamics of hydrazone crosslinking in hyaluronic acid-based hydrogels, which can be exploited for designing self-gelling bioinks with improved stability.417

Although still in its infancy, 4D bioprinting attempts are also beginning to emerge in bottom-up tissue engineering approaches, motivated by establishment of shape-shifting polymers and advent of actuating constructs.418 Recent reports focused on the development of shape-morphing bioinks comprising methacrylated alginate/hyaluronic acid biopolymers and mouse bone marrow stromal cells, which could self-fold under aqueous conditions from sheet-based configuration into hollow tubes.419 Such swelling-driven capillary assemblies displayed small internal diameters (>20 μm) and are thus more similar to smaller blood vessels, which are currently unattained by typical bioprinting techniques. Recently, 4D bioprinting of alginate/GelMA-based bioinks patterned with alginate/polydopamine inks, were used to generate 3D cell-laden constructs with programmed shape-morphing features via NIR light-triggered local deswelling of the hydrogel.420 On the same context these approaches can be further improved since, stereolithography-based grayscale digital light processing is now emerging as an enabling tool for manufacturing functionally graded materials with location-specific properties. This could allow 4D bioprinting of constructs with programmable buckling/deformation sequences.421 Multiphoton technology is also capable of eliciting topographical changes in protein-based hydrogels via inner contraction of the structural network, thus allowing manipulation of cell microenvironment in 4D, but is still constrained by complex operation conditions and slow patterning rate.422, 433 Recent studies are also starting to modulate the mechanical properties of bioprinted constructs and the impact of cell-generated forces in the maturation of multicellular structures.423 With increased understanding of tissue developmental processes, cells can potentially serve as sophisticated bioactuators in bioprinting, where cell-driven microtissue contraction/compaction effects can be leveraged for increasing the effective spatial resolution of bioprinted construct features or implementing programmable structural design motifs with living cells as the driving force.424 Alternatively, 4D biomolecule-driven microtissue maturation could be explored on the emerging research subfield of prokaryotic bioprinting. Microgels encapsulating bioengineered bacteria can serve as autonomous biofactories that can potentially be bioprinted and continuously provide 4D biochemical cue presentation (e.g., rhBMP-2) to neighboring human cells along time.425

4 Combined Multicomponent-Multiscale Bioarchitectures

The combination of cell-rich/cell–biomaterial constructs into multiscale organotypic assemblies (i.e., from nano to macrolevel) arises as the most challenging, but conceivably, the

most promising approach for better recapitulating native tissues structure, connective organization and physiology in 3D macroconstructs. Apart from improving biofunctionality and biomimicry, the bottom-up combination of multiblock 3D assemblies into higher order multiscale architectures with biospecific designs is envisioned to provide a seamless biointegration into host tissues upon constructs implantation (Figure 1). After this stage, obtaining a self-regulated response to local/systemic biomacromolecular cues is key for assuring 3D microtissues commitment toward tissue-specific functions. Unsurprisingly, mimicking human tissues bioarchitecture while assuring microenvironment-sensing and physiological response in implantable multiscale assemblies is remarkably complex.

An elegant approach that involves the deconstruction of nature into its fundamental building blocks (i.e., cells/materials/soluble factors) as means to manipulate each component and encode action/response biofeedback networks has been recognized as a valuable reductionistic alternative to fabricate multiscale macrotissues with better biofunctionality and higher translational potential.

Gathering on these fundaments researchers used advanced 3D biofabrication technologies to fabricate large scale constructs with a multicomponent, multiscale bone bioarchitecture incorporating osteoinductive silica nanoplatelets within constructs. This was essential for promoting osteodifferentiation of hMSCs.426 In this work, VEGF-functionalized GelMA cell-laden cylinders were stacked in a pyramidal construction (comprising 28 rods), ultimately obtaining a perfusable lumen with HUVECs and pericytes, surrounded by differentiated osteoblasts.

Also inspired by these concepts researchers generated compartmentalized multilayered micro/macrocapsules as hierarchic, self-regulated 3D living systems that support stem cells differentiation toward osteogenic or chondrogenic lineages depending on core/surrounding microenvironment cues and cell/biomaterial combinations.427, 428 This hierarchically structured and compartmentalized system is composed of PLLA microparticle–cell building blocks encapsulated in permselective liquefied microenvironments that assure gas/nutrients/waste exchange and sustain enclosed 3D microtissues viability during prolonged periods in vitro and in vivo.427 In a similar line, the development of vascularized hierarchic microtissue assemblies based on cell confinement in ECM mimetic environments has also been recently described.428 Such approach involved a highly controlled fabrication of cell laden alginate-collagen microcapsules in microfluidic chips, followed by their random impregnation into a hydrogel shell. The hierarchically assembled construct was then employed as a template for build-up and maturation of stromal cells and endothelial cells into primitive vascular networks.429 Despite focusing on cancer cells and the establishment of a close-to-native tumor microenvironment, the underlying concept of this multicomponent platform can be translated for bottom-up tissue engineering and regenerative medicine applications. Nevertheless, the build-up of such 3D multicomponents was highly random and no control over vascular networks spatial distribution was obtained. Such is paramount when considering the effects of 3D engineered constructs vascularization in the overall outcome after implantation.

To overcome this inherent unpredictability, researchers are investigating precision chemistry approaches and biofabrication techniques that unlock the possibility to direct bottom-up assembly of multicomponent, multiscale microtissues. In this sense, by using modular cell–biomaterial bioink combinations researchers have successfully bioprinted multiscale constructs with decoupled micro- and microenvironments and multiscale bioarchitectures.19

Overall, combining distinct assembly mechanisms (i.e., self-assembly, guided assembly, direct assembly, etc.) and synchronizing them toward the development of spatially coded complex bioarchitectures, will be essential for manufacturing living multicomponent modules across several length scales.10 The emerging tools for engineering heterogenous assemblies with high precision and biofunctionality at cellular and biomaterial scale are now more established than ever, hence their interface with pioneering assembly technologies that can manipulate such building blocks could collectively accelerate the design from micro- to macroscale living 3D constructs. In this process bioengineers will be challenged with design trade-offs by having to assure the fabrication of biologically relevant modules while keeping production cost and scalability at reach.

5. Concluding Remarks

In a holistic view, human organs display a robust, yet highly regulated cellular framework that combines both structural and functional properties for maintaining a living organism. Interestingly, the human body does not require a pre-existing scaffold for generating full-sized organs and mature tissues. In fact, the natural assembly of tissues into hierarchic modules is intrinsically a bottom-up process through interaction among cellular building blocks and cell-fabricated matrix throughout development, growth, homeostasis, and aging. Nature does this balance effortlessly in the human body but achieving this complexity in de novo engineered architectures remains remarkably challenging.

The bioinspired philosophy in modular bottom-up engineering strategies provides immense design flexibility in the generation of unitary building blocks (i.e., cells and biomaterials) with tailored biochemical features, as well as specific biophysical cues which are potentiated by their interaction and combination. To date, bottom-up engineered micro/macrotissue assemblies have proven their biomedical value and further developments are envisioned considering the constant improvement and discovery of new nano/micro assembly technologies, precision chemistry/genetic engineering tools, 3D biofabrication approaches, as well as the increasing understanding of basic biological regeneration processes and tissues physiology.430 We therefore anticipate an accelerated offer of bottom-up tools that allow the development of tissues or organs with higher complexity and functionalities. Such bioengineered structures may not necessarily exhibit the exact anatomical characteristics of native tissues but should possess the required physiological performance. In this sense, there is currently an analytical challenge regarding the specific biomarkers and pathways that should be characterized in engineered 3D micro/macrotissues. Fortunately, with an increasingly widespread access to the vast toolbox offered by Omics sciences (e.g., metabolomics, lipidomics, glycomics, transcriptomics, etc.) researchers will be able to better evaluate the quality of the fabricated 3D living assemblies and their maturation during in vitro culture and evolution postimplantation in vivo. The latter can also be complemented with the noninvasive follow up of implanted 3D constructs via sophisticated in vivo bioimaging probes. Still, regarding in vivo implantation, a significant effort has been put toward improving living 3D modular constructs biointegration into surrounding host tissues by controlling/stimulating angiogenesis with the inclusion of morphogens or mechanical cues.431 This remains one of the most challenging aspects of bottom-up tissue engineering but with the advent of sophisticated volumetric light-based 3D biofabrication-based approaches for generating flow-functional multivascular networks,401 we anticipate that the ex vivo development of functional prevascularized modular tissue constructs will improve in the upcoming years. The scalability and speed of 3D bioprocessing techniques have been recently improved with elegant approaches for rapid printing of anatomically sized living architectures.[432] Nonetheless, minimizing complexity while pursuing optimal microtissue biofunctionality and physiological responsiveness to its surrounding

microenvironment will be critical for pushing more realistic bottom-up assembled constructs toward preclinical applications.

Acknowledgements

V.M.G. and P.L. contributed equally to this work. The authors would like to acknowledge the support of the European Research Council for project ATLAS, grant agreement ERC-2014-ADG-669858. This work was developed within the scope of the project CICECO - Aveiro Institute of Materials, FCT Ref. UID/CTM/50011/2019, financed by national funds through the FCT/MCTES. This work was also supported by the Programa Operacional Competitividade e Internacionalização (POCI), in the component FEDER, and by national funds (OE) through FCT/MCTES, in the scope of the projects PANGEIA (PTDC/BTM-SAL/30503/2017), TranSphera (PTDC/BTM-ORG/30770/2017), Margel (PTDC/ BTM-MAT/31498/2017), and by the Programa Operacional Regional do Centro - Centro 2020, in the component FEDER, and by national funds (OE) through FCT/MCTES, in the scope of the project SUPRASORT (PTDC/QUI-OUT/30658/2017, CENTRO-01-0145-FEDER-030658). The PANGEIA project is acknowledged for the individual Junior Researcher contract of V.M.G. The authors also acknowledge financial support by FCT through a Ph.D. grant (SFRH/BD/141834/2018, P.L.) and through individual contracts (CEECIND/03202/2017, J.B.; CEECIND/03605/2017, M.O.).

Received: ((will be filled in by the editorial staff))
Revised: ((will be filled in by the editorial staff))
Published online: ((will be filled in by the editorial staff))

References

1. S. M. Oliveira, R. L. Reis, J. F. Mano, Biotechnol. Adv. 2015, 33, 842.

2. A. Ovsianikov, A. Khademhosseini, V. Mironov, Trends Biotechnol. 2018, 36, 348.

3. M. Karin, H. Clevers, Nature 2016, 529, 307.

4. Y. Okabe, R. Medzhitov, Nat. Immunol. 2016, 17, 9.

5. R. M. Harland, Science 2018, 360, 967.

6. C. A. Custódio, R. L. Reis, J. F. Mano, Adv. Healthcare Mater. 2014, 3, 797.

7. T. Kamperman, M. Karperien, S. Le Gac, J. Leijten, Trends Biotechnol. 2018, 36, 850.

8. G. S. Hussey, J. L. Dziki, S. F. Badylak, Nat. Rev. Mater. 2018, 3, 159.

9. C. Bonnans, J. Chou, Z. Werb, Nat. Rev. Mol. Cell Biol. 2014, 15, 786.

10. S. Guven, P. Chen, F. Inci, S. Tasoglu, B. Erkmen, U. Demirci, Trends Biotechnol. 2015, 33, 269.

11. E.-K. Ehmoser-Sinner, C.-W. D. Tan, Lessons on Synthetic Bioarchitectures, Springer, Cham, Switzerland 2018, pp. 29– 39.

12. Z. Shtein, O. Shoseyov, Proc. Natl. Acad. Sci. USA 2017, 114, 428.

13A. I. Neto, P. A. Levkin, J. F. Mano, Mater. Horiz. 2018, 5, 379.

14. A. M. Rosales, S. L. Vega, F. W. DelRio, J. A. Burdick, K. S. Anseth, Angew. Chem., Int. Ed. 2017, 56, 12132.

15. L. Li, J. Eyckmans, C. S. Chen, Nat. Mater. 2017, 16, 1164.

16. K. F. Bruggeman, R. J. Williams, D. R. Nisbet, Adv. Healthcare Mater. 2018, 7, 1700836.

17. J. M. Sobral, S. G. Caridade, R. A. Sousa, J. F. Mano, R. L. Reis, Acta Biomater. 2011, 7, 1009.

18. T. Kamperman, S. Henke, A. van den Berg, S. R. Shin, A. Tamayol, A. Khademhosseini, M. Karperien, J. Leijten, Adv. Healthcare Mater. 2017, 6, 1600913.

19. J. S. Liu, Z. J. Gartner, Trends Cell Biol. 2012, 22, 683.

20. I. Derényi, G. J. Szöllősi, Nat. Commun. 2017, 8, 14545.

21. C. Alvarado, N. A. Fider, H. J. Wearing, N. L. Komarova, PLoS Comput. Biol. 2018, 14, e1005967.

22. M. Darnell, D. J. Mooney, Nat. Mater. 2017, 16, 1178.

23. T. Sasagawa, T. Shimizu, S. Sekiya, Y. Haraguchi, M. Yamato, Y. Sawa, T. Okano, Biomaterials 2010, 31, 1646.

24. J. M. Kelm, M. Fussenegger, Adv. Drug Delivery Rev. 2010, 62, 753.

25. J. Yang, M. Yamato, C. Kohno, A. Nishimoto, H. Sekine, F. Fukai, T. Okano, Biomaterials 2005, 26, 6415.

26. M. Mirbagheri, V. Adibnia, B. R. Hughes, S. D. Waldman, X. Banquy, D. K. Hwang, Mater. Horiz. 2019, 6, 45.

27. I. Elloumi-Hannachi, M. Yamato, T. Okano, J. Intern. Med. 2010, 267, 54.

28.N. Matsuda, T. Shimizu, M. Yamato, T. Okano, Adv. Mater 2007, 19, 3089.

29. R. M. P. Da Silva, J. F. Mano, R. L. Reis, Trends Biotechnol. 2007, 25, 577.

30. J. Yang, M. Yamato, T. Shimizu, H. Sekine, K. Ohashi, M. Kanzaki, T. Ohki, K. Nishida, T. Okano, 2007, 28, 5033.

31T. Shimizu, M. Yamato, Y. Isoi, T. Akutsu, T. Setomaru, K. Abe, A. Kikuchi, M. Umezu, T. Okano, Circ. Res. 2002, 90, e40.

32. M. Yamato, M. Utsumi, A. Kushida, C. Konno, A. Kikuchi, T. Okano, Tissue Eng. 2001, 7, 473.

33. H. Takahashi, T. Okano, Adv. Drug Delivery Rev. 2019, 138, 276.

34.B. B. Shotorbani, H. André, A. Barzegar, N. Zarghami, R. Salehi, E. Alizadeh, J. Mater. Sci.: Mater. Med. 2018, 29, 170.

35. S. Hong, J. H. Sunwoo, J. S. Kim, H. Tchah, C. Hwang, Biomater. Sci. 2019, 7, 139.

36. Y. Bin Lee, Y. M. Shin, E. M. Kim, J. Lim, J.-Y. Lee, H. Shin, Adv. Healthcare Mater. 2016, 5, 2305.

37. Y. Bin Lee, S.-j. Kim, E. M. Kim, H. Byun, H.-k. Chang, J. Park, Y. S. Choi, H. Shin, Acta Biomater. 2017, 61, 75.

38. G. V. Martins, J. F. Mano, N. M. Alves, Langmuir 2011, 27, 8415.

39. N. G. Patel, G. Zhang, Organogenesis 2013, 9, 93.

40. J. Kobayashi, A. Kikuchi, T. Aoyagi, T. Okano, J. Biomed. Mater. Res., Part A 2019, 107, 955.

41. M. A. Koo, S. Hee Hong, M. Hee Lee, B. J. Kwon, G. Mi Seon, M. Sung Kim, D. Kim, K. Chang Nam, J. C. Park, Acta Biomater. 2019, 95, 418.

42. C. Liu, Y. Zhou, M. Sun, Q. Li, L. Dong, L. Ma, K. Cheng, W. Weng, M. Yu, H. Wang, ACS Appl. Mater. Interfaces 2017, 9, 36513.

43. A. Ito, K. Ino, T. Kobayashi, H. Honda, Biomaterials 2005, 26, 6185.

44.S. Gil, C. R. Correia, J. F. Mano, Adv. Healthcare Mater. 2015, 4, 883.

45. M. Noh, Y. H. Choi, Y. H. An, D. Tahk, S. Cho, J. W. Yoon, N. L. Jeon, T. H. Park, J. Kim, N. S. Hwang, ACS Biomater. Sci. Eng. 2019, 5, 3909.

46. C. Vaquette, P. T. Sudheesh Kumar, E. B. Petcu, S. Ivanovski, J. Biomed. Mater. Res., Part B 2018, 106, 399.

47. T. Kikuchi, T. Shimizu, M. Wada, M. Yamato, T. Okano, Biomaterials 2014, 35, 2428.

48. M. A. Rowland, J. M. Greenbaum, E. J. Deeds, Nat. Commun. 2017, 8, 16009.

49. H. Zhang, S. Liu, B. Zhu, Q. Xu, Y. Ding, Y. Jin, Stem Cell Res. Ther. 2016, 7, 168.

50 S. N. Bhatia, G. H. Underhill, K. S. Zaret, I. J. Fox, Sci. Transl. Med. 2014, 6, 245sr2.

51. N. Tanaka, H. Ota, K. Fukumori, J. Miyake, M. Yamato, T. Okano, Biomaterials 2014, 35, 9802.

52. L. Wong, J. D. Pegan, B. Gabela-Zuniga, M. Khine, K. E. McCloskey, Biofabrication 2017, 9, 021001.

53. Y. Tsuda, A. Kikuchi, M. Yamato, G. Chen, T. Okano, Biochem. Biophys. Res. Commun. 2006, 348, 937.

54. Y. Tsuda, A. Kikuchi, M. Yamato, A. Nakao, Y. Sakurai, M. Umezu, T. Okano, Biomaterials 2005, 26, 1885.

55. D. R. Albrecht, G. H. Underhill, T. B. Wassermann, R. L. Sah, S. N. Bhatia, Nat. Methods 2006, 3, 369.

56. C.-Y. Fu, C.-Y. Lin, W.-C. Chu, H.-Y. Chang, Tissue Eng., Part C 2011, 17, 871.

57. C.-T. Ho, R.-Z. Lin, R.-J. Chen, C.-K. Chin, S.-E. Gong, H.-Y. Chang, H.-L. Peng, L. Hsu, T.-R. Yew, S.-F. Chang, Lab Chip 2013, 13, 3578.

58. Y. Zheng, J. Chen, M. Craven, N. W. Choi, S. Totorica, A. Diaz-Santana, P. Kermani, B. Hempstead, C. Fischbach-Teschl, J. A. López, A. D. Stroock, Proc. Natl. Acad. Sci. USA 2012, 109, 9342.

59. E. Bakirci, B. Toprakhisar, M. C. Zeybek, G. O. Ince, B. Koc, Biofabrication 2017, 9, 024105.

60. H. Takahashi, T. Shimizu, M. Nakayama, M. Yamato, T. Okano, Biomaterials 2013, 34, 7372.

61. Q. Xing, Z. Qian, M. Tahtinen, A. H. Yap, K. Yates, F. Zhao, Adv. Healthcare Mater. 2017, 6, 1601333.

62. B. Yuan, Y. Jin, Y. Sun, D. Wang, J. Sun, Z. Wang, W. Zhang, X. Jiang, Adv. Mater. 2012, 24, 890.

63. Q. He, T. Okajima, H. Onoe, A. Subagyo, K. Sueoka, K. Kuribayashi-Shigetomi, Sci. Rep. 2018, 8, 4556.

64. A. Chanda, C. Callaway, Appl. Bionics Biomech. 2018, 2018, 4838157.

65. M. Valderrábano, Prog. Biophys. Mol. Biol. 2007, 94, 144.

66. T. Shimizu, M. Yamato, A. Kikuchi, T. Okano, Biomaterials 2003, 24, 2309.

67. Y. Haraguchi, T. Shimizu, M. Yamato, A. Kikuchi, T. Okano, Biomaterials 2006, 27, 4765.

68. T. Shimizu, H. Sekine, Y. Isoi, M. Yamato, A. Kikuchi, T. Okano, Tissue Eng. 2006, 12, 499.

69. K. Sakaguchi, T. Shimizu, T. Okano, J. Controlled Release 2015, 205, 83.

70. S. Sekiya, T. Shimizu, M. Yamato, A. Kikuchi, T. Okano, Biochem. Biophys. Res. Commun. 2006, 341, 573.

71. R. Keller, D. Shook, BMC Biol. 2011, 9, 90.

72. H. Kubo, T. Shimizu, M. Yamato, T. Fujimoto, T. Okano, Biomaterials 2007, 28, 3508.

73. M. Kanzaki, M. Yamato, H. Hatakeyama, C. Kohno, J. Yang, T. Umemoto, A. Kikuchi, T. Okano, T. Onuki, Tissue Eng. 2006, 12, 1275.

74. R. Gauvin, T. Ahsan, D. Larouche, P. Lévesque, J. Dubé, F. A. Auger, R. M. Nerem, L. Germain, Tissue Eng., Part A 2010, 16, 1737.

75. Q. He, T. Okajima, H. Onoe, A. Subagyo, K. Sueok, Sci. Rep. 2018, 8, 4556.

76. T. Shimizu, Circ. J. 2014, 78, 2594.

77. F. Kawecki, W. P. Clafshenkel, F. A. Auger, J. M. Bourget, J. Fradette, R. Devillard, Biofabrication 2018, 10, 035006.

78. Y. Seto, R. Inaba, T. Okuyama, F. Sassa, H. Suzuki, J. Fukuda, Biomaterials 2010, 31, 2209.

79. D. Sasaki, K. Matsuura, H. Seta, Y. Haraguchi, T. Okano, T. Shimizu, PLoS One 2018, 13, e0198026.

80. T. Osaki, V. Sivathanu, R. D. Kamm, Biomaterials 2018, 156, 65.

81. H. D. Himel IV, G. Bub, P. Lakireddy, N. El-Sherif, Heart Rhythm 2012, 9, 2077.

82. Y. Haraguchi, T. Shimizu, T. Sasagawa, H. Sekine, K. Sakaguchi, T. Kikuchi, W. Sekine, S. Sekiya, M. Yamato, M. Umezu, T. Okano, Nat. Protoc. 2012, 7, 850.

83. H. Sekine, T. Shimizu, K. Sakaguchi, I. Dobashi, M. Wada, M. Yamato, E. Kobayashi, M. Umezu, T. Okano, Nat. Commun. 2013, 4, 1310.

84. L. P. Ferreira, V. M. Gaspar, J. F. Mano, Biomaterials 2018, 185, 155.

85. K. Mubyana, D. T. Corr, Tissue Eng., Part A 2018, 24, 1808.

86. M. Asmani, S. Velumani, Y. Li, N. Wawrzyniak, I. Hsia, Z. Chen, B. Hinz, R. Zhao, Nat. Commun. 2018, 9, 2066.

87. T. W. Ridky, J. M. Chow, D. J. Wong, P. A. Khavari, Nat. Med. 2010, 16, 1450.

88. M. W. Laschke, M. D. Menger, Trends Biotechnol. 2017, 35, 133.

89. E. Fennema, N. Rivron, J. Rouwkema, C. van Blitterswijk, J. De Boer, Trends Biotechnol. 2013, 31, 108.

90. M. W. Laschke, M. D. Menger, Biotechnol. Adv. 2017, 35, 782.

91. F. Pampaloni, E. G. Reynaud, E. H. K. Stelzer, Nat. Rev. Mol. Cell Biol. 2007, 8, 839.

92. J. Eyckmans, C. S. Chen, J. Cell Sci. 2017, 130, 63.

93. M. A. Gionet-Gonzales, J. K. Leach, Biomed. Mater. 2018, 13, 034109.

94. O. B. Matthys, T. A. Hookway, T. C. McDevitt, Curr. Stem Cell Rep. 2016, 2, 43.

95. E. Castro, J. F. Mano, J. Biomed. Nanotechnol. 2013, 9, 1129.

96. M. E. Katt, A. L. Placone, A. D. Wong, Z. S. Xu, P. C. Searson, Front. Bioeng. Biotechnol. 2016, 4, 12.

97. L. P. Ferreira, V. M. Gaspar, J. F. Mano, Acta Biomater. 2018, 75, 11.

98. T.-M. Achilli, J. Meyer, J. R. Morgan, Expert Opin. Biol. Ther. 2012, 12, 1347.

99. G. H. Lee, J. S. Lee, X. Wang, S. H. Lee, Adv. Healthcare Mater. 2016, 5, 56.

100. F. Urciuolo, G. Imparato, A. Totaro, P. A. Netti, Methodist DeBakey Cardiovasc. J. 2013, 9, 213.

101. S. M. Z. M. D. Ferreira, G. P. Domingos, D. D. S. Ferreira, T. G. R. Rocha, R. Serakides, C. M. De Faria Rezende, V. N. Cardoso, S. O. A. Fernandes, M. C. Oliveira, Bioorg. Med. Chem. Lett. 2012, 22, 4605.

102. T. R. Olsen, F. Alexis, J. Bioprocess. Biotech. 2014, 4, e112.

103. T. Y. Kim, C. M. Kofron, M. King, A. R. Markes, A. O. Okundaye, Z. Qu, U. Mende, B.-R. Choi, Biophys. J. 2018, 114, 626a.

104. L. S. Baptista, G. S. Kronemberger, K. R. Silva, J. M. Granjeiro, Front. Biosci. 2018, 23, 1969.

105. S. Inglis, J. M. Kanczler, R. O. C. Oreffo, FASEB J. 2019, 33, 3279.

106. R. Walser, W. Metzger, A. Görg, T. Pohlemann, M. D. Menger, M. W. Laschke, Eur. Cells Mater. 2013, 26, 222.

107. E. Bauman, T. Feijao, D. T. O. Carvalho, P. L. Granja, C. C. Barrias, Sci. Rep. 2018, 8, 230.

108. A. P. Rago, D. M. Dean, J. R. Morgan, Biotechnol. Bioeng. 2009, 102, 1231.

109. M. Kato-Negishi, Y. Tsuda, H. Onoe, S. Takeuchi, Biomaterials 2010, 31, 8939.

110. E. Vrij, J. Rouwkema, V. Lapointe, C. Van Blitterswijk, R. Truckenmüller, N. Rivron, Adv. Mater. 2016, 28, 4032.

111. N. C. Rivron, E. J. Vrij, J. Rouwkema, S. Le Gac, A. van den Berg, R. K. Truckenmuller, C. A. van Blitterswijk, Proc. Natl. Acad. Sci. USA 2012, 109, 6886.

112. C. Norotte, F. S. Marga, L. E. Niklason, G. Forgacs, Biomaterials 2009, 30, 5910.

113. N. I. Moldovan, N. Hibino, K. Nakayama, Tissue Eng., Part B 2017, 23, 237.

114. T. R. Olsen, B. Mattix, M. Casco, A. Herbst, C. Williams, A. Tarasidis, D. Simionescu, R. P. Visconti, F. Alexis, Acta Biomater. 2015, 13, 188.

115. B. Mattix, T. R. Olsen, Y. Gu, M. Casco, A. Herbst, D. T. Simionescu, R. P. Visconti, K. G. Kornev, F. Alexis, Acta Biomater. 2014, 10, 623.

116. X. Yin, B. E. Mead, H. Safaee, R. Langer, J. M. Karp, O. Levy, Cell Stem Cell 2016, 18, 25.

117. T. Takahashi, Annu. Rev. Pharmacol. Toxicol. 2019, 59, 447.

118. M. J. Kratochvil, A. J. Seymour, T. L. Li, S. P. Paşca, C. J. Kuo, S. C. Heilshorn, Nat. Rev. Mater. 2019, 4, 606.

119. C. R. Marti-Figueroa, R. S. Ashton, Acta Biomater. 2017, 54, 35.

120. S. Grebenyuk, A. Ranga, Front. Bioeng. Biotechnol. 2019, 7, 39.

121. J. Candiello, T. S. P. Grandhi, S. K. Goh, V. Vaidya, M. Lemmon-Kishi, K. R. Eliato, R. Ros, P. N. Kumta, K. Rege, I. Banerjee, Biomaterials 2018, 177, 27.

122. T. Takebe, J. M. Wells, Science 2019, 364, 956.

123. H. Onoe, S. Takeuchi, Drug Discovery Today 2015, 20, 236.

124. S. V. Murphy, A. Atala, Nat. Biotechnol. 2014, 32, 773.

125. A. Lee, A. R. Hudson, D. J. Shiwarski, J. W. Tashman, T. J. Hinton, S. Yerneni, J. M. Bliley, P. G. Campbell, A. W. Feinberg, Science 2019, 365, 482.

126. T. J. Hinton, Q. Jallerat, R. N. Palchesko, J. H. Park, M. S. Grodzicki, H.-J. Shue, M. H. Ramadan, A. R. Hudson, A. W. Feinberg, Sci. Adv. 2015, 1, e1500758.

127. M. Akbari, A. Tamayol, S. Bagherifard, L. Serex, P. Mostafalu, N. Faramarzi, M. H. Mohammadi, A. Khademhosseini, Adv. Healthcare Mater. 2016, 5, 751.

128. C. Rinoldi, M. Costantini, E. Kijeńska-Gawrońska, S. Testa, E. Fornetti, M. Heljak, M. Ćwiklińska, R. Buda, J. Baldi, S. Cannata, Adv. Healthcare Mater. 2019, 8, 1801218.

129. M. Zhong, X. Liu, D. Wei, J. Sun, L. Guo, H. Zhu, Y. Wan, H. Fan, Mater. Sci. Eng., C 2019, 101, 370.

130. H. Onoe, T. Okitsu, A. Itou, M. Kato-Negishi, R. Gojo, D. Kiriya, K. Sato, S. Miura, S. Iwanaga, K. Kuribayashi-Shigetomi, Nat. Mater. 2013, 12, 584.

131.Y. Yu, K. K. Moncal, J. Li, W. Peng, I. Rivero, J. A. Martin, I. T. Ozbolat, Sci. Rep. 2016, 6, 28714.

132. O. Jeon, Y. Bin Lee, H. Jeong, S. J. Lee, D. Wells, E. Alsberg, Mater. Horiz. 2019, 6, 1625.

133.Y. Wu, M. Hospodiuk, W. Peng, H. Gudapati, T. Neuberger, S. Koduru, D. J. Ravnic, I. T. Ozbolat, Biofabrication 2018, 11, 015009.

134.J. Kalisky, J. Raso, C. Rigothier, M. Rémy, R. Siadous, R. Bareille, J.-C. Fricain, J. Amedée-Vilamitjana, H. Oliveira, R. Devillard, Sci. Rep. 2016, 6, 33328.

135. N. R. Schiele, R. A. Koppes, D. B. Chrisey, D. T. Corr, Tissue Eng., Part A 2013, 19, 1223.

136. A. Fallahi, A. Khademhosseini, A. Tamayol, Trends Biotechnol. 2016, 34, 683.

137.J. Leijten, J. Seo, K. Yue, G. Trujillo-de Santiago, A. Tamayol, G. U. Ruiz-Esparza, S. R. Shin, R. Sharifi, I. Noshadi, M. M. Álvarez, Y. S. Zhang, A. Khademhosseini, Mater. Sci. Eng., R 2017, 119, 1.

138. M. Akbari, A. Tamayol, V. Laforte, N. Annabi, A. H. Najafabadi, A. Khademhosseini, D. Juncker, Adv. Funct. Mater. 2014, 24, 4060.

139. B. J. Kim, H. Cho, J. H. Park, J. F. Mano, I. S. Choi, Adv. Mater. 2018, 30, 1706063.

140. C. A. Custódio, J. F. Mano, ChemNanoMat 2016, 2, 376.

141. S. Toda, L. R. Blauch, S. K. Y. Tang, L. Morsut, W. A. Lim, Science 2018, 162, 156.

142. E. M. Sletten, C. R. Bertozzi, Angew. Chem., Int. Ed. 2009, 48, 6974.

143. B. Cheng, R. Xie, L. Dong, X. Chen, ChemBioChem 2016, 17, 11.

144. L. K. Mahal, K. J. Yarema, C. R. Bertozzi, Science 1997, 276, 1125.

145. E. Saxon, C. R. Bertozzi, Science 2000, 287, 2007.

146. C. J. Capicciotti, C. Zong, M. O. Sheikh, T. Sun, L. Wells, G. Boons, J. Am. Chem. Soc. 2017, 139, 13342.

147. J. Wang, B. Cheng, J. Li, Z. Zhang, W. Hong, X. Chen, P. R. Chen, Angew. Chem., Int. Ed. 2015, 54, 5364.

148. N. J. Agard, J. A. Prescher, C. R. Bertozzi, J. Am. Chem. Soc. 2004, 126, 15046.

149. Y. Sun, S. Hong, R. Xie, R. Huang, R. Lei, B. Cheng, D. Sun, Y. Du, C. M. Nycholat, J. C. Paulson, X. Chen, J. Am. Chem. Soc. 2018, 140, 3592.

150. B. Layek, T. Sadhukha, S. Prabha, Biomaterials 2016, 88, 97.

151. S. Y. Lee, S. Lee, J. Lee, J. Y. Yhee, H. I. Yoon, S.-J. Park, H. Koo, S.-H. Moon, H. Lee, Y. W. Cho, S. W. Kang, S.-Y. Lee, K. Kim, Biochem. Biophys. Res. Commun. 2016, 479, 779.

152. D. Alberti, C. Grange, S. Porta, S. Aime, L. Tei, S. Geninatti Crich, ACS Omega 2018, 3, 8097.

153. L. Du, H. Qin, T. Ma, T. Zhang, D. Xing, ACS Nano 2017, 11, 8930.

154. A. Mongis, F. Piller, V. Piller, Bioconjugate Chem. 2017, 28, 1151.

155. S. Li, B. Yu, J. Wang, Y. Zheng, H. Zhang, M. J. Walker, Z. Yuan, H. Zhu, J. Zhang, P. G. Wang, B. Wang, ACS Chem. Biol. 2018, 13, 1686.

156. S.-G. Sampathkumar, A. V. Li, M. B. Jones, Z. Sun, K. J. Yarema, Nat. Chem. Biol. 2006, 2, 149.

157. A. I. P. M. Smits, C. V. C. Bouten, Curr. Opin. Biomed. Eng. 2018, 6, 17.

158. A.-K. Späte, J. E. G. A. Dold, E. Batroff, V. F. Schart, D. E. Wieland, O. R. Baudendistel, V. Wittmann, ChemBioChem 2016, 17, 1374.

159. V. F. Schart, J. Hassenrück, A.-K. Späte, J. E. G. A. Dold, R. Fahrner, V. Wittmann, ChemBioChem 2019, 20, 166.

160. R. M. F. Tomás, B. Martyn, T. L. Bailey, M. I. Gibson, ACS Macro Lett. 2018, 7, 1289.

161. J. Niu, D. J. Lunn, A. Pusuluri, J. I. Yoo, M. A. O'Malley, S. Mitragotri, H. T. Soh, C. J. Hawker, Nat. Chem. 2017, 9, 537.

162. H. Koo, S. K. Hahn, S. H. Yun, Bioconjugate Chem. 2016, 27, 2601.

163. P. Shi, E. Ju, Z. Yan, N. Gao, J. Wang, J. Hou, Y. Zhang, J. Ren, X. Qu, Nat. Commun. 2016, 7, 13088.

164. W. Luo, A. Pulsipher, D. Dutta, B. M. Lamb, M. N. Yousaf, Sci. Rep. 2014, 4, 6313.

165. Z. J. Gartner, C. R. Bertozzi, Proc. Natl. Acad. Sci. USA 2009, 106, 4606.

166. H. Wang, R. Wang, K. Cai, H. He, Y. Liu, J. Yen, Z. Wang, M. Xu, Y. Sun, X. Zhou, Q. Yin, L. Tang, I. T. Dobrucki, L. W. Dobrucki, E. J. Chaney, S. A. Boppart, T. M. Fan, S. Lezmi, X. Chen, L. Yin, J. Cheng, Nat. Chem. Biol. 2017, 13, 415.

167. H. I. Yoon, J. Y. Yhee, J. H. Na, S. Lee, H. Lee, S. W. Kang, H. Chang, J. H. Ryu, S. Lee, I. C. Kwon, Y. W. Cho, K. Kim, Bioconjugate Chem. 2016, 27, 927.

168. S. Lee, H. I. Yoon, J. H. Na, S. Jeon, S. Lim, H. Koo, S. Han, S. Kang, S. Park, S. Moon, J. H. Park, Y. W. Cho, B.-S. Kim, S. K. Kim, T. Lee, D. Kim, S. Lee, M. G. Pomper, I. C. Kwon, K. Kim, Biomaterials 2017, 139, 12.

169. X. Ai, L. Lyu, Y. Zhang, Y. Tang, J. Mu, F. Liu, Y. Zhou, Z. Zuo, G. Liu, B. Xing, Angew. Chem., Int. Ed. 2017, 56, 3031.

170. H. Y. Yoon, H. Koo, K. Kim, I. C. Kwon, Biomaterials 2017, 132, 28.

171. S. T. Laughlin, J. M. Baskin, S. L. Amacher, C. R. Bertozzi, Science 2008, 320, 664.

172.C. T. Saeui, A. V. Nairn, M. Galizzi, C. Douville, P. Gowda, M. Park, V. Dharmarha, S. R. Shah, A. Clarke, M. Austin, K. W. Moremen, K. J. Yarema, PLoS One 2018, 13, e0195812.

173. J. Rong, J. Han, L. Dong, Y. Tan, H. Yang, L. Feng, Q.-W. Wang, R. Meng, J. Zhao, S.-Q. Wang, X. Chen, J. Am. Chem. Soc. 2014, 136, 17468.

174A. Shajahan, S. Parashar, S. Goswami, S. M. Ahmed, P. Nagarajan, S.-G. Sampathkumar, J. Am. Chem. Soc. 2017, 139, 693.

175. X. Bi, J. Yin, A. Chen Guanbang, C. F. Liu, Chem. - Eur. J. 2018, 24, 8042.

176. S. A. Whitehead, C. D. McNitt, S. I. Mattern-Schain, A. J. Carr, S. Alam, V. V. Popik, M. D. Best, Bioconjugate Chem. 2017, 28, 923.

177. S. Kube, N. Hersch, E. Naumovska, T. Gensch, J. Hendriks, A. Franzen, L. Landvogt, J.-P. Siebrasse, U. Kubitscheck, B. Hoffmann, R. Merkel, A. Csiszár, Langmuir 2017, 33, 1051.

178. D. Dutta, A. Pulsipher, W. Luo, H. Mak, M. N. Yousaf, Bioconjugate Chem. 2011, 22, 2423.

179. D. Dutta, A. Pulsipher, W. Luo, M. N. Yousaf, J. Am. Chem. Soc. 2011, 133, 8704.

180. P. J. O'Brien, W. Luo, D. Rogozhnikov, J. Chen, M. N. Yousaf, Bioconjugate Chem. 2015, 26, 1939.

181. D. Rogozhnikov, W. Luo, S. Elahipanah, P. J. O'Brien, M. N. Yousaf, Bioconjugate Chem. 2016, 27, 1991.

182. D. Rogozhnikov, P. J. O'Brien, S. Elahipanah, M. N. Yousaf, Sci. Rep. 2016, 6, 39806.

183. N. Hersch, B. Wolters, Z. Ungvari, T. Gautam, D. Deshpande, R. Merkel, A. Csiszar, B. Hoffmann, A. Csiszár, J. Biomater. Appl. 2016, 30, 846.

184. J. F. Reuther, S. D. Dahlhauser, E. Van Anslyn, Angew. Chem., Int. Ed. 2018, 58, 74.

185. P. Chidchob, H. F. Sleiman, Curr. Opin. Chem. Biol. 2018, 46, 63.

186. R. J. Weber, A. E. Cerchiari, L. S. Delannoy, J. C. Garbe, M. A. LaBarge, T. A. Desai, Z. J. Gartner, ACS Biomater. Sci. Eng. 2016, 2, 1851.

187. S. Toda, L. R. Blauch, S. K. Y. Tang, L. Morsut, W. A. Lim, Science 2018, 2, 156.

188. M. Good, X. Trepat, Nature 2018, 563, 188.

189. C. Gilbert, T. Ellis, ACS Synth. Biol. 2018, 8, 1.

190. J. Santos-Moreno, Y. Schaerli, Adv. Biosyst. 2018, 3, 1800280.

191. M. B. Oliveira, J. Hatami, J. F. Mano, Chem. - Asian J. 2016, 11, 1753.

192. J. T. Wilson, W. Cui, E. L. Chaikof, Nano Lett. 2008, 8, 1940.

193P. T. Hammond, Adv. Mater. 2004, 16, 1271.

194. J. Borges, J. F. Mano, Chem. Rev. 2014, 114, 8883.

195. J. Borges, L. C. Rodrigues, R. L. Reis, J. F. Mano, Adv. Funct. Mater. 2014, 24, 5624.

196. J. J. Richardson, M. Björnmalm, F. Caruso, Science 2015, 348, aaa2491.

197. J. J. Richardson, J. Cui, M. Bjornmalm, J. A. Braunger, H. Ejima, F. Caruso, Chem. Rev. 2016, 116, 14828.

198. F.-X. Xiao, M. Pagliaro, Y.-J. Xu, B. Liu, Chem. Soc. Rev. 2016, 45, 3088.

199. M. Matsusaki, K. Kadowaki, Y. Nakahara, M. Akashi, Angew. Chem., Int. Ed. 2007, 46, 4689.

200. C. Monge, J. Almodóvar, T. Boudou, C. Picart, Adv. Healthcare Mater. 2015, 4, 811.

201. T. Boudou, T. Crouzier, K. Ren, G. Blin, C. Picart, Adv. Mater. 2010, 22, 441.

202. J. Park, B. Andrade, Y. Seo, M.-J. Kim, S. C. Zimmerman, H. Kong, Chem. Rev. 2018, 118, 1664.

203. J. Yang, Y. Yang, N. Kawazoe, G. Chen, Biomaterials 2019, 197, 317.

204. A. Matsuzawa, M. Matsusaki, M. Akashi, Langmuir 2013, 29, 7362.

205. J. T. Wilson, W. Cui, V. Kozlovskaya, E. Kharlampieva, D. Pan, Z. Qu, V. R. Krishnamurthy, J. Mets, V. Kumar, J. Wen, Y. Song, V. V. Tsukruk, E. L. Chaikof, J. Am. Chem. Soc. 2011, 133, 7054.

206. K. M. Gattás-Asfura, C. L. Stabler, ACS Appl. Mater. Interfaces 2013, 5, 9964.

207. K. Kadowaki, M. Matsusaki, M. Akashi, Langmuir 2010, 26, 5670.

208. A. Nishiguchi, H. Yoshida, M. Matsusaki, M. Akashi, Adv. Mater. 2011, 23, 3506.

209. M. Matsusaki, Bull. Chem. Soc. Jpn. 2012, 85, 401.

210. M. Matsusaki, K. Kadowaki, E. Adachi, T. Sakura, U. Yokoyama, Y. Ishikawa, M. Akashi, J. Biomater. Sci., Polym. Ed. 2012, 23, 63.

211. K. Sasaki, T. Akagi, T. Asaoka, H. Eguchi, Y. Fukuda, Y. Iwagami, D. Yamada, T. Noda, H. Wada, K. Gotoh, Biomaterials 2017, 133, 263.

212. M. Matsusaki, K. Fujimoto, Y. Shirakata, S. Hirakawa, K. Hashimoto, M. Akashi, J. Biomed. Mater. Res., Part A 2015, 103, 3386.

213. A. Nishiguchi, M. Matsusaki, M. R. Kano, H. Nishihara, D. Okano, Y. Asano, H. Shimoda, S. Kishimoto, S. Iwai, M. Akashi, Biomaterials 2018, 179, 144.

214. Y. Amano, A. Nishiguchi, M. Matsusaki, H. Iseoka, S. Miyagawa, Y. Sawa, M. Seo, T. Yamaguchi, M. Akashi, Acta Biomater. 2016, 33, 110.

215. F. Shima, H. Narita, A. Hiura, H. Shimoda, M. Akashi, J. Biomed. Mater. Res., Part A 2017, 105, 814.

216. M. Matsusaki, K. Sakaue, K. Kadowaki, M. Akashi, Adv. Healthcare Mater. 2013, 2, 534.

217. S. Mauquoy, C. Dupont-Gillain, Colloids Surf., B 2016, 147, 54.

218. J. M. Silva, R. L. Reis, J. F. Mano, Small 2016, 12, 4308.

219. M. Matsusaki, M. Akashi, Polym. J. 2014, 46, 524.

220. J. Borges, M. P. Sousa, G. Cinar, S. G. Caridade, M. O. Guler, J. F. Mano, Adv. Funct. Mater. 2017, 27, 1605122.

221. J. Boekhoven, S. I. Stupp, Adv. Mater. 2014, 26, 1642.

222. I. W. Hamley, Chem. Rev. 2017, 117, 14015.

223. K. S. Hellmund, B. Koksch, Front. Chem. 2019, 7, 172.

224. R. J. Wade, J. A. Burdick, Mater. Today 2012, 15, 454.

225. M. Yang, E. Kang, J. W. Shin, J. Hong, Sci. Rep. 2017, 7, 4464.

226. D. Choi, J. Park, J. Heo, T. I. Oh, E. Lee, J. Hong, ACS Appl. Mater. Interfaces 2017, 9, 12264.

227Y. Teramura, H. Iwata, Soft Matter 2010, 6, 1081.

228. R. F. Fakhrullin, A. I. Zamaleeva, R. T. Minullina, S. A. Konnova, V. N. Paunov, Chem. Soc. Rev. 2012, 41, 4189.

229. J. T. Wilson, W. Cui, V. Kozlovskaya, E. Kharlampieva, D. Pan, Z. Qu, V. R. Krishnamurthy, J. Mets, V. Kumar, J. Wen, J. Am. Chem. Soc. 2011, 133, 7054.

230. P. R. Leroueil, S. Hong, A. Mecke, J. R. Baker Jr., B. G. Orr, M. M. Banaszak Holl, Acc. Chem. Res. 2007, 40, 335.

231. S. Krol, S. Del Guerra, M. Grupillo, A. Diaspro, A. Gliozzi, P. Marchetti, Nano Lett. 2006, 6, 1933.

232. J. T. Wilson, V. R. Krishnamurthy, W. Cui, Z. Qu, E. L. Chaikof, J. Am. Chem. Soc. 2009, 131, 18228.

233. J. M. Mets, J. T. Wilson, W. Cui, E. L. Chaikof, Adv. Healthcare Mater. 2013, 2, 266.

234. Y. Teramura, H. Iwata, Bioconjugate Chem. 2008, 19, 1389.

235. Y. Teramura, Y. Kaneda, H. Iwata, Biomaterials 2007, 28, 4818.

236. Y. Teramura, Biomaterials 2015, 48, 119.

237. Y. Teramura, O. P. Oommen, J. Olerud, J. Hilborn, B. Nilsson, Biomaterials 2013, 34, 2683.

238. V. Kozlovskaya, S. Harbaugh, I. Drachuk, O. Shchepelina, N. Kelley-Loughnane, M. Stone, V. V Tsukruk, Soft Matter 2011, 7, 2364.

239. V. Kozlovskaya, O. Zavgorodnya, Y. Chen, K. Ellis, H. M. Tse, W. Cui, J. A. Thompson, E. Kharlampieva, Adv. Funct. Mater. 2012, 22, 3389.

240. V. Kozlovskaya, B. Xue, W. Lei, L. E. Padgett, H. M. Tse, E. Kharlampieva, Adv. Healthcare Mater. 2015, 4, 686.

241. K. McNamara, S. A. M. Tofail, Adv. Phys.: X 2017, 2, 54.

242. J. Jeevanandam, A. Barhoum, Y. S. Chan, A. Dufresne, M. K. Danquah, Beilstein J. Nanotechnol. 2018, 9, 1050.

243. X. Hu, X. Dong, Y. Lu, J. Qi, W. Zhao, W. Wu, Drug Discovery Today 2017, 22, 382.

244. N. Kamaly, B. Yameen, J. Wu, O. C. Farokhzad, Chem. Rev. 2016, 116, 2602.

245. B. Sarkar, P. Alexandridis, Prog. Polym. Sci. 2015, 40, 33.

246. M. Elsabahy, K. L. Wooley, Chem. Soc. Rev. 2012, 41, 2545.

247. D. Kim, K. Shin, S. G. Kwon, T. Hyeon, Adv. Mater. 2018, 30, 1802309.

248. X. Mao, L. Liu, L. Cheng, R. Cheng, L. Zhang, L. Deng, X. Sun, Y. Zhang, B. Sarmento, W. Cui, J. Controlled Release 2019, 297, 91.

249. S. Mura, J. Nicolas, P. Couvreur, Nat. Mater. 2013, 12, 991.

250. P. Lavrador, V. M. Gaspar, J. F. Mano, J. Controlled Release 2018, 273, 51.

251. X. Fu, J. Cai, X. Zhang, W.-D. Li, H. Ge, Y. Hu, Adv. Drug Delivery Rev. 2018, 132, 169.

252. J. A. Champion, Y. K. Katare, S. Mitragotri, Proc. Natl. Acad. Sci. USA 2007, 104, 11901.

253. X. Yu, Z. Liu, J. Janzen, I. Chafeeva, S. Horte, W. Chen, R. K. Kainthan, J. N. Kizhakkedathu, D. E. Brooks, Nat. Mater. 2012, 11, 468.

254. .X. Mo, Q. Li, L. W. Yi Lui, B. Zheng, C. H. Kang, B. Nugraha, Z. Yue, R. R. Jia, H. X. Fu, D. Choudhury, T. Arooz, J. Yan, C. T. Lim, S. Shen, C. Hong Tan, H. Yu, Biomaterials 2010, 31, 7455.

255 N. Su, L.-Y. Jiang, X. Wang, P.-L. Gao, J. Zhou, C.-Y. Wang, Y. Luo, Biomacromolecules 2019, 20, 1007.

256. A. Meddahi-Pellé, A. Legrand, A. Marcellan, L. Louedec, D. Letourneur, L. Leibler, Angew. Chem., Int. Ed. 2014, 53, 6369.

257. S. Rose, A. Prevoteau, P. Elzière, D. Hourdet, A. Marcellan, L. Leibler, Nature 2014, 505, 382.

258. G. Beaune, U. Nagarajan, F. Brochard-Wyart, F. M. Winnik, Langmuir 2019, 35, 7396.

259. B. M. Mattix, T. R. Olsen, M. Casco, L. Reese, J. T. Poole, J. Zhang, R. P. Visconti, A. Simionescu, D. T. Simionescu, F. Alexis, Biomaterials 2014, 35, 949.

260. M. T. Stephan, J. J. Moon, S. H. Um, A. Bersthteyn, D. J. Irvine, Nat. Med. 2010, 16, 1035.

261. M. T. Stephan, S. B. Stephan, P. Bak, J. Chen, D. J. Irvine, Biomaterials 2012, 33, 5776.

262. L. Tang, Y. Zheng, M. B. Melo, L. Mabardi, A. P. Castaño, Y.-Q. Xie, N. Li, S. B. Kudchodkar, H. C. Wong, E. K. Jeng, M. V Maus, D. J. Irvine, Nat. Biotechnol. 2018, 36, 707.

263. M. Obana, B. R. Silverman, D. A. Tirrell, J. Am. Chem. Soc. 2017, 139, 14251.

264. B. Brunel, G. Beaune, U. Nagarajan, S. Dufour, F. Brochard-Wyart, F. M. Winnik, Soft Matter 2016, 12, 7902.

265. A. C. Daquinag, G. R. Souza, M. G. Kolonin, Tissue Eng., Part C 2013, 19, 336.

266. S. Yaman, M. Anil-Inevi, E. Ozcivici, H. C. Tekin, Front. Bioeng. Biotechnol. 2018, 6, 192.

267. F. Mazuel, A. Espinosa, N. Luciani, M. Reffay, R. Le Borgne, L. Motte, K. Desboeufs, A. Michel, T. Pellegrino, Y. Lalatonne, ACS Nano 2016, 10, 7627.

268. B. R. Whatley, X. Li, N. Zhang, X. Wen, J. Biomed. Mater. Res., Part A 2014, 102, 1537.

269. A. Seidi, M. Ramalingam, I. Elloumi-Hannachi, S. Ostrovidov, A. Khademhosseini, Acta Biomater. 2011, 7, 1441.

270. J. F. Mano, Mater. Lett. 2015, 141, 198.

271. X. Zhang, L. Chen, K. H. Lim, S. Gonuguntla, K. W. Lim, D. Pranantyo, W. P. Yong, W. J. T. Yam, Z. Low, W. J. Teo, H. P. Nien, Q. W. Loh, S. Soh, Adv. Mater. 2019, 31, 1804540.

272. D. W. Howell, C. W. Peak, K. J. Bayless, A. K. Gaharwar, Adv. Biosyst. 2018, 2, 1800092.

273. L. M. Cross, J. K. Carrow, X. Ding, K. A. Singh, A. K. Gaharwar, ACS Appl. Mater. Interfaces 2019, 11, 6741.

274. C. Li, J. P. Armstrong, I. J. Pence, W. Kit-Anan, J. L. Puetzer, S. Correia Carreira, A. C. Moore, M. M. Stevens, Biomaterials 2018, 176, 24.

275. E. Guisasola, A. Baeza, L. Asín, J. M. de la Fuente, M. Vallet-Regí, Small Methods 2018, 2, 1800007.

276. L. R. Polstein, M. Juhas, G. Hanna, N. Bursac, C. A. Gersbach, ACS Synth. Biol. 2017, 6, 2003.

277. K. Huang, Q. Dou, X. J. Loh, RSC Adv. 2016, 6, 60896.

278. P. Cai, B. Hu, W. R. Leow, X. Wang, X. J. Loh, Y. Wu, X. Chen, Adv. Mater. 2018, 30, 1800572.

279. M. Mehrali, A. Thakur, C. P. Pennisi, S. Talebian, A. Arpanaei, M. Nikkhah, A. Dolatshahi-Pirouz, Adv. Mater. 2016, 29, 1603612.

280. K. Ashtari, H. Nazari, H. Ko, P. Tebon, M. Akhshik, M. Akbari, S. N. Alhosseini, M. Mozafari, B. Mehravi, M. Soleimani, R. Ardehali, M. Ebrahimi Warkiani, S. Ahadian, A. Khademhosseini, Adv. Drug Delivery Rev. 2019, 144, 162.

281. A. J. Ryan, C. J. Kearney, N. Shen, U. Khan, A. G. Kelly, C. Probst, E. Brauchle, S. Biccai, C. D. Garciarena, V. Vega-mayoral, P. Loskill, S. W. Kerrigan, D. J. Kelly, K. Schenke-Layland, J. N. Coleman, F. J. O'Brien, Adv. Mater. 2018, 30, 1706442.

282. T. Dvir, B. P. Timko, M. D. Brigham, S. R. Naik, S. S. Karajanagi, O. Levy, H. Jin, K. K. Parker, R. Langer, D. S. Kohane, Nat. Nanotechnol. 2011, 6, 720.

283. D. J. Richards, Y. Tan, R. Coyle, Y. Li, R. Xu, N. Yeung, A. Parker, D. R. Menick, B. Tian, Y. Mei, Nano Lett. 2016, 16, 4670.

284. J. Ge, E. Neofytou, T. J. Cahill III, R. E. Beygui, R. N. Zare, ACS Nano 2012, 6, 227.

285. G. Thrivikraman, S. K. Boda, B. Basu, Biomaterials 2018, 150, 60.

286. N. Ashammakhi, S. Ahadian, C. Xu, H. Montazerian, H. Ko, R. Nasiri, N. Barros, A. Khademhosseini, Mater. Today Bio 2019, 1, 100008.

287. G. Bouguéon, T. Kauss, B. Dessane, P. Barthélémy, S. Crauste-Manciet, Drug Discovery Today 2018, 24, 163.

288. S. Hong, D. Sycks, H. F. Chan, S. Lin, G. P. Lopez, F. Guilak, K. W. Leong, X. Zhao, Adv. Mater. 2015, 27, 4034.

289. J. R. Xavier, T. Thakur, P. Desai, M. K. Jaiswal, N. Sears, E. Cosgriff-Hernandez, R. Kaunas, A. K. Gaharwar, ACS Nano 2015, 9, 3109.

290. G. Cidonio, C. R. Alcala-Orozco, K. S. Lim, M. Glinka, I. Mutreja, Y.-H. Kim, J. I. Dawson, T. B. F. Woodfield, R. O. C. Oreffo, Biofabrication 2019, 11, 035027.

291. S. Afewerki, L. S. S. M. Magalhães, A. D. R. Silva, T. D. Stocco, E. C. Silva Filho, F. R. Marciano, A. O. Lobo, Adv. Healthcare Mater. 2019, 8, 1900158.

292. C. W. Peak, K. A. Singh, M. Adlouni, J. Chen, A. K. Gaharwar, Adv. Healthcare Mater. 2019, 8, 1801553.

293. C. W. Peak, J. Stein, K. A. Gold, A. K. Gaharwar, Langmuir 2018, 34, 917.

294. D. Chimene, C. W. Peak, J. L. Gentry, J. K. Carrow, L. M. Cross, E. Mondragon, G. B. Cardoso, R. Kaunas, A. K. Gaharwar, ACS Appl. Mater. Interfaces 2018, 10, 9957.

295. K. Zhu, S. R. Shin, T. van Kempen, Y.-C. Li, V. Ponraj, A. Nasajpour, S. Mandla, N. Hu, X. Liu, J. Leijten, Y.-D. Lin, M. A. Hussain, Y. S. Zhang, A. Tamayol, A. Khademhosseini, Adv. Funct. Mater. 2017, 27, 1605352.

296. M. S. Mannoor, Z. Jiang, T. James, Y. L. Kong, K. A. Malatesta, W. O. Soboyejo, N. Verma, D. H. Gracias, M. C. McAlpine, Nano Lett. 2013, 13, 2634.

297. S. Shin, H. Kwak, J. Hyun, ACS Appl. Mater. Interfaces 2018, 10, 23573.

298. M. Lee, K. Bae, P. Guillon, J. Chang, Ø. Arlov, M. Zenobi-Wong, ACS Appl. Mater. Interfaces 2018, 10, 37820.

299. T. J. McKee, G. Perlman, M. Morris, S. V Komarova, Sci. Rep. 2019, 9, 10542.

300. M. Betsch, C. Cristian, Y. Lin, A. Blaeser, J. Schöneberg, M. Vogt, E. M. Buhl, H. Fischer, D. F. Duarte Campos, Adv. Healthcare Mater. 2018, 7, 1800894.

301. R. H. Fang, A. V. Kroll, W. Gao, L. Zhang, Adv. Mater. 2018, 30, 1706759.

302. Q. D. Mac, D. V. Mathews, J. A. Kahla, C. M. Stoffers, O. M. Delmas, B. A. Holt, A. B. Adams, G. A. Kwong, Nat. Biomed. Eng. 2019, 3, 281.

303. E. Trampe, K. Koren, A. R. Akkineni, C. Senwitz, F. Krujatz, A. Lode, M. Gelinsky, M. Kühl, Adv. Funct. Mater. 2018, 28, 1804411.

304 K. M. Z. Hossain, U. Patel, I. Ahmed, Prog. Biomater. 2015, 4, 1.

305. M. B. Oliveira, J. F. Mano, Biotechnol. Prog. 2011, 27, 897.

306. M. D. Neto, M. B. Oliveira, J. F. Mano, Trends Biotechnol. 2019, 37, 1011.

307. S. Bale, A. Khurana, A. S. S. Reddy, M. Singh, C. Godugu, Crit. Rev. Ther. Drug Carrier Syst. 2016, 33, 309.

308. J. Xu, D. H. C. Wong, J. D. Byrne, K. Chen, C. Bowerman, J. M. DeSimone, Angew. Chem., Int. Ed. 2013, 52, 6580.

309. W. Li, L. Zhang, X. Ge, B. Xu, W. Zhang, L. Qu, C.-H. Choi, J. Xu, A. Zhang, H. Lee, Chem. Soc. Rev. 2018, 47, 5646.

310. T. Nisisako, T. Torii, Adv. Mater. 2007, 19, 1489.

311. R. K. Kankala, J. Zhao, C.-G. Liu, X.-J. Song, D.-Y. Yang, K. Zhu, S.-B. Wang, Y. S. Zhang, A.-Z. Chen, Small 2019, 15, 1901397.

312. M. Hayakawa, H. Onoe, K. H. Nagai, M. Takinoue, Sci. Rep. 2016, 6, 20793.

313. A. C. Lima, P. Sher, J. F. Mano, Expert Opin. Drug Delivery 2012, 9, 231.

314. C. A. Custódio, M. T. Cerqueira, A. P. Marques, R. L. Reis, J. F. Mano, Biomaterials 2015, 43, 23.

315. C. C. Ahrens, Z. Dong, W. Li, Acta Biomater. 2017, 62, 64.

316. D. L. Elbert, Curr. Opin. Biotechnol. 2011, 22, 674.

317. D. Smith, C. Herman, S. Razdan, M. R. Abedin, W. Van Stoecker, S. Barua, ACS Appl. Bio Mater. 2019, 2, 2791.

318. W. Leong, D. A. Wang, Trends Biotechnol. 2015, 33, 653.

319. J. C. Rose, L. De Laporte, Adv. Healthcare Mater. 2018, 7, 1701067.

320. A. Leferink, D. Schipper, E. Arts, E. Vrij, N. Rivron, M. Karperien, K. Mittmann, C. Van Blitterswijk, L. Moroni, R. Truckenmüller, Adv. Mater. 2014, 26, 2592.

321. A. M. Bratt-Leal, A. H. Nguyen, K. A. Hammersmith, A. Singh, T. C. McDevitt, Biomaterials 2013, 34, 7227.

322A. K. Kudva, A. D. Dikina, F. P. Luyten, E. Alsberg, J. Patterson, Acta Biomater. 2019, 90, 287.

323. Y. Zhang, H. Mao, C. Gao, S. Li, Q. Shuai, J. Xu, K. Xu, L. Cao, R. Lang, Z. Gu, T. Akaike, J. Yang, Adv. Healthcare Mater. 2016, 5, 1949.

324. S. Aday, J. Zoldan, M. Besnier, L. Carreto, J. Saif, R. Fernandes, T. Santos, L. Bernardino, R. Langer, C. Emanueli, Nat. Commun. 2017, 8, 747.

325. H. Y. Kim, S. Y. Kim, H.-Y. Lee, J. H. Lee, G.-J. Rho, H.-J. Lee, H.-C. Lee, J.-H. Byun, S. H. Oh, Biomacromolecules 2019, 20, 1087.

326. D. X. Wei, J. W. Dao, G. Q. Chen, Adv. Mater. 2018, 30, 1802273.

327. N. Dinh, R. Luo, M. T. A. Christine, W. N. Lin, W. Shih, J. C. Goh, C. Chen, Small 2017, 13, 1700684.

328. S. Yoshida, M. Takinoue, H. Onoe, 2016 IEEE 29th Int. Conf. on Micro Electro Mechanical Systems, IEEE, Piscataway, NJ, USA 2016, pp. 263– 266.

329. S. Yoshida, M. Takinoue, H. Onoe, Adv. Healthcare Mater. 2017, 6, 1601463.

330. H. Zheng, W. Du, Y. Duan, K. Geng, J. Deng, C. Gao, ACS Appl. Mater. Interfaces 2018, 10, 36776.

331. S. M. Bittner, J. L. Guo, A. G. Mikos, Bioprinting 2018, 12, e00032.

332. Y. Luo, X. Wei, P. Huang, J. Biomed. Mater. Res., Part B 2019, 107, 1695.

333. M. T. Poldervaart, H. Gremmels, K. van Deventer, J. O. Fledderus, F. C. Öner, M. C. Verhaar, W. J. A. Dhert, J. Alblas, J. Controlled Release 2014, 184, 58.

334 M. T. Poldervaart, H. Wang, J. van der Stok, H. Weinans, S. C. G. Leeuwenburgh, F. C. Öner, W. J. A. Dhert, J. Alblas, PLoS One 2013, 8, e72610.

335. S. Hu, B. M. Ogle, K. Cheng, Curr. Opin. Cell Biol. 2018, 54, 37.

336. R. Levato, J. Visser, J. A. Planell, E. Engel, J. Malda, M. A. Mateos-Timoneda, Biofabrication 2014, 6, 035020.

337. K. S. Sen, D. F. Duarte Campos, M. Köpf, A. Blaeser, H. Fischer, Adv. Healthcare Mater. 2018, 7, 1800343.

338. A. Kosik-Kozioł, M. Costantini, A. Mróz, J. Idaszek, M. Heljak, J. Jaroszewicz, E. Kijeńska, K. Szöke, N. Frerker, A. Barbetta, J. E. Brinchmann, W. Święszkowski, Biofabrication 2019, 11, 035016.

339. J. Idaszek, M. Costantini, T. A. Karlsen, J. Jaroszewicz, C. Colosi, S. Testa, E. Fornetti, S. Bernardini, M. Seta, K. Kasarełło, R. Wrzesień, S. Cannata, A. Barbetta, C. Gargioli, J. E. Brinchman, W. Święszkowski, Biofabrication 2019, 11, 044101.

340. G. Huang, F. Li, X. Zhao, Y. Ma, Y. Li, M. Lin, G. Jin, T. J. Lu, G. M. Genin, F. Xu, Chem. Rev. 2017, 117, 12764.

341. E. Cukierman, R. Pankov, D. R. Stevens, K. M. Yamada, Science 2001, 294, 1708.

342. Y. Luo, M. S. Shoichet, Nat. Mater. 2004, 3, 249.

343. C. A. DeForest, D. A. Tirrell, Nat. Mater. 2015, 14, 523.

344. C. A. DeForest, K. S. Anseth, Nat. Chem. 2011, 3, 925.

345. C. K. Arakawa, B. A. Badeau, Y. Zheng, C. A. DeForest, Adv. Mater. 2017, 29, 1703156.

346. A. M. Kloxin, A. M. Kasko, C. N. Salinas, K. S. Anseth, Science 2009, 324, 59.

347. J. C. Culver, J. C. Hoffmann, R. A. Poché, J. H. Slater, J. L. West, M. E. Dickinson, Adv. Mater. 2012, 24, 2344.

348. C. Jungnickel, M. V. Tsurkan, K. Wogan, C. Werner, M. Schlierf, Adv. Mater. 2017, 29, 1603327.

349. M. V Tsurkan, C. Jungnickel, M. Schlierf, C. Werner, J. Am. Chem. Soc. 2017, 139, 10184.

350. S. Zhang, Nat. Biotechnol. 2003, 21, 1171.

351. C. Huang, D. Quinn, S. Suresh, K. J. Hsia, Proc. Natl. Acad. Sci. USA 2018, 115, 70.

352. W. Y. Seow, C. A. E. Hauser, Mater. Today 2014, 17, 381.

353. A. Aggeli, M. Bell, N. Boden, J. N. Keen, P. F. Knowles, T. C. McLeish, M. Pitkeathly, S. E. Radford, Nature 1997, 386, 259.

354. S. Zhang, T. Holmes, C. Lockshin, A. Rich, Proc. Natl. Acad. Sci. USA 1993, 90, 3334.

355. G. Fichman, E. Gazit, Acta Biomater. 2014, 10, 1671.

356. X.-Q. Dou, C.-L. Feng, Adv. Mater. 2017, 29, 1604062.

357. J. P. Schneider, D. J. Pochan, B. Ozbas, K. Rajagopal, L. Pakstis, J. Kretsinger, J. Am. Chem. Soc. 2002, 124, 15030.

358. M. Reches, E. Gazit, Nano Lett. 2004, 4, 581.

359. C. Tomasini, N. Castellucci, Chem. Soc. Rev. 2013, 42, 156.

360. K. Sato, W. Ji, L. C. Palmer, B. Weber, M. Barz, S. I. Stupp, J. Am. Chem. Soc. 2017, 139, 8995.

361. A. Schneider, J. A. Garlick, C. Egles, PLoS One 2008, 3, e1410.

362. M. E. Davis, J. P. M. Motion, D. A. Narmoneva, T. Takahashi, D. Hakuno, R. D. Kamm, S. Zhang, R. T. Lee, Circulation 2005, 111, 442.

363. R. G. Ellis-Behnke, Y.-X. Liang, S.-W. You, D. K. C. Tay, S. Zhang, K.-F. So, G. E. Schneider, Proc. Natl. Acad. Sci. USA 2006, 103, 5054.

364. C. E. Semino, J. R. Merok, G. G. Crane, G. Panagiotakos, S. Zhang, Differentiation 2003, 71, 262.

365. A. N. Edelbrock, Z. Àlvarez, D. Simkin, T. Fyrner, S. M. Chin, K. Sato, E. Kiskinis, S. I. Stupp, Nano Lett. 2018, 18, 6237.

366. R. N. Shah, N. A. Shah, M. M. D. R. Lim, C. Hsieh, G. Nuber, S. I. Stupp, Proc. Natl. Acad. Sci. USA 2010, 107, 3293.

367. T.-Y. Cheng, M.-H. Chen, W.-H. Chang, M.-Y. Huang, T.-W. Wang, Biomaterials 2013,

368. E. J. Berns, S. Sur, L. Pan, J. E. Goldberger, S. Suresh, S. Zhang, J. A. Kessler, S. I. Stupp, Biomaterials 2014, 35, 185.

369. A. J. Matsuoka, Z. A. Sayed, N. Stephanopoulos, E. J. Berns, A. R. Wadhwani, Z. D. Morrissey, D. M. Chadly, S. Kobayashi, A. N. Edelbrock, T. Mashimo, C. A. Miller, T. L. McGuire, S. I. Stupp, J. A. Kessler, PLoS One 2017, 12, e0190150.

370. E. J. Berns, Z. Alvarez, J. E. Goldberger, J. Boekhoven, J. A. Kessler, H. G. Kuhn, S. I. Stupp, Acta Biomater. 2016, 37, 50.

371. M. Miotto, R. M. Gouveia, A. M. Ionescu, F. Figueiredo, I. W. Hamley, C. J. Connon, Adv. Funct. Mater. 2019, 29, 1807334.

372. L. Liu, J. A. Shadish, C. K. Arakawa, K. Shi, J. Davis, C. A. DeForest, Adv. Biosyst. 2018, 2, 1800240.

373. K. T. Dicker, J. Song, A. C. Moore, H. Zhang, Y. Li, D. L. Burris, X. Jia, J. M. Fox, Chem. Sci. 2018, 9, 5394.

374. .K. T. Dicker, A. C. Moore, N. Garabedian, H. Zhang, S. L. Scinto, R. E. Akins, D. L. Burris, J. M. Fox, X. Jia, ACS Appl. Mater. Interfaces 2019, 11, 16402.

375 H. Wang, S. C. Heilshorn, Adv. Mater. 2015, 27, 3717.

376. M. Hörning, M. Nakahata, P. Linke, A. Yamamoto, M. Veschgini, S. Kaufmann, Y. Takashima, A. Harada, M. Tanaka, Sci. Rep. 2017, 7, 7660.

377. C. B. Rodell, A. L. Kaminski, J. A. Burdick, Biomacromolecules 2013, 14, 4125.

378. A. C. Gaffey, M. H. Chen, C. M. Venkataraman, A. Trubelja, C. B. Rodell, P. V. Dinh, G. Hung, J. W. MacArthur, R. V. Soopan, J. A. Burdick, P. Atluri, J. Thorac. Cardiovasc. Surg. 2015, 150, 1268.

379. K. Wei, X. Chen, R. Li, Q. Feng, L. Bian, Chem. Mater. 2017, 29, 8604.

380. X.-Q. Dou, J. Zhang, C. Feng, ACS Appl. Mater. Interfaces 2015, 7, 20786.

381. K. M. Park, J.-A. Yang, H. Jung, J. Yeom, J. S. Park, K.-H. Park, A. S. Hoffman, S. K. Hahn, K. Kim, ACS Nano 2012, 6, 2960.

382. B. W. Hwang, Y.-E. Kim, M. Kim, S. Han, S. Bok, K. M. Park, A. Shrinidhi, K. S. Kim, G.-O. Ahn, S. K. Hahn, RSC Adv. 2018, 8, 18771.

383. H. Jung, J. S. Park, J. Yeom, N. Selvapalam, K. M. Park, K. Oh, J.-A. Yang, K. H. Park, S. K. Hahn, K. Kim, Biomacromolecules 2014, 15, 707.

384. H. D. Lu, M. B. Charati, I. L. Kim, J. A. Burdick, Biomaterials 2012, 33, 2145.

385. I. Willner, Acc. Chem. Res. 2017, 50, 657.

386. J. Jin, Y. Xing, Y. Xi, X. Liu, T. Zhou, X. Ma, Z. Yang, S. Wang, D. Liu, Adv. Mater. 2013, 25, 4714.

387. H. Stoll, H. Steinle, K. Stang, S. Kunnakattu, L. Scheideler, B. Neumann, J. Kurz, I. Degenkolbe, N. Perle, C. Schlensak, Macromol. Biosci. 2017, 17, 1600252.

388. F. Ding, Q. Mou, Y. Ma, G. Pan, Y. Guo, G. Tong, C. H. J. Choi, X. Zhu, C. Zhang, Angew. Chem., Int. Ed. 2018, 57, 3064.

389 C. Li, A. Faulkner-Jones, A. R. Dun, J. Jin, P. Chen, Y. Xing, Z. Yang, Z. Li, W. Shu, D. Liu, Angew. Chem., Int. Ed. 2015, 54, 3957.

390. C. Wang, M. Fadeev, M. Vázquez-González, I. Willner, Adv. Funct. Mater. 2018, 28, 1803111.

391. C. Li, M. J. Rowland, Y. Shao, T. Cao, C. Chen, H. Jia, X. Zhou, Z. Yang, O. A. Scherman, D. Liu, Adv. Mater. 2015, 27, 3298.

392. Y. Hu, C. M. Niemeyer, Adv. Mater. 2019, 31, 1806294.

393. N. Park, S. H. Um, H. Funabashi, J. Xu, D. Luo, Nat. Mater. 2009, 8, 432.

394. T. Xu, W. Zhao, J.-M. Zhu, M. Z. Albanna, J. J. Yoo, A. Atala, Biomaterials 2013, 34, 130.

395. S. Yoon, J. A. Park, H.-R. Lee, W. H. Yoon, D. S. Hwang, S. Jung, Adv. Healthcare Mater. 2018, 7, 1800050.

396. K. Christensen, C. Xu, W. Chai, Z. Zhang, J. Fu, Y. Huang, Biotechnol. Bioeng. 2015, 112, 1047.

397. A. Negro, T. Cherbuin, M. P. Lutolf, Sci. Rep. 2018, 8, 17099.

398. M. A. Heinrich, W. Liu, A. Jimenez, J. Yang, A. Akpek, X. Liu, Q. Pi, X. Mu, N. Hu, R. M. Schiffelers, J. Prakash, J. Xie, Y. S. Zhang, Small 2019, 15, 1805510.

399. W. Liu, Y. S. Zhang, M. A. Heinrich, F. De Ferrari, H. L. Jang, S. M. Bakht, M. M. Alvarez, J. Yang, Y.-C. Li, G. Trujillo-de Santiago, A. K. Miri, K. Zhu, P. Khoshakhlagh, G. Prakash, H. Cheng, X. Guan, Z. Zhong, J. Ju, G. H. Zhu, X. Jin, S. R. Shin, M. R. Dokmeci, A. Khademhosseini, Adv. Mater. 2017, 29, 1604630.

400. A. K. Miri, D. Nieto, L. Iglesias, H. Goodarzi Hosseinabadi, S. Maharjan, G. U. Ruiz-Esparza, P. Khoshakhlagh, A. Manbachi, M. R. Dokmeci, S. Chen, S. R. Shin, Y. S. Zhang, A. Khademhosseini, Adv. Mater. 2018, 30, 1800242.

401. P. N. Bernal, P. Delrot, D. Loterie, Y. Li, J. Malda, C. Moser, R. Levato, Adv. Mater. 2019, 1904209.

402. O. Jeon, Y. B. Lee, T. J. Hinton, A. W. Feinberg, E. Alsberg, Mater. Today Chem. 2019, 12, 61.

403. G. Ying, N. Jiang, S. Maharjan, Y. Yin, R. Chai, X. Cao, J. Yang, A. K. Miri, S. Hassan, Y. S. Zhang, Adv. Mater. 2018, 30, 1805460.

404. W. Jia, P. S. Gungor-Ozkerim, Y. S. Zhang, K. Yue, K. Zhu, W. Liu, Q. Pi, B. Byambaa, M. R. Dokmeci, S. R. Shin, A. Khademhosseini, Biomaterials 2016, 106, 58.

405. Q. Pi, S. Maharjan, X. Yan, X. Liu, B. Singh, A. M. van Genderen, F. Robledo-Padilla, R. Parra-Saldivar, N. Hu, W. Jia, C. Xu, J. Kang, S. Hassan, H. Cheng, X. Hou, A. Khademhosseini, Y. S. Zhang, Adv. Mater. 2018, 30, 1706913.

406. C. Colosi, S. R. Shin, V. Manoharan, S. Massa, M. Costantini, A. Barbetta, M. R. Dokmeci, M. Dentini, A. Khademhosseini, Adv. Mater. 2016, 28, 677.

407. W. Zhu, X. Qu, J. Zhu, X. Ma, S. Patel, J. Liu, P. Wang, C. S. E. Lai, M. Gou, Y. Xu, K. Zha.ng, S. Chen, Biomaterials 2017, 124, 106.

408. X. Ma, X. Qu, W. Zhu, Y.-S. Li, S. Yuan, H. Zhang, J. Liu, P. Wang, C. S. E. Lai, F. Zanella, G.-S. Feng, F. Sheikh, S. Chien, S. Chen, Proc. Natl. Acad. Sci. USA 2016, 113, 2206.

409. .K. Zhu, N. Chen, X. Liu, X. Mu, W. Zhang, C. Wang, Y. S. Zhang, Macromol. Biosci. 2018, 18, 1800127.

410. C. L. Hedegaard, E. C. Collin, C. Redondo-Gómez, L. T. H. Nguyen, K. W. Ng, A. A. Castrejón-Pita, J. R. Castrejón-Pita, A. Mata, Adv. Funct. Mater. 2018, 28, 1703716.

411 J. S. Lee, Y. H. Roh, Y. S. Choi, Y. Jin, E. J. Jeon, K. W. Bong, S. Cho, Adv. Funct. Mater. 2019, 29, 1807803.

412. A. Blaeser, D. F. Duarte Campos, U. Puster, W. Richtering, M. M. Stevens, H. Fischer, Adv. Healthcare Mater. 2016, 5, 326.

413. C. B. Highley, C. B. Rodell, J. A. Burdick, Adv. Mater. 2015, 27, 5075.

414. O. Chaudhuri, Biomater. Sci. 2017, 5, 1480.

415. M. de Ruijter, A. Ribeiro, I. Dokter, M. Castilho, J. Malda, Adv. Healthcare Mater. 2019, 8, 1800418.

416. H. W. Kang, S. J. Lee, I. K. Ko, C. Kengla, J. J. Yoo, A. Atala, Nat. Biotechnol. 2016, 34, 312.

417. J. Lou, F. Liu, C. D. Lindsay, O. Chaudhuri, S. C. Heilshorn, Y. Xia, Adv. Mater. 2018, 30, 1705215.

418. S. C. Carreira, R. Begum, A. W. Perriman, Adv. Healthcare Mater. 2019,

419. A. Kirillova, R. Maxson, G. Stoychev, C. T. Gomillion, L. Ionov, Adv. Mater. 2017, 29, 1703443.

420. Y. Luo, X. Lin, B. Chen, X. Wei, Biofabrication 2019, 11, 045019.

421. X. Kuang, J. Wu, K. Chen, Z. Zhao, Z. Ding, F. Hu, D. Fang, H. J. Qi, Sci. Adv. 2019, 5, eaav5790.

422. D. S. Hernandez, E. T. Ritschdorff, J. L. Connell, J. B. Shear, J. Am. Chem. Soc. 2018, 140, 14064.

423. C. D. Morley, S. T. Ellison, T. Bhattacharjee, C. S. O'Bryan, Y. Zhang, K. F. Smith, C. P. Kabb, M. Sebastian, G. L. Moore, K. D. Schulze, S. Niemi, W. G. Sawyer, D. D. Tran, D. A. Mitchell, B. S. Sumerlin, C. T. Flores, T. E. Angelini, Nat. Commun. 2019, 10, 3029.

424. Z. Gartner, A. Hughes, Nature 2019, 572, 38.

425. K. Witte, A. Rodrigo-Navarro, M. Salmeron-Sanchez, Mater. Today Bio 2019, 2, 100011.

426. B. Byambaa, N. Annabi, K. Yue, G. Trujillo-de de Santiago, M. M. Alvarez, W. Jia, M. Kazemzadeh-Narbat, S. R. Shin, A. Tamayol, A. Khademhosseini, Adv. Healthcare Mater. 2017, 6, 1700015.

427. C. R. Correia, S. Gil, R. L. Reis, J. F. Mano, Adv. Healthcare Mater. 2016, 5, 1346.

428. C. R. Correia, R. P. Pirraco, M. T. Cerqueira, A. P. Marques, R. L. Reis, J. F. Mano, Sci. Rep. 2016, 6, 21883.

429. P. Agarwal, H. Wang, M. Sun, J. Xu, S. Zhao, Z. Liu, K. J. Gooch, Y. Zhao, X. Lu, X. He, ACS Nano 2017, 11, 6691.

430. D. L. Lopes, C. Martins-Cruz, M. B. Oliveira, J. F. Mano, Biomaterials 2018, 185, 240.

431. J. Zhang, P. Padmanaban, J. Rouwkema, Controlling Vascularisation Within Tissue Building Blocks Using Internal and External Mechanical Cues, https://ris.utwente.nl/ws/portalfiles/portal/74570230/NBTE_2018.pdf (accessed: September 2019).

432. B. Grigoryan, S. J. Paulsen, D. C. Corbett, D. W. Sazer, C. L. Fortin, A. J. Zaita, P. T. Greenfield, N. J. Calafat, J. P. Gounley, A. H. Ta, Science 2019, 364, 458.

433C. B. Highley, K. H. Song, A. C. Daly, J. A. Burdick, Adv. Sci. 2019, 6, 1801076.

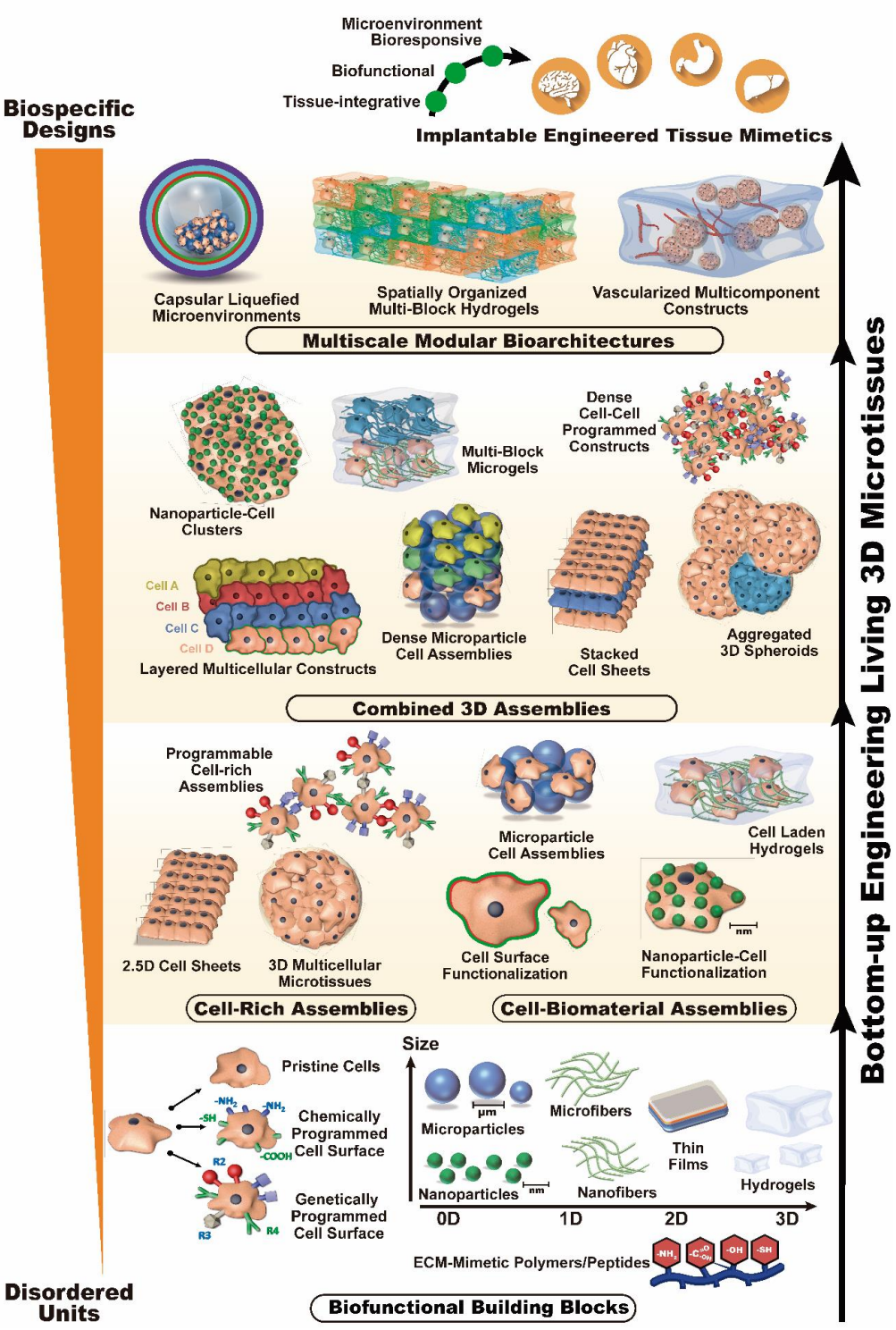

Figure 1. Schematics of tissue engineered constructs fabrication via modular bottom-up assembly methodologies based on cell-rich assemblies or cell-biomaterial assemblies and their combinations. The use of advanced packing methods such as those based on chemically or genetically controlled programming allows the design of microtissues with higher control over microarchitectural and biological features. Ultimately, engineered bottom-up living microtissues are expected to exhibit organ-specific biofunctionality, successful host-integration and microenvironment bioresponsiveness throughout time.

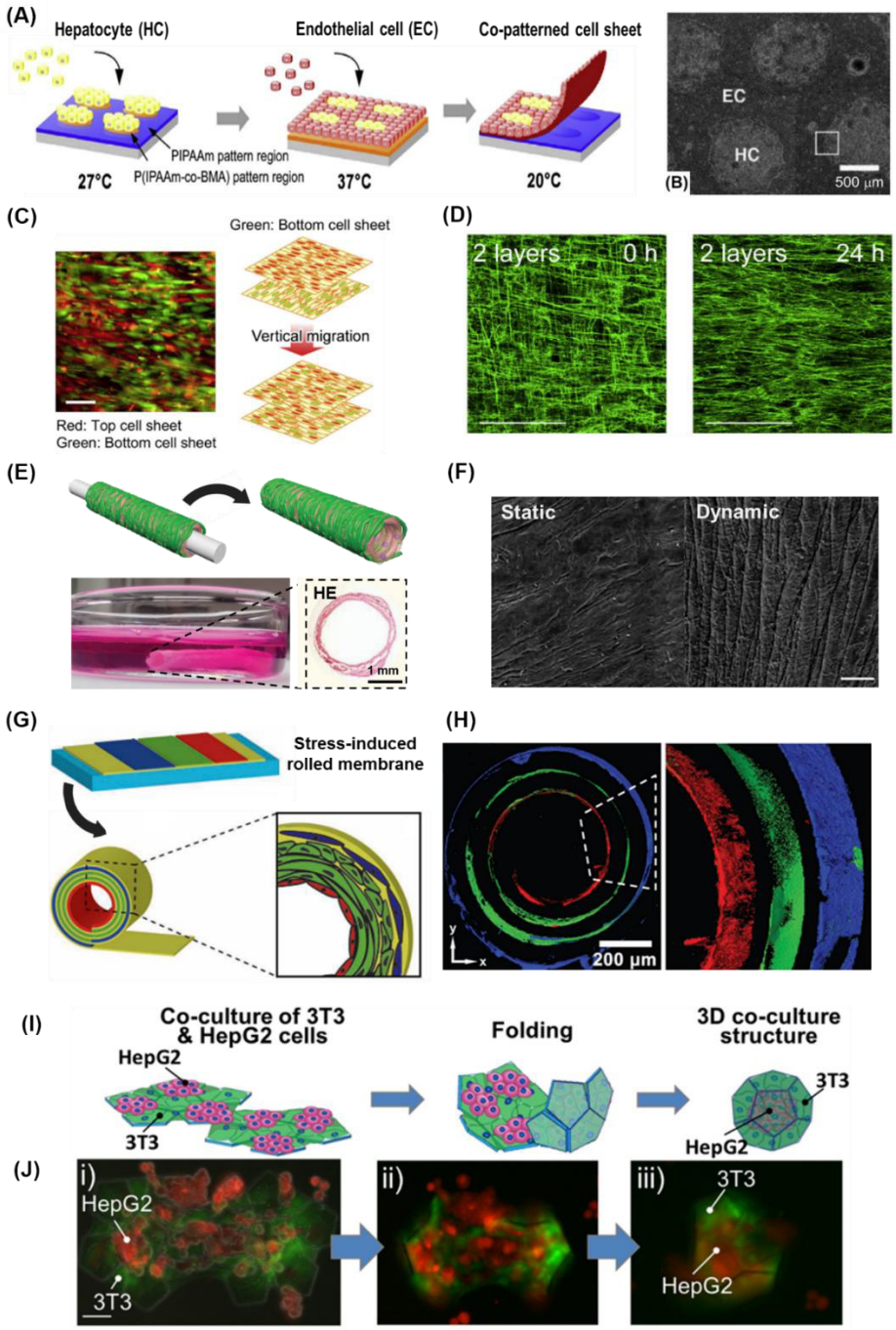

Figure 2. Assembling cell-rich multilayered constructs with advanced cell sheet engineering. **(A-B)** Co-patterned cell sheet with rat primary hepatocytes and endothelial cells in a spatially-defined distribution. Reproduced with permission.[53,54] Copyright 2005 and 2006, Elsevier. **(C-D)** Anisotropic skeletal muscle microtissue obtained by stacking aligned myoblast sheets, highlighting transferable anisotropy to bottom layers via myoblast vertical migration. Reproduced with permission.[60] Copyright 2005 and 2013 Elsevier. **(E-F)** hMSCs cell sheets rolled on a mandrel to obtain a macroscopic vascular graft that can be matured in static or dynamic conditions, yielding well-defined parallel grooves on the external surface of bioreactor-matured tubules. Reproduced with permission.[61] Copyright 2017, John Wiley & Sons, Inc. **(G-H)** Stress-induced rolling of surface patterned with multiple cell types, distributing in 3D akin to blood vessels, red shows endothelial cells, green shows SMCs, blue shows fibroblasts. Reproduced with permission.[62] Copyright 2012, John Wiley & Sons, Inc. **(I-J)** Self-folding origami inspired co-culture structures assembled from cell sheets. Reproduced with permission.[63] Copyright 2018, Nature Publishing Group.

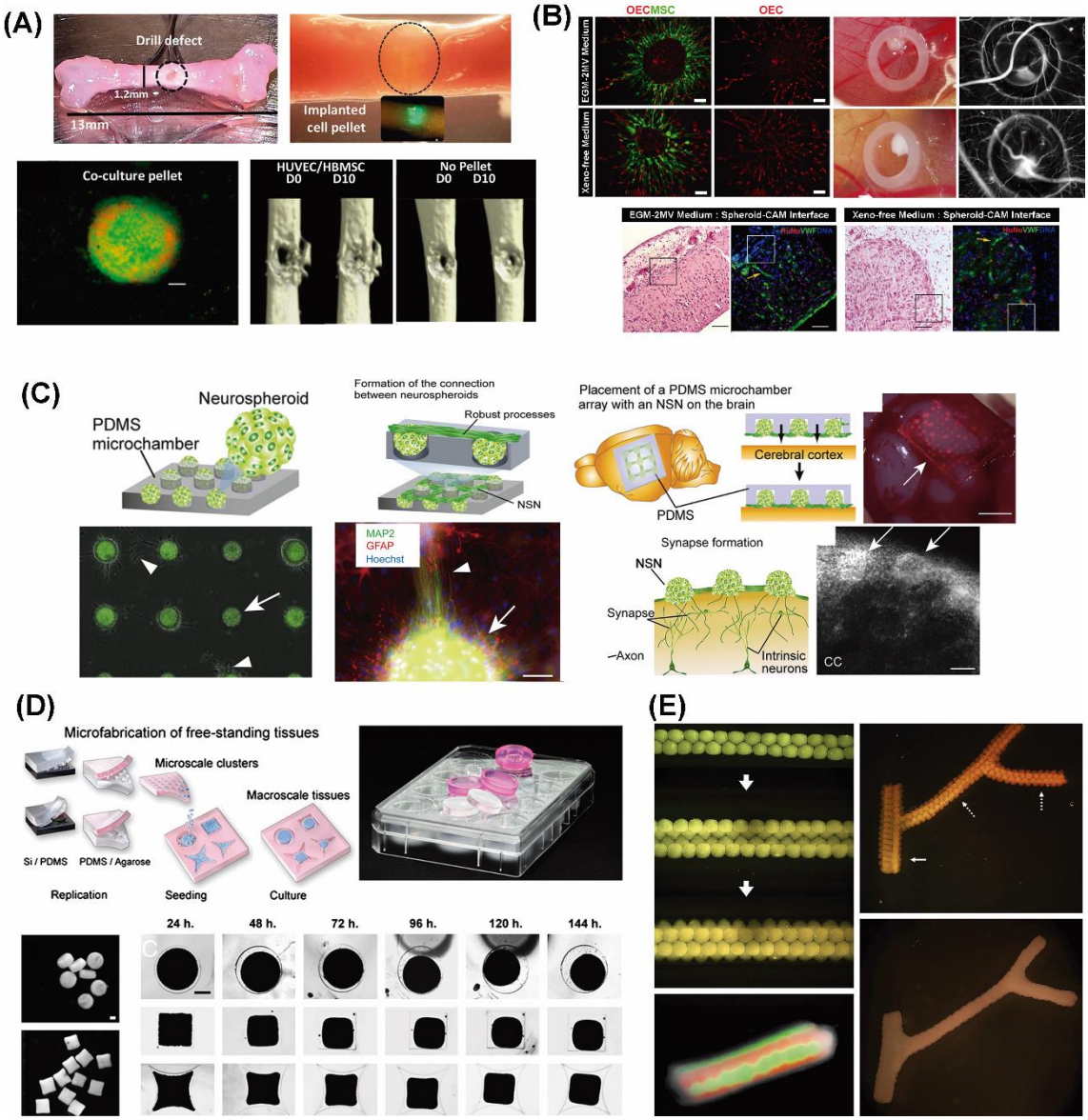

Figure 3. 3D cell-rich spheroids bottom-up tissue engineering. **(A)** 3D co-culture HUVEC/HBMSCs spheroids for improving bone healing in the osteogenic niche after implantation. Reproduced with permission.[98] Copyright 2018, Creative Commons Attribution 4.0 International (CC BY 4.0). **(B)** Co-culture OEC-MSC 3D spheroids improved angiogenic sprouting and integration into CAM under xeno-free conditions. Reproduced with permission.[100] Copyright 2018, Nature Publishing Group. **(C)** 3D neurospheroids produced in PDMS microchambers that promoted spheroids interconnection via neural processes. Scaffold-free 3D neurospheroids microarrays implantation *in vivo* led to fusion with the neuronal tissue and synapses formation. Reproduced with permission.[101] Copyright 2010, Elsevier. **(D)** Microfabricated microtissues with different architectures assembled from cell-rich 3D spheroids. Upon confinement these unitary building blocks fuse into more complex constructs. Reproduced with permission.[102] Copyright 2012, National Academy of Sciences of the United States of America. **(E)** Scaffold-free bioprinting of a complex bi-furcated vascular-like network comprised by human skin fibroblast 3D spheroids as building blocks. Reproduced with permission.[103] Copyright 2009, Elsevier.

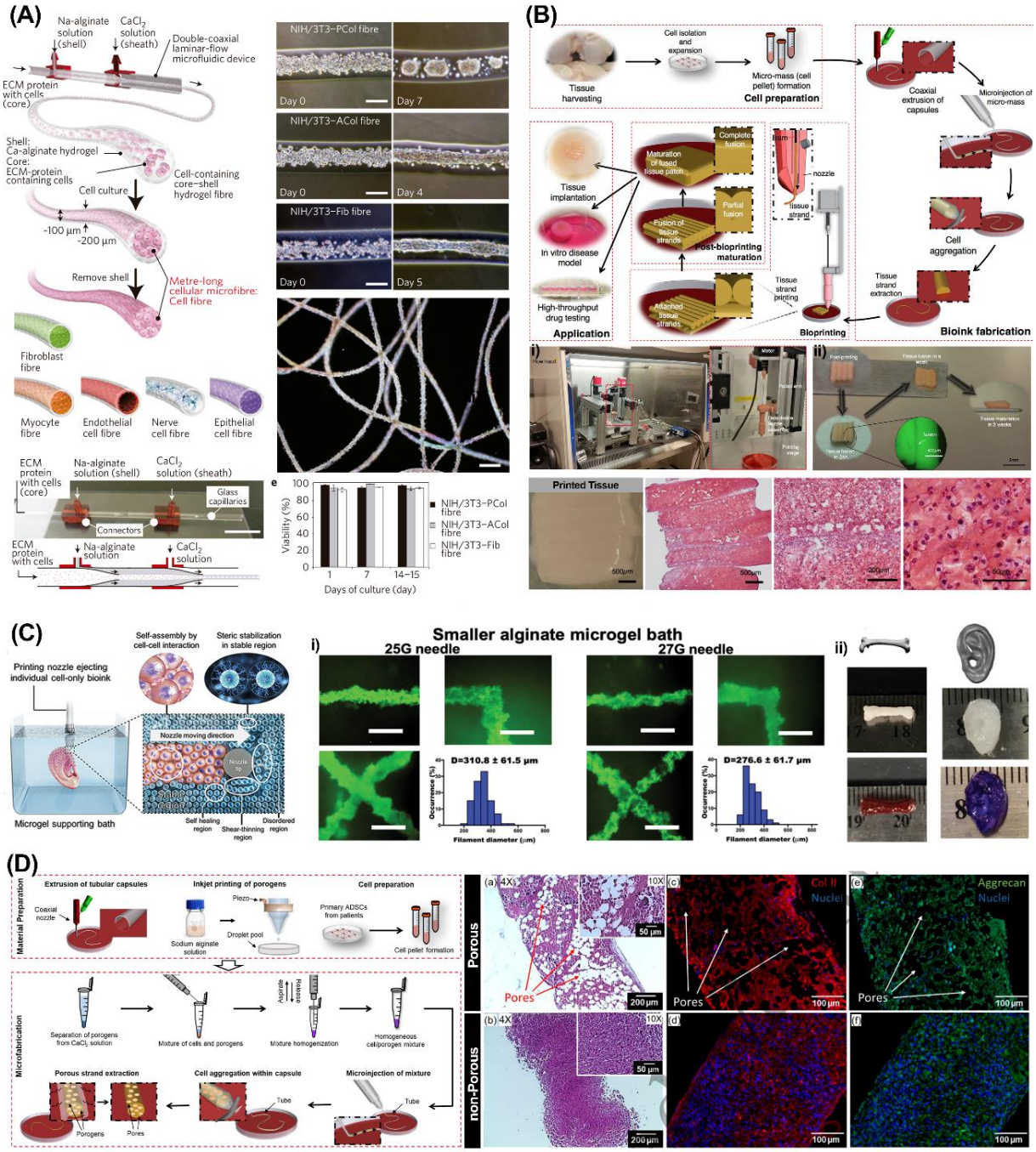

Figure 4. Fiber-shaped constructs for bottom-up tissue engineering. **(A)** Fabrication of metre-long core-shell microfibers comprised by cells-ECM protein/calcium-alginate core by using a double-coaxial microfluidic apparatus. NIH/3T3 cells encapsulation in different fiber constructs and maturation along time (Acid-solubilized type-I collagen (ACol); pepsin-solubilized type-I collagen (PCol); Fibrin (F). Reproduced with permission.[132] Copyright 2013, Nature Publishing Group. **(B)** Schematic illustration and apparatus used for 3D printing process using tissue strand bioinks. Microtissues maturation along 3 weeks of incubation exhibiting strand fusion (Green fluorescence images). Histological examination of 3D printed microfiber-based tissues exhibiting Safranin-O/Fast green proteoglycan positive staining. Reproduced with permission.[133] Copyright 2016, Creative Commons Attribution 4.0 International (CC BY 4.0). **(C)** Schematics of 3D bioprinting process with cell-rich bioink into shear-thinning and self-healing OMA alginate microgel supporting bath. Representative optical images of the printing process of letter "c" by using the stem cell-rich bioink. i) Live/dead fluorescence micrographs of 3D hMSCs cell-rich filaments, with different diameters, after bioprinting with different

nozzles. ii) Digital sketch and 3D bioprinted anatomical-inspired constructs using the cell-only bioink and the supporting medium. Reproduced with permission.[134] Copyright 2019, Royal Society of Chemistry. **(D)** Schematics of microporous tissue strands microfabrication process comprised by adipose derived MSCs (ASCs) and their improved chondrogenic differentiation in comparison to their non-porous counterparts Immunocytochemistry analysis of cartilage-specific biomarkers expression in porous (a, c, e) and non-porous (b, d, f) (Aggrecan – green channel; Collagen type II – red channel, Nuclei – blue channel). Reproduced with permission.[135] Copyright 2018, IOP Publishing Ltd.

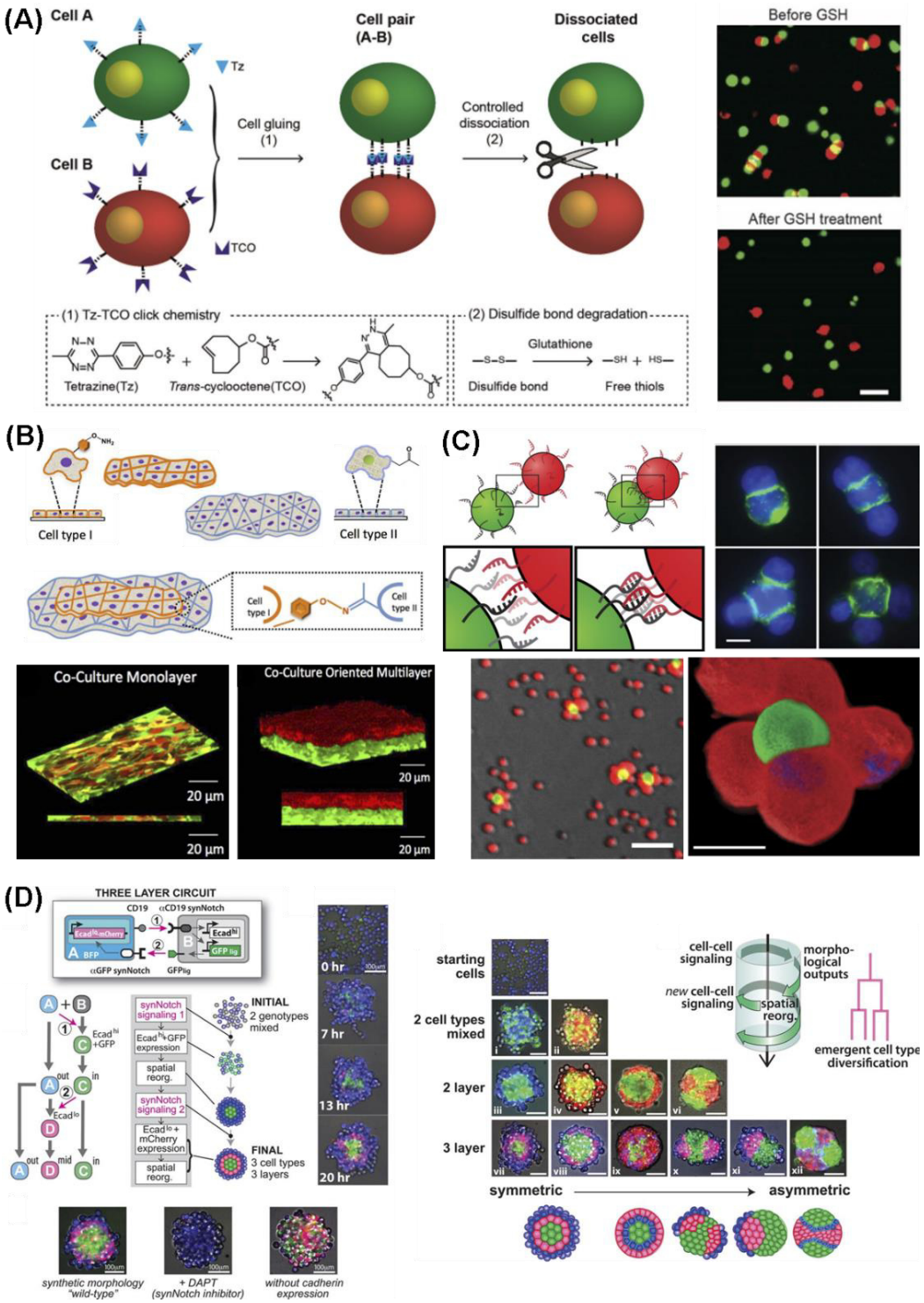

Figure 5. Cell-rich assemblies established via cell surface engineering. **(A)** Schematic illustration of redox-sensitive cell glue system based on selective click chemistry linkers. Cellular aggregates readily disassemble upon GSH treatment evidencing the stimuli-responsive features of this system. Reproduced with permission.[164] Copyright 2016, American Chemical Society. **(B)** Use of chemical surface programming via liposomal fusion technology for constructing multi-layered microtissues comprised of photo-oxyamine MSCs and ketone functionalized fibroblasts. The two cell populations assembled into co-cultured monolayers and also user-oriented multi-layers via the oxyamine linkage. Reproduced with permission.[180] Copyright 2014, Nature Publishing Group. **(C)** Schematics of programmed cell-cell selective adhesion via interaction of complementary ssDNA aptamer sequences installed at cells surface. Fluorescent labeling of Jurkat cells indicate that ssDNA clusters form at the cell-cell interface.

Assembled cell-rich 3D microtissues with controlled cellular stoichiometries (1:50) for establishing neighboring selective microenvironments. Reproduced with permission.[181] Copyright 2009, National Academy of Sciences of the United States of America. **(D)** Engineering self-organizing multicellular spheroids via genetic engineering using a 3-layer circuit approach. Cell fate is governed by reciprocal interactions established between A-type and B-type cells which give rise to bifurcated phenotypes. The system is based on two disordered cell genotypes and self-assembles into 3 different cell phenotypes organized in 3 different layers. The synNotch-adhesion programming kit leads to a gallery of self-driven, spatially organized compartments and increasing shape asymmetry, sharing similarities with natural cell-cell signaling and tissue morphogenesis. Reproduced with permission.[143] Copyright 2018, American Association for the Advancement of Science (AAAS).

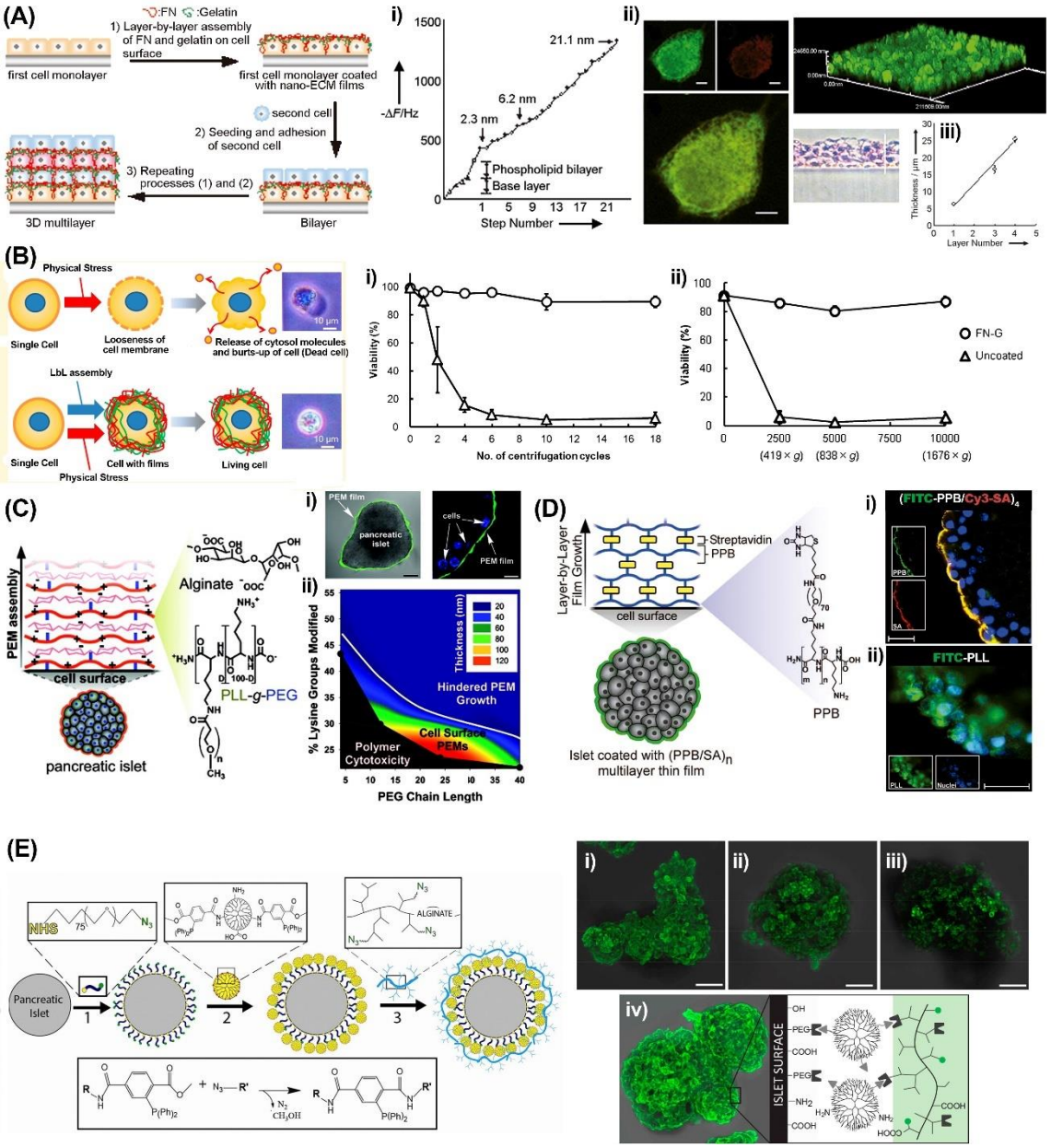

Figure 6. Layer-by-layer technologies for cell-surface functionalization and bottom-up assembly of microtissue constructs. **(A)** Schematics of cell surface functionalization with nanometer-sized coatings and 3D cellular multilayers fabrication process. i) QCM evaluation of the LbL assembly process of FN/G onto a phospholipid bilayer (DPPC/DPPA 4:1). ii) CLSM micrographs of L929 fibroblasts coated with seven-bilayers of FN/G and CLSM 3D reconstruction and histological analysis of four-layered L929 constructs. iii) Linear correlation between L929 cell layer number and constructs mean thickness via CLSM. Reproduced with permission.[201] Copyright 2007, John Wiley & Sons, Inc. **(B)** Schematics of LbL cell surface functionalization and physical stress effect on cellular activity/viability during nanocoating via centrifugation. i and ii) Cell viability of HepG2 cell with and without FN/G protection after various centrifugations and at different rotational speeds, respectively. Reproduced with permission.[206] Copyright 2013, American Chemical Society. **(C)** Schematic illustration of islets coated with PLL-*g*-PEG polyelectrolyte multilayered (PEM) films. i and ii) Successful islets functionalization and contour plot demonstrating the relationship between film thickness, copolymer structure and cellular toxicity, respectively. Reproduced with permission.[207] Copyright 2011, American Chemical Society. **(D)** Schematics of Islet sequential coating with

PPB/SA and consequent film growth. i) Fluorescence micrographs of $(PPB/SA)_4$ multilayer films localized on cells surface and islets periphery. ii) FITC-PLL is observed in cells nuclei and distributed across the cytoplasm. (Blue channel – nuclei). Reproduced with permission.[194] Copyright 2008, American Chemical Society. **(E)** Schematics of ultrathin coatings assembly comprised by MDT-PAMAM (2) on the surface of pancreatic islets via a combination of NHS-amine (1) and Staudinger ligation (3 - inset box). 3D projection of CLSM micrographs of rat pancreatic islets LbL functionalization with 6 layers of Alginate-PAMAM. i) MDT-PAMAM 15/0 and Alg-N_3 film. ii) NHS-PEG-N_3 primary coating followed by 3 bilayers of MDT-PAMAM 15/20 and Alg-N_3. iii) NHS-PEG-N_3 primary coating followed by 3 bilayers of MDT-PAMAM 15/40 and Alg-N_3 (Green channel hyperbranched Alg-N_3). iv) schematic illustration of islets coating via multiple chemical interactions. Reproduced with permission.[208] Copyright 2013, American Chemical Society.

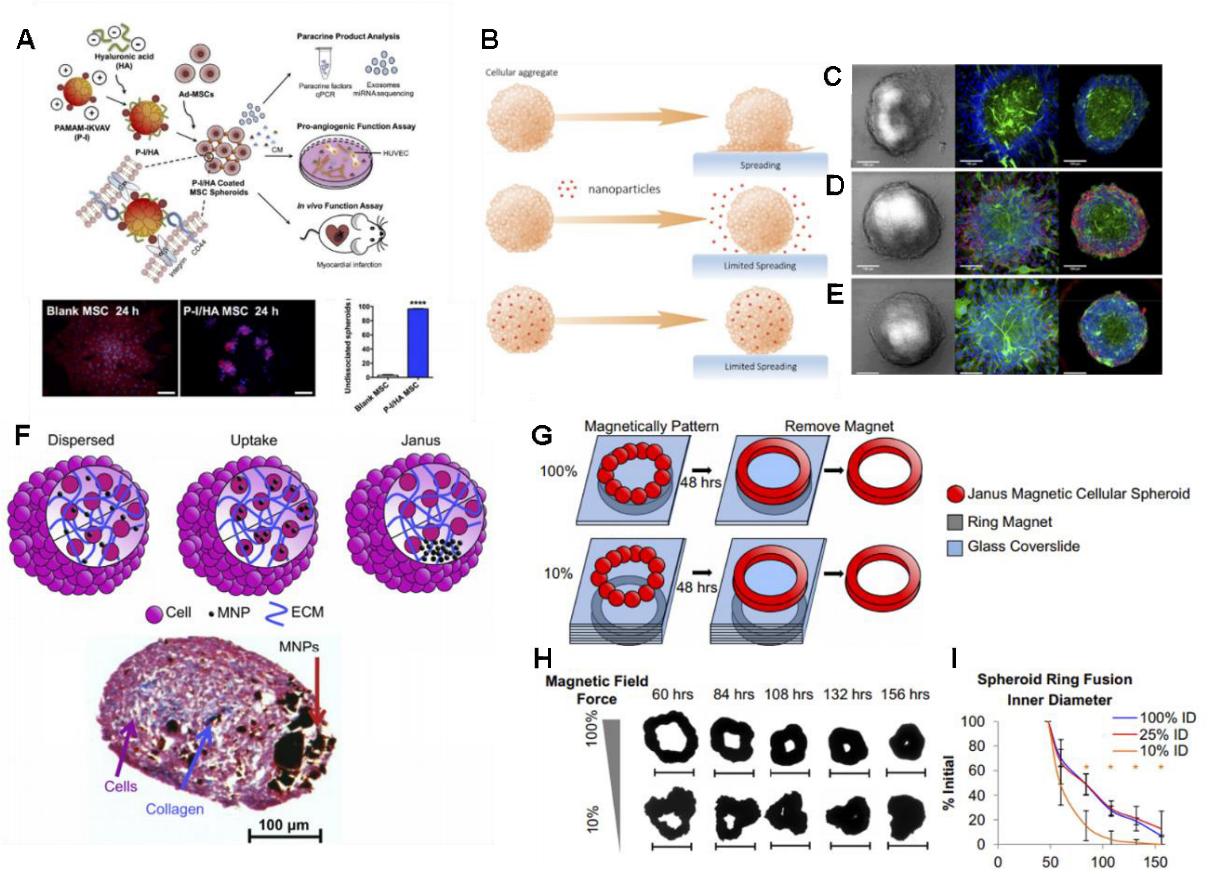

Figure 7. Bottom-up assembly of higher order cell-rich structures by using nanoparticles as interfacial linkers. **(A)** IKVAV-functionalized dendrimers promote the assembly of MSCs into dense 3D spheroid constructs. Reproduced with permission.[258] Copyright 2019, American Chemical Society. **(B)** Nanoparticle-mediated limitation of cells spreading for 3D cell-rich constructs. i) Control 3D cell agglomerates; ii and iii) 3D cell agglomerates incubated with carboxylated polystyrene nanoparticles of 20 nm and 200 nm, respectively. Reproduced with permission.[262] Copyright 2019, American Chemical Society. **(C)** Schematics and histological analysis of Magnetic 3D Janus magnetic multicellular spheroids. Reproduced with permission.[263] Copyright 2014, Elsevier. **(D)** Schematics of janus magnetic spheroids assembly. i and ii) Effect of magnet strength in 3D spheroids fusion and structural maintenance of complex ring/tubular structures along time. Reproduced with permission.[263] Copyright 2014, Elsevier.

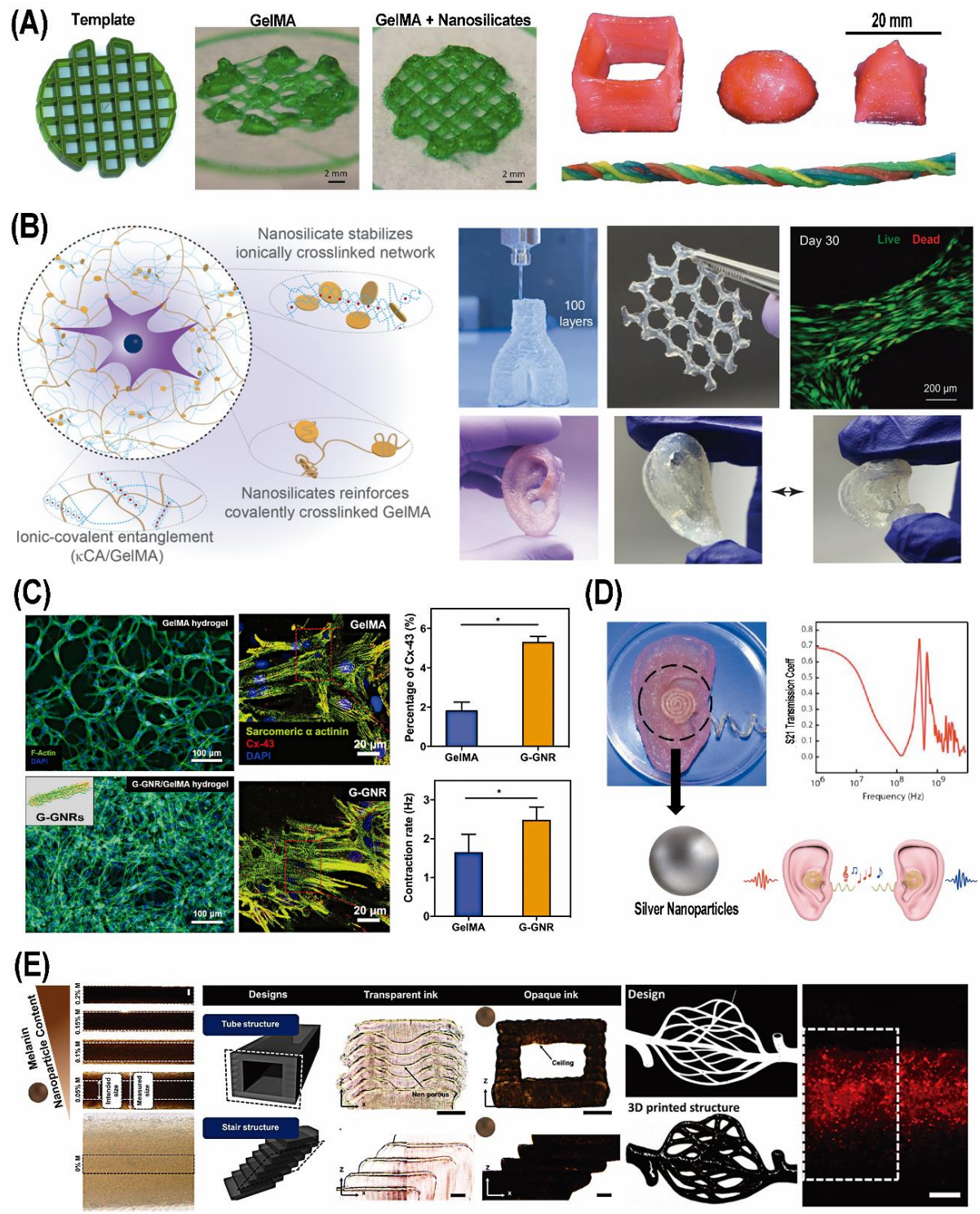

Figure 8. Nanoengineered bioinks for bioprinting complex microtissues with enhanced mechanical properties and improved biofunctionality. **(A)** Hybridization of conventional bioinks (e.g. PEG-diacrylate/Alginate and GelMA) with nanosilicates resulted in improved printability and mechanical robustness of 3D bioprinted constructs. Reproduced with permission.[298,299] Copyright 2015, John Wiley & Sons, Inc and American Chemical Society, respectively. **(B)** Nanoengineered ionic covalent entanglement (NICE) bioinks enabled bioprinting of large vertical constructs with human-scale 3D anatomical structures that are mechanically robust. Reproduced with permission.[297] Copyright 2018, American Chemical Society. **(C)** Electrically-conductive bioink nanoengineered with gold nanorods improved cardiac cell adhesion/organization and promoted electrical communication, which lead to

improved cardiac phenotypic expression as well as increased microtissue beating rate frequency over pristine bioink. Reproduced with permission.[300] Copyright 2017, John Wiley & Sons, Inc. **(D)** Silver nanoparticles embedded in alginate-based matrices were used for fabricating 3D bionic ears with imparted auditory sensing for radio frequency reception. Reproduced with permission.[301] Copyright 2013, American Chemical Society. **(E)** Nanoengineered bioinks with melanin nanoparticles that have intrinsic light absorption capacities enabling enhanced z-axis resolution for 3D-projection stereolithography. Micrographs represent the fabrication of complex hollow/tilted constructs and perfusable blood vessel networks. Reproduced with permission.[302] Copyright 2018, American Chemical Society.

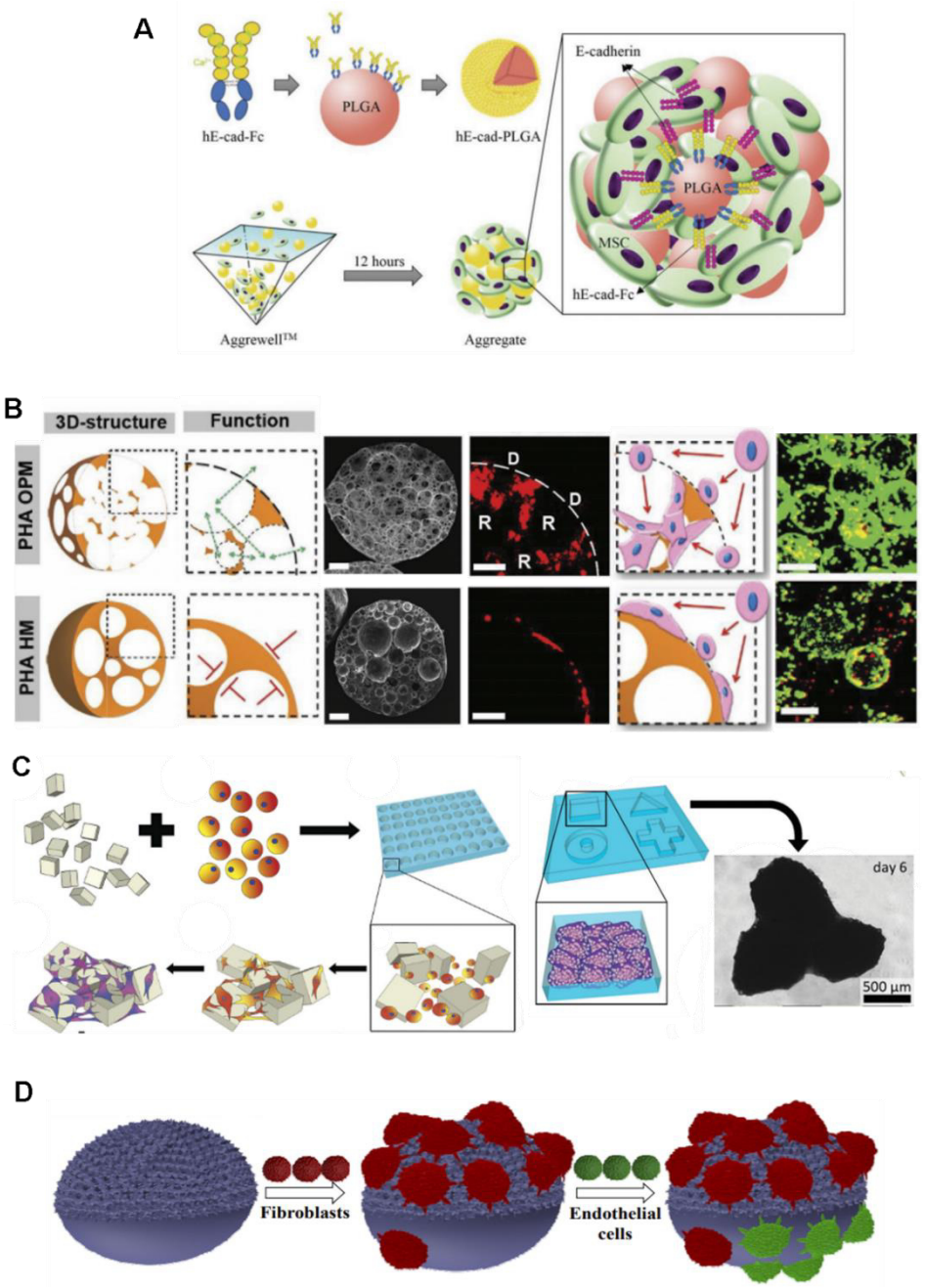

Figure 9. Microparticle enabled bottom-up assemblies of higher order microtissue constructs. **(A)** Schematics of E-cadherin fusion protein surface functionalized PLGA microparticles as cell-anchoring and cell-supportive platforms for 3D microtissues generation. Reproduced with permission.[255] Copyright 2016, John Wiley & Sons, Inc. **(B)** Fabrication of highly open porous polyhydroxyalkanoate (PHA) microspheres (PHA OPM) and hollow microspheres (PAH HM). SEM micrographs of particles interior. Fluorescence micrographs of MSCs migration in the particles volume. Red channel: hMSCs; D: surface pore (room); R: inner pore (room). Live/dead analysis of hMSCs cells under culture for 10 days. Red channel: dead; Green channel: live cells. Reproduced with permission. [258] Copyright 2018, John Wiley & Sons, Inc. **(C)** Schematics of bottom-up microtissue assembly based on cells-microparticles building blocks. Macro-tissue formed after 7 days of micro-aggregates fusion in confined microarray platforms. Reproduced with permission.[252] Copyright 2014, John Wiley and Sons, Inc. **(D)** Schematics of anisotropic PCL microparticles selective cell adhesion concept; particles display a Janus structure with fuzzy or smooth surface. Reproduced with permission.[259] Copyright 2018, American Chemical Society.

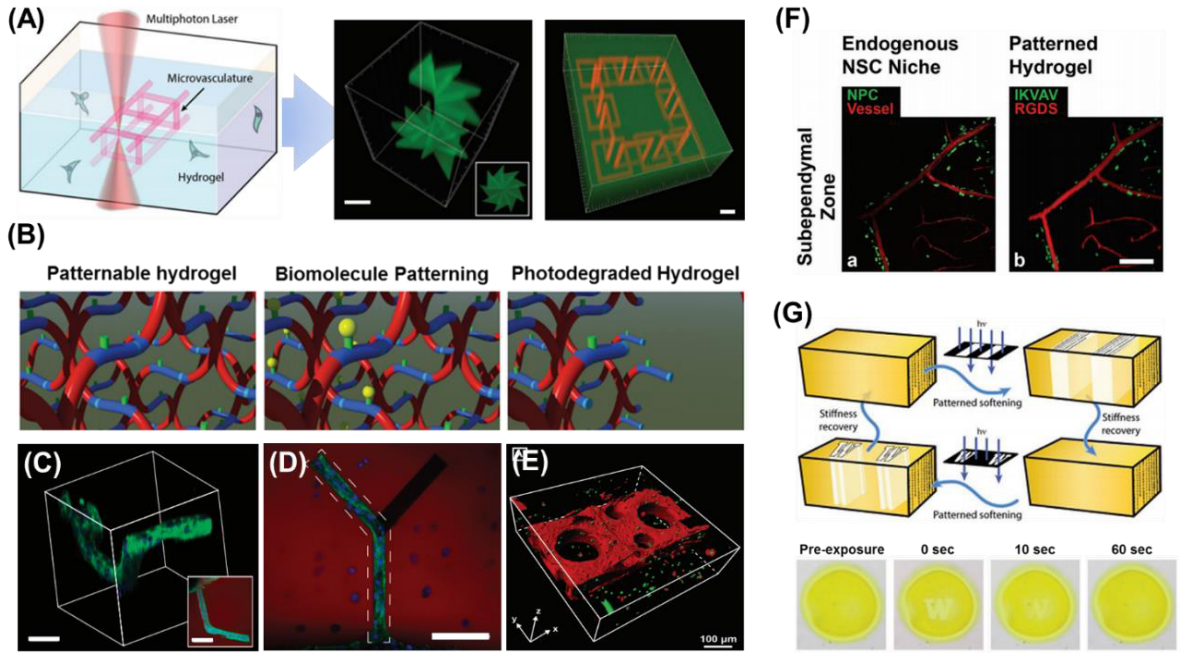

Figure 10. Hydrogel-based approaches for bottom-up tissue engineering of 3D microtissues. **(A)** Multiphoton-enabled true 3D spatial patterning of bioactive proteins within self-assembled hydrogels. Reproduced with permission.[268] Copyright 2015, Nature Publishing Group. **(B-E)** Light-cleavable hydrogel backbone allows for complex 3D control over cell attachment and hydrogel network degradation. Reproduced with permission.[269,278] Copyright 2011 and 2017, Nature Publishing Group and John Wiley and Sons, Inc. **(F)** Image-guided accurate patterning of cell-laden hydrogels reproducing the organization of native tissue niches. Reproduced with permission.[272] Copyright 2012, John Wiley and Sons, Inc. **(G)** Hydrogels with patternable and cyclic stiffness moduli, as shown by the softening of the hydrogel on specific regions (white color). Reproduced with permission.[279] Copyright 2018, John Wiley and Sons, Inc.

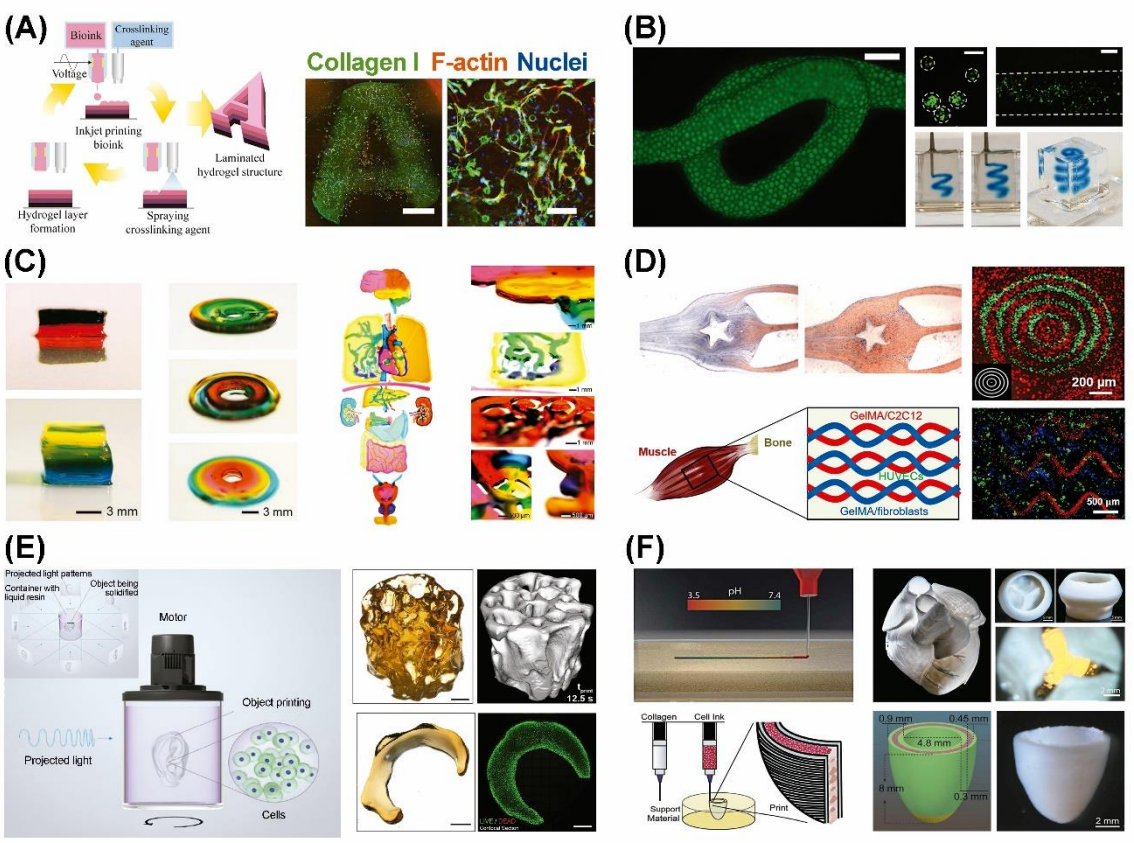

Figure 11. Bioprinting of cell-laden hydrogels for bottom-up assembly of living architectures with defined geometries. **(A)** Inkjet-spray bioprinting for fabricating large-scale laminated hydrogel constructs with suitable cell spreading/proliferation. Reproduced with permission.[407] Copyright 2018, John Wiley and Sons Inc. **(B)** Extrusion-based bioprinting of densely-packed granular inks comprised of fibroblast-laden microgels. Adapted with permission. Copyright 2019, John Wiley and Sons Inc. **(C)** Digitally-tunable extrusion-based bioprinting can be leveraged for continuous multi-material deposition of up to seven different bioinks, enabling the assembly of multilayered blocks, pyramids, blood vessel-like rings and seamless segments, as well as other organ-mimicking anatomical constructs. Reproduced with permission.[410] Copyright 2016, John Wiley and Sons Inc. **(D)** Microfluidics-enabled stereolithographic bioprinting for layer-by-layer photofabrication of multi-biomaterial constructs with different design layouts (e.g. circular patterns and muscle bundle-like organization) and spatial control over cell distribution. Reproduced with permission.[411] Copyright 2018, John Wiley and Sons Inc. **(E)** Tomography-inspired volumetric bioprinting enables rapid fabrication of large-scale anatomically-shaped constructs in shear stress-free conditions, combining unprecedented printing speed with high cell viability. Reproduced with permission.[412] Copyright 2019, John Wiley and Sons Inc. **(F)** Exploiting the pH-induced collagen self-assembly for FRESH v2.0-enabled 3D bioprinting of human cardiac ventricles, functional tri-leaflet valves and organ-scale neonatal hearts. Reproduced with permission.[413] Copyright 2019, The American Association for the Advancement of Science.

Author Photograph

Author Bibiography

João F. Mano is a Full Professor at the Chemistry Department of University of Aveiro, and member of CICECO – Aveiro Institute of Materials. His current research interests include the use of biomaterials and cells towards the progress of transdisciplinary concepts to be employed in regenerative and personalised medicine. João F. Mano is author of 550+ papers in international journals (16500+ citations, *h*=63). He has been part of a series of scientific societies and editorial boards of international journals. He has been coordinating or involved in many national and European research projects, including an Advanced Grant and Proof of Concept grant from the European Research Council.

The recapitulation of native tissues hierarchy and biofunctionality remains a remarkable challenge. Bottom-up tissue engineering as arisen as the most promising approach for designing modular biomimetic 3D microtissues that can better display the biofunctionality and biospecific design of living architectures. This review showcases the most recent advances in integrative bottom-up engineering of functional microtissues.

Keyword Tissue Engineering, Living Building Blocks, Bottom-up Assembly, 3D Bioarchitectures

Vítor M. Gaspar*, Pedro Lavrador, João Borges, Mariana B. Oliveira, João F. Mano*
Corresponding Authors*

Title Advanced Bottom-up Engineering of Living Architectures

ToC figure: